REPORT 1389

CHARACTERISTICS OF THE LANGLEY 8-FOOT TRANSONIC TUNNEL WITH SLOTTED TEST SECTION [1]

By Ray H. Wright, Virgil S. Ritchie, and Albin O. Pearson

SUMMARY

A large wind tunnel, approximately 8 feet in diameter, has been converted to transonic operation by means of slots in the boundary extending in the direction of flow. The usefulness of such a slotted wind tunnel, already known with respect to the reduction of the subsonic blockage interference and the production of continuously variable supersonic flows, has been augmented by devising a slot shape with which a supersonic test region with excellent flow quality could be produced. The flow in this ⅛-open slotted test section was surveyed extensively and calibrated at Mach numbers up to about 1.14. The uniformity and angularity characteristics of the flow were entirely satisfactory for testing purposes. The uniform Mach number in the test region was infinitely variable up to supersonic Mach numbers without change of tunnel geometry. The power required for operation of the slotted tunnel was considerably in excess of that for the closed tunnel but could be somewhat reduced. The flow principles involved in the operation of such a wind tunnel are discussed in some detail.

The reliability of pressure-distribution measurements for a fineness-ratio-12 nonlifting body of revolution in the slotted test section was established by comparisons with body pressure distributions obtained from theory, from free-fall tests, and from other wind-tunnel tests. The effects of boundary interference on the body pressure distributions measured in the slotted test section were shown to be negligible at subsonic Mach numbers and at the higher supersonic Mach numbers obtained. At low supersonic Mach numbers, however, portions of the body pressure distributions were influenced by boundary-reflected disturbances which increased in intensity and moved downstream with increase in Mach number. The effect of the disturbances on body pressures was ascertained and their effect on body drag was shown to be small, particularly when the body was located off the test-section center line to reduce focusing of the reflected disturbance waves.

Experimental locations of detached shock waves ahead of axially symmetric bodies at low supersonic speeds in the slotted test section agreed satisfactorily with predictions obtained by use of existing approximate methods.

INTRODUCTION

In reference 1, a type of wind tunnel having a slotted test section is described in which the tunnel boundary interference due to solid blockage can be greatly decreased or reduced to zero and in which tunnel choking does not exist. The stream Mach number in the slotted test section can be varied continuously up to and through a value of 1.0 and the Mach number in the supersonic range is, moreover, continuously variable.

In order to take advantage of these favorable characteristics the Langley 8-foot high-speed tunnel, which was operated with an axisymmetrical fixed nozzle to produce subsonic Mach numbers up to 0.99 and a supersonic Mach number of 1.2 (see ref. 2), was converted to slotted-tunnel operation early in 1950 and henceforth will be designated as the Langley 8-foot transonic tunnel. The present paper describes this modification and the subsequent changes necessary to produce a test section with uniform Mach number. In addition, an investigation was made (1) to survey and calibrate the flow in the slotted test section and (2) to ascertain the reliability of pressure-distribution measurements for a typical nonlifting transonic model in the slotted test section. The latter part of the investigation included extensive pressure measurements and schlieren observations needed to evaluate the nature and approximate magnitude of test-section boundary effects on the model pressures.

SYMBOLS

a	speed of sound in air
C_D	body drag coefficient based on body frontal area
L_M	axial distance required for free-stream Mach line, starting at model nose, to traverse the supersonic flow to test-section boundary and reflect back to surface of model near test-section center line
L_S	axial distance required for model nose shock to traverse the supersonic flow to test-section boundary and reflect back to surface of model near test-section center line
l	basic length of body-of-revolution model
M	Mach number, V/a
M_{TC}	Mach number corresponding to ratio of stream total pressure to pressure in test chamber surrounding the slotted section
M_o	average Mach number in test section; stream Mach number; Mach number ahead of shock
M_1	Mach number behind shock
P	pressure coefficient, $\frac{p_l-p_o}{q_o}$

[1] Supersedes NACA Research Memorandum L51H10 by Ray H. Wright and Virgil S. Ritchie, 1951, and NACA Research Memorandum L51K14 by Virgil S. Ritchie and Albin O. Pearson, 1952.

$(\Delta P)_{max}$ maximum change in pressure coefficient at model surface due to effect of boundary-reflected distrubances at supersonic speeds

P_{sonic} pressure coefficient corresponding to the speed of sound

p_l local static pressure

p_o stream static pressure

q_o stream dynamic pressure, $\frac{1}{2}\rho V^2$

V airspeed

x axial distance downstream of slot origin; distance downstream of model nose

x_{SB} axial distance from sonic point on body to location of detached shock ahead of body nose

y radial distance from tunnel center line

y_{SB} radial distance from body center line to sonic point on body surface

α angle of attack of model

β acute angle between weak shock wave and the flow direction

θ_v mean flow inclination to the horizontal (measured in vertical plane through center line of tunnel), positive for upflow, deg

ρ mass density of air

APPARATUS AND METHODS

DESIGN OF TEST SECTION

The modification of the Langley 8-foot high-speed tunnel was limited by the desire to preserve intact the original reinforced concrete structure. The length available for the test section was therefore restricted to the 15-foot-long region between the downstream end of the entrance cone and the upstream end of the diffuser; the maximum transverse dimension could not exceed the approximately 96-inch minimum diameter of the entrance cone and diffuser. Moreover, because of the necessity of taking into the diffuser the low-speed air from the mixing region at the slots and because of the expansion required for supersonic flow, the cross-sectional area at the throat had to be reduced to a value less than that at the diffuser entrance—about 20 percent less as suggested by the experiments of reference 1.

In order to accomplish this reduction of area at the throat, a liner was inserted into the original tunnel. The liner and test section were made polygonal in cross section to facilitate construction and to provide plane surfaces for windows. The twelve-sided regular polygon was chosen, as it provided a sufficiently near approach to the circular cross section of the entrance and diffuser to make enough space available for the supporting structure at all points between the original entrance cone and the liner and to allow the fairing into the circular diffuser entrance to be relatively easy. The sides were sufficiently wide to accommodate windows approximately 12 inches square. A cutaway view of the installation is shown in figure 1.

The shape of the entrance liner, given in figure 2, was based on that of the plaster nozzle described in reference 2. This entrance shape, which near its downstream end diverged to an angle of 5 minutes with the center line of the tunnel, was designed to produce a very gradual expansion, so that the Mach number at tunnel station 0 (origin for tapered slots) is nearly uniform and, for all supersonic test-section Mach numbers, is equal to unity all over the cross section. The boundary-layer development is responsible (see ref. 2) for the fact that the effective minimum section (cross section at which the Mach number is unity) exists at or near the slot origin rather than 32 inches upstream at the geometric minimum section. With this liner the maximum possible ratio of diffuser-entrance cross-sectional area to throat cross-sectional area is about 1.18.

The test section was made of steel panels reinforced on the back and supported at the ends. Between the panels, at the corners of the polygon, slot spaces were left sufficiently wide to permit the attachment of strips forming rounded slot edges. By changing these slot edges, constructed of wood to facilitate their modification, various slot shapes (plan forms) could be tested. The spaces between the panels were made sufficiently wide to permit slot widths considerably in excess of the width corresponding to a total opening of one-ninth of the periphery, which is the ratio of open to total jet boundary judged from reference 1 to be required (with 12 equally spaced slots) for zero solid blockage.

In the original design, windows were placed in three panels on each side of the test section, but in assembly, in order to facilitate model observation, one of these glazed panels was interchanged with the top panel (fig. 1, section C-C).

The panels were originally installed with a divergence angle of 45 minutes relative to the center line of the tunnel. To reach this divergence from the 5-minute divergence at the downstream end of the approach section, the upstream end of every panel was gradually curved over the first 18 inches. The shape of this curved region is shown in figure 3 (a).

The stream-side surfaces of the panels and of the downstream 10 feet of the entrance cone were carefully machined, and precautions were taken to assure the smoothness and continuity of the surface. In particular, considerable care was exercised to minimize any differences in surface level at the juncture between the panels and the entrance cone. Inaccuracies in window installation caused disturbances which were removed by fairing the edges or by reinstallation.

At 125.6 inches from their upstream ends the panels joined with a transition section (fig. 3 (a)) which led into the circular diffuser entrance at the 180-inch station. This transition section was made up of curved elements and flat triangular parts as shown in figure 1. The triangular flats made an angle of approximately 2°30′ with the center line of the tunnel so that a discontinuity in slope existed at the 125.6-inch station. The transition section was slotted but the slots could be filled and thus stopped at any position between the 125.6- and 180-inch stations. Because the panels were of essentially constant width, the slot width in this divergent region increased from 2.6 inches to about 3.5 inches.

As indicated in figure 1, section C-C, the structure of the panels was such that open channels existed under the slots. Because of the turbulent mixing at the slots and the expansion to supersonic flow, the jet must expand into the channels. Continuity then requires, since the chamber surrounding the slots is sealed, that air which came out through the slots

must reenter and pass into the diffuser. In order to guide this air into the diffuser entrance, noses were placed in the channels at the downstream ends of the slots as shown in figure 3. Several different nose shapes were tried, the first of which is indicated in figure 1. The nose shape used for most of the test discussed in this report is shown in figure 4 (a). This nose could be moved upstream or downstream to match the position of the downstream end of the slot. A later modification (fig. 4 (b)), including side plates which restricted the downstream channel width, was designed to reduce the power consumption. (See ref. 3.) The flap (fig. 4 (b)), which was open for subsonic operation and closed for supersonic operation, was designed to relieve a subsonic negative Mach number gradient introduced into the test region by this nose shape.

The original dome-shaped test chamber was used as the sealed tank surrounding the slots. (See fig. 1.) This chamber was adequately large, having a maximum diameter of 40 feet. It nowhere approached the slotted test section closer than 6 feet. Glass observation ports were provided in the top, at one side, and in the chamber door.

SLOT SHAPES

The slot shapes tested are shown in figure 5. For the rectangular shape (number 10) originally designed, the edges were made of steel, and two of these edges contained rows of pressure orifices. Figure 6 shows the location of these and other orifice rows. The other slot shapes tested were constructed with wood edges to facilitate their modification.

FLOW-SURVEY INSTRUMENTATION AND METHODS

The characteristics of the flow in the slotted test section were investigated by means of pressure measurements and schlieren observations near the center line and by means of pressure measurements at the wall.

Pressure and temperature measurements.—Static-pressure measurements were obtained from 0.031-inch-diameter orifices located in the surfaces along the center lines of diametrically opposed wall panels 5 and 11, and in the surface of a 2-inch-diameter cylindrical survey tube (fig. 1). The wall orifices were located approximately 2 inches apart axially in the slotted section and as far as 60 inches upstream of the slot origin. The cylindrical-tube orifices were arranged in four axial rows spaced 90° apart. A single row contained orifices located 6 inches apart in a 60-inch-long region immediately upstream of the slot origin, 2 inches apart in a 24-inch-long region just downstream of the slot origin, 6 inches apart in the 24- to 60-inch downstream region, and 2 inches apart in the region extending from 60 to 160 inches downstream of the slot origin. The three other rows contained orifices spaced 2 inches apart in the region from about 72 to 112 inches downstream of the slot origin; in this region the orifice locations in the four rows were staggered so that static-pressure measurements could be obtained at ½-inch intervals. The surface of the cylindrical tube was kept free of irregularities in the vicinity of pressure orifices.

The cylindrical survey tube was alined approximately parallel to the geometric center line of the slotted test section. The nose of the tube was located about 9 feet upstream of the slot origin and was held in position by means of three 0.060-inch-diameter stay wires spaced 120° apart angularly; the downstream end was located in the tunnel diffuser and was supported by means of the model-support system shown in figure 1. A small amount of sag existed along the unsupported length of the tube but this did not affect the pressure measurements. The tube was capable of axial movement to permit measurements at intervals as close as desired. Interchangeable offset adapters were used to locate the tube 6 inches and 15 inches off the center line at any desired angular position.

Local static-pressure measurements obtained by means of the orifices in the wall panel and in the cylindrical-tube surfaces were assumed to be equal to those outside the boundary layer except in the vicinity of a shock where the pressure changes would occur over an axial distance greater at the surface than outside the boundary layer.

Stream total-pressure measurements were obtained in the subsonic flow region upstream of the slot origin by means of several total-pressure tubes, one located in the ellipsoidal nose of the cylindrical survey tube (fig. 1) and the others in the low-speed section upstream of the contraction cone. Measurements also were obtained near the center line of the slotted test section by using a total-pressure rake consisting of eight 0.050-inch-diameter tubes, 3 inches long, mounted ahead of a 1° included-angle wedge.

Pressures were measured by use of multiple-tube manometers containing tetrabromoethane and by use of U-tubes containing kerosene. All manometer tubes were photographed simultaneously.

The temperature of the flow mixture in the tunnel was controlled in order to reduce possible humidity effects on the flow in the test section. Temperature measurements were obtained at a number of stations between the tunnel center line and wall in the low-speed section upstream of the contraction cone by use of thermocouples in conjunction with a recording potentiometer.

Schlieren optical system.—In order to supplement the pressure measurements, schlieren observations of flow phenomena were made by use of the temporary single-pass system shown in figure 7. This system utilized 1-foot-diameter parabolic mirrors and was mounted on large movable support structures which permitted observations at any desired test-section windows in the horizontal plane or in a plane 30° from the horizontal. A spark source was used for photographic recording. The entire system was located within the test chamber and was operated by remote control.

Determination of Mach number.—The flow Mach number, the parameter used for presenting most of the results of the present surveys, was obtained by relating simultaneously measured values of the stream total pressure and local static pressures. Indications of the flow Mach number were also obtained from measured values of the angularity of weak shock waves produced by small two-dimensional surface irregularities on opposite wall panels. Conical shock waves produced by a 10° included-angle cone of 1-inch maximum diameter were used not only for indicating the value of the stream Mach number but also for indicating the degree of flow uniformity in the slotted test section.

Flow angularity measurements.—The mean angularity of the flow with respect to a horizontal plane near the center line of the slotted test section was measured by use of the null-pressure-type instrument shown in figure 8. This instrument, a 3° included-angle cone, contained 0.010-inch-diameter static-pressure orifices located symmetrically in opposite surfaces. The sensitivity of this instrument to angle-of-attack changes, expressed in terms of the pressure differential between orifices in opposite surfaces and in the plane of angle change, was about 0.6 percent of the stream dynamic pressure per degree change of angle in the transonic speed range. This sensitivity, though not great, was within the possible error in instrument-attitude measurements. Such measurements, obtained by careful use of a cathetometer during actual testing, were estimated to include possible inaccuracies not exceeding 0.1°. The procedure for measuring the flow inclination consisted of, first, orienting the instrument so that pressure orifices in opposite surfaces were situated in the vertical plane of measurement, and second, varying the instrument attitude by means of a remotely controlled angle-changing mechanism in the support system until the pressures at the opposite surfaces were equal. The instrument attitude was determined carefully by means of cathetometer readings for this indicated null-pressure condition, and the procedure was repeated with the instrument inverted. The arithmetical average of instrument-attitude measurements made with the instrument erect and inverted was assumed to compensate for possible asymmetry of the instrument and to indicate the mean direction of the flow.

Rapid variations of the flow angularity with time were indicated by means of pressure-fluctuation measurements in the slotted test section. For these measurements a 3° included-angle cone was equipped with a small electrical pressure cell (mounted inside the cone) which connected directly with static-pressure orifices located 180° apart in the cone surface. Periodic differences in pressure between the orifices in opposite surfaces of the cone were measured by means of a recording oscillograph. The indicated pressure differences were expressed in terms of flow-angularity changes by use of a steady-state calibration of the pressure differential between orifices in opposite surfaces of the cone with respect to cone-attitude changes in the plane of the orifices. This pressure differential in the transonic range was about 5 pounds per square foot per degree change in cone attitude with respect to the flow, whereas the sensitivity of the pressure cell was approximately 0.25 pound per square foot. The accuracy of the pressure cell was maintained over a frequency range from 0 to 300 cycles per second.

Jet-boundary interference effects.—In order to ascertain the value of the slotted test section for testing purposes a high-fineness-ratio body of revolution was tested at zero angle of attack through the Mach number range from about 0.60 to 1.14 and the measured body-surface pressure distributions were compared with essentially interference-free distributions from other sources. The particular body shape used in this investigation, a fineness-ratio-12 body for which coordinates are given in reference 4, was selected because of the availability of theoretical and experimental pressure distributions. The wind-tunnel model consisted of the forward 83.7 percent (33.5 inches) of a 40-inch-long basic body; a 3.25° semiangle support sting joined the body at the 83.7-percent station (see fig. 9). This model contained static-pressure orifices (0.020 inch in diameter) spaced 2 inches apart axially along the length of the body and arranged in rows at various angular locations (ref. 5) but only the pressure measurements at the upper and lower surfaces were used for the comparisons shown in this report. Small surface discontinuities existed at model-component junctures, at an embedded mirror in the upper surface, and at faired surfaces over filled bolt holes.

The reflection of disturbances from the slotted-test-section boundary and the effect of such reflections on model pressure distributions were examined by testing both the body of revolution (fig. 9) and a wing-body combination (fig. 10) at supersonic speeds and correlating the measured pressures at model and wall surfaces with schlieren pictures of the flow field near the model surface. The wing-body combination consisted of the previously described body of revolution (fig. 9 (c)) fitted with a 45° sweptback airfoil of NACA 65A006 section, 12-inch semispan, and 1-square-foot planform area. Static-pressure orifices (0.020 inch in diameter) were located in the upper and lower surfaces of the airfoil at five semispan stations (see ref. 5) but for the present surveys pressures were measured mainly at the 60-percent and 80-percent semispan stations where the airfoil chords were about 5.70 and 5.05 inches, respectively. Pressure orifices at these wing stations were located at chordwise intervals no greater than 10 percent of the chord. Static-pressure orifices (0.018 inch in diameter) also were located at axial intervals of about 0.75 inch along the length of the model-support sting in order to measure pressures in the compression region at the base of the model and to aid in locating wall-reflected disturbances. Transition was fixed at 10-percent-chord and 12-percent-body-length stations for the wing and body of revolution, respectively.

The control of model attitude during tests in the slotted test section was effected by means of cathetometer observations and a remotely controlled angle-changing mechanism in the model-support system.

PRECISION OF DATA

The maximum random error in the indicated Mach number, as obtained from pressure measurements throughout the transonic range covered by these surveys, was estimated to be no greater than 0.003 in shock-free flow. For measurements behind shocks an additional error in the indicated Mach number was possible because of failure to correct for changes of the stream total pressure through the shocks; this error, however, was negligible at the lower supersonic Mach numbers and did not exceed 0.002 for normal shocks at a Mach number of 1.14.

Probable errors in Mach numbers indicated by angularity measurements of weak shocks in supersonic flow were about 0.002. This error corresponds to an estimated inaccuracy of 0.2° in the measurement of the angularity of two-dimensional shocks from the test section walls. The angularity of

sharply defined conical shocks could be measured with an inaccuracy of only about 0.1°.

The differences between Mach numbers determined from pressure measurements and those from shock-angularity measurements at supersonic speeds corresponded closely to the estimated probable errors in determining the Mach number. (See fig. 11.)

Estimated possible errors in the model-surface pressure coefficients obtained from tests in the slotted test section were generally about 0.005 and did not exceed about 0.010.

The sensitivity of the schlieren optical system, when properly adjusted, was sufficient to permit the detection of a conical shock whose strength corresponded to a Mach number change of about 0.003.

The maximum possible error in measuring the flow angularity was estimated to be about 0.1°. A like error in measuring the model angularity introduced the possibility of errors as great as 0.2° in model alinement with respect to the flow direction.

RESULTS AND DISCUSSION

PRELIMINARY INVESTIGATIONS

Inasmuch as the 8-foot transonic tunnel was the first large slotted tunnel constructed at the Langley Laboratory, the first task was to study its general characteristics. Such a study was facilitated by the large size of the test chamber, which permitted direct observation during tunnel operation from positions near the slots. Such observation was limited, however, by the noise, which became painful at Mach numbers greater than about 0.6, and by the danger of a sudden large pressure increase due to power failure at large Mach number, which might result in physical injury to the observer. The test chamber was also uncomfortably hot because of the necessity of operating the tunnel with high stagnation temperature, up to 180° F, in order to prevent condensation difficulties.

In an investigation of the noise, the natural fundamental frequency of the system of test chamber and slots was roughly estimated at about 3 cycles per second. Measurements of the frequency and intensity of the sound in the test chamber indicated a vibration with about this frequency, but the greater part of the energy was rather widely distributed in general noise. This noise, which arose from the tunnel fan, from the vorticity and general turbulence in the slots, and from the general diffuser flow, reached an intensity in excess of 130 decibels at Mach numbers near unity. In addition, sections of the test-chamber floor vibrated, apparently with their natural frequencies, but these vibrations were not excessive. To minimize noise and vibration, blunt diffuser entrance noses are believed to be desirable, because sharp noses might be expected to produce oscillations when struck by the vortices proceeding downstream just outside the slots.

In addition to the vibration, a general circulatory movement of the air in the test chamber was observed. The scrubbing action at the slots entrains air from the test chamber and carries it along toward the diffuser entrance, where it is separated from the tunnel flow at the diffuser entrance noses, deflected out into the surrounding chamber, and circulated back toward the upstream ends of the slots.

The first tests were made with the rectangular slot shape and with a panel divergence of 45 minutes. The indicated Mach number distributions at the various orifice rows are shown in figure 6. In this figure M_{TC} is the Mach number corresponding to test chamber pressure. The total pressure for these and all other Mach number distributions presented in this report is that near the center of the tunnel stream.

The Mach number distribution shown in figure 6 is evidently unsatisfactory for model testing. As pointed out in reference 2, the flow disturbances in a circular tunnel are concentrated at the center; as might be expected, the 12-sided tunnel with regular polygonal cross section behaves in a similar manner, that is, the Mach number oscillations shown in figure 6 are considerably greater near the center of the tunnel than at the center of a panel. Special care is therefore required to obtain a model test region with uniform Mach number. The solution to this problem was deduced from tests with various slot widths and shapes, from additional tests which had previously been carried out in the apparatus of reference 1, and from a fundamental conception of the part to be played by the slots in producing the supersonic flow. Previous tests had already led to the belief that one of the most important causes of the Mach number oscillations was the overexpansion in the upstream part of the slotted section, similar to that which occurs when a supersonic jet debouches into a region having a pressure less than that at the jet exit. The function of the slot shape is conceived to be the control of this expansion in such a way that the Mach number will gradually approach its final test-section value without exceeding this value at any section. With the 45-minute divergence of the panels such control was found to be impossible, although a number of different slot shapes were tried, because the flow expansion produced by the curvature and divergence of the panels already exceeded that required.

The possibility existed of removing most of this divergence by turning end-for-end the part of the panels between stations 0 and 125.6 inches. This modification as accomplished is shown in figure 3 (b). The panels are straight for the first 107 inches with a 5-minute slope continuous with that of the entrance cone. The curved part of the plates now lies between the 107- and 125.6-inch stations, and curved liners have been added between the 125.6- and 141.6-inch stations in order to relieve the discontinuity in slope at that station and thus to prevent large flow disturbances with attendant shocks in this region.

The efficacy of changing the panel divergence from 45 to 5 minutes is shown in figure 12. A considerable reduction in the Mach number oscillations has been obtained, particularly near the center of the tunnel. The slot is now fulfilling its function of controlling the development of the supersonic flow, and changes in slot shape might therefore be utilized to improve the Mach number distribution at the center of the tunnel.

INVESTIGATION OF SLOT SHAPES

The establishment of supersonic flow suitably uniform for model testing in the slotted region of the Langley 8-foot transonic tunnel was the primary purpose of the investigation of slot shapes, since the production of satisfactorily

uniform flow at speeds up to and slightly exceeding the speed of sound was easily achieved simply by the installation of rectangular-plan-form slots. (See fig. 13.) The performance of rectangular slots, reported in reference 1 for the case of a 12-inch-diameter throat, was verified experimentally in the 88-inch effective-diameter throat of the Langley 8-foot transonic tunnel. A characteristic feature of supersonic flow in a throat equipped with rectangular slots is a rapid initial expansion and a subsequent compression of the flow immediately downstream of the slot origin. At Mach numbers greater than about 1.02 disturbances associated with the initial expansion-compression appear in the slotted-test-section flow, and the magnitude of the disturbances increases with Mach number. This performance is illustrated in figure 13, which presents the results of flow surveys in the 8-foot tunnel with rectangular slots and with the throat geometry of figure 3 (b). The disturbances shown in figure 13 are sufficiently severe to preclude the use of rectangular-plan-form slots at supersonic speeds in this test section.

The use of tapered slots to reduce the rapidity of the initial flow expansion and the severity of the accompanying disturbances, which was originally reported in reference 6, was followed in investigating suitable slot shapes for the Langley 8-foot transonic tunnel. For this investigation the tunnel throat geometry of figure 3 (b) was maintained. For some of these tests, the curved liner shown in figure 3 was replaced by a "boat-tail" as indicated at the top of figure 14, but this change did not significantly affect the flow in the test section. The first slot shape investigated was a straight-taper design, somewhat similar to one for which fairly good flow characteristics were reported in reference 6. This slot shape is identified in figure 5 as shape 1. The slot originated as a point at the effective minimum section of the tunnel (station 0) and opened with an angle of 0.77° between the edge and center line of the slot. The tapered portion extended 96 inches (1.09 jet diameters) downstream, after which the slot width remained constant. In this region of constant slot width, the open portion of the boundary comprised approximately one-ninth of the total periphery of the tunnel wall. The flow characteristics of the slotted section equipped with slot shape 1 (see fig. 14) corresponded approximately to those for the tapered slot reported in reference 6 for a 12-inch-diameter tunnel throat. The supersonic flow in both tunnels attained approximately the same maximum and minimum Mach numbers at equivalent distances (jet diameters) downstream of the slot origin. The existence of the compression region following the initial expansion was sufficient, however, to justify investigating the control of slotted-section flow characteristics by means of slot-shape modifications.

Other tapered slots were then investigated in an attempt to reduce the initial flow overexpansion and the compression that followed. The flow characteristics for slot shapes 4 and 9, which opened with only about half the angle of slot shape 1 over the first 48 inches downstream of the slot origin (see fig. 5), are shown in figures 15 and 16, respectively. Comparison of these data with those for slot shape 1 indicated that the reduction in the initial rate of opening of the tapered slot produced a corresponding reduction in the rate of flow expansion; also, the slight overexpansion and following compression of the supersonic flow produced by slot shape 1 was practically eliminated by use of shape 9. The flow expansions produced by slots 4 and 9 were almost identical in spite of the fact that slot shape 4 opens more abruptly downstream of the 48-inch station. In the test section the degree of flow uniformity was slightly less for shape 4 than for shape 9, and it is therefore surmised that small flow-uniformity gains may be expected by changing the slot shape gradually over the downstream portion of its taper.

Slot shapes 6 and 7 (see fig. 5) utilized over their first 12 inches of length essentially the same initial taper angles as were employed for shapes 9 and 1, respectively; but following this 12-inch straight-taper region slots 6 and 7 opened with greater angles of divergence than did shapes 9 and 1 and attained their full-open widths at 76 and 74 inches downstream of the slot origin. The results of flow surveys for these slot shapes, presented in figures 17 and 18, revealed that the supersonic flow downstream of the initial straight-taper region expanded more rapidly and compressed more severely than did the flow for slot shapes 9 and 1. The data for slot shapes 1, 9, 6, and 7 indicated that, for tapered slots whose initial opening angles are no greater than the 0.77-degree half-angle taper used for shape 1, the important factor in controlling the flow expansion and compression is the proper shaping of the slot over the long region in which most of the opening to full slot width takes place.

Slot shape 8, which opened in a straight taper of 1.18° half angle over its first 48 inches from the slot origin (see fig. 5), produced the Mach number distributions shown in figure 19. The supersonic-flow expansion occurred more rapidly for slot shape 8 than for any of the other tapered shapes investigated, as might be expected from the greater angle at which it opened. At the higher Mach numbers the distribution became saddle-shaped.

From the center-line Mach number distributions corresponding to slot shapes 1, 4, 6, 7, 8, and 9, the possibility now existed of relating slot-shape changes to the corresponding Mach number changes and thereby effecting modifications designed to improve the distribution. For the direction and a qualitative indication of the magnitude of the slot-width changes required, the conception of the function of the slots in producing the supersonic flow served as a guide. Thus, for instance, if at some point along the center line the flow has expanded to a Mach number in excess of that indicated by the test-chamber pressure, this overexpansion can be traced back along a Mach line to a region on the tunnel boundary; if in this region the pressure on the panels is greater than that in the test chamber, a decrease in slot width is indicated in order to reduce the flow expansion at that section.

In selecting a slot shape to serve as a basis for the new design, shape 9 was chosen because it already produced a supersonic flow of considerable uniformity. In addition to the changes intended to improve the flow uniformity, which were accomplished by interpolating among the slot shapes previously tested and by applying the ideas discussed in the previous paragraph, a further modification was made in order to decrease the length required for establishment of

the uniform flow. For this purpose the angle of taper at the upstream end was increased to a value approaching that for shape 8. This increase in taper angle at the upstream end was consistent with a decrease between the 55- and 75-inch stations, where such a decrease was believed to be desirable in order to decrease the Mach number oscillations in the test region. The final slot shape is shown as number 11 in figure 5.

The results of the flow surveys with slot shape 11, which are presented in figure 20, show a slight improvement in flow uniformity at Mach numbers greater than 1.1. The over-expansion with subsequent compression is practically eliminated, and, moreover, this uniform flow is reached in a shorter distance than with slot shape 9. The length of the essentially gradient-free region available for testing purposes varies from about 80 inches at a stream Mach number of 1.07 to approximately 40 inches at a stream Mach number of about 1.13. Extensive surveys, including static-pressure measurements at axial intervals as close as ¼ inch, in the slotted section equipped with tapered slot shape 11 indicated Mach number deviations no greater than those shown in figure 20. In a typical model-testing region approximately 36 inches long and 30 inches in diameter, the Mach number deviations increased with Mach number to values not exceeding ± 0.006 at a stream Mach number of 1.13. This degree of flow uniformity was considered satisfactory for model-testing purposes, and slot shape 11 was therefore chosen for the final test-section configuration.

The coordinates for slot shape 11 are given in figure 21. Also included in this figure is the approximate shape of the slot edge, which was slightly over 0.5-inch thick and which remained essentially the same for all the slot shapes investigated. Immediately outside the slot edges, the channel between the edges and the test chamber opened abruptly as indicated in section C-C of figure 1. If the thickness of the slot edges and the size of the channel immediately outside the slot opening had been greatly different, the characteristics of the flow through the slots might have been influenced sufficiently to have resulted in a final slot shape somewhat different from shape 11. The large size of the channels results in the maintenance of the pressure just outside the slots at a value very close to that in the test chamber; and the thinness of the slot edges tends to reduce the inertia effects due to flow in the slots, which might aggravate the oscillation in the test region. The rounding of the slot edges may not be necessary, but was taken as a precaution against disturbances that might arise from flow separation at sharp corners.

TEST-SECTION CALIBRATION

Flow uniformity.—The results of extensive pressure surveys in the slotted test section using slot shape 11 are presented in figures 22 and 23 in terms of the local Mach number. The stream total pressure used, in conjunction with local static pressures, to determine the Mach number distributions of figures 22 and 23 was found to be essentially constant throughout the survey region near the test-section center line and was in close agreement with values measured in low-speed regions upstream of the slotted section. The Mach number distributions shown in figure 22 are associated with the flow characteristics soon after installation of the slotted throat and with a diffuser-entrance nose located 142.5 inches downstream of the slot origin (nose A). Figure 23 presents wall and center-line Mach number distributions obtained from surveys conducted at a later date and with a longer diffuser-entrance nose (nose B, ref. 3) located 114.6 inches downstream of the slot origin.

The Mach number distributions in the slotted test section with diffuser-entrance nose A (fig. 22) indicated that (1) the flow in the slotted test section was essentially free of gradients (except in the Mach number range from about 0.90 to 1.08 where a slight positive Mach number gradient existed), (2) the length of the uniform-flow region available for model-testing purposes decreased with Mach number but was approximately 60 inches long at a Mach number of 1.13, (3) the Mach numbers measured near the center line of the uniform-flow region agreed reasonably well with those at the wall, and (4) the quality of the flow in the slotted test section with slot shape 11 was fully equal to that in the most carefully designed two-dimensional solid nozzles. This result is the more remarkable when it is realized that the slot shape was reached without the benefit of any such theory as is available for the solid nozzle design and that, moreover, this uniform-flow test region was attained in a tunnel of approximately circular cross section, for which the solid nozzle design is particularly critical. It seems reasonable, therefore, to conclude that the design is much less critical for the slotted nozzle than for the solid nozzle. This easing of the design requirements is perhaps due to the fact that the slots in conjunction with the panels produce an effective integrated damped elastic pressure boundary in contrast to the unyielding solid boundary of the solid nozzle. This pressure boundary is incapable of supporting the large pressure gradients that can exist at a completely solid boundary and, therefore, all disturbances at the boundary tend to be spread out into shallow oscillations instead of being concentrated into shocks as may occur in a solid nozzle.

In other respects the flow in the slotted nozzle is similar to that in a solid nozzle. Thus, just as in a solid nozzle, irregularities on the solid surfaces produce disturbances extending into the interior of the flow. Disturbances produced by strings 0.010 inch in diameter on the top and bottom panels at a Mach number of 1.074 are shown by the schlieren photograph inset in figure 24. These disturbances are propagated along lines at angles very close to the Mach angle. This behavior corresponds with the assumption, involved in the derivation of the slot shapes, that the only part of a slot effective at a point of the flow is that upstream of the intersection of that slot with the upstream Mach cone through the point.

The results of surveys in the slotted test section after a long period of model testing and with diffuser-entrance nose B (fig. 23) indicate that the Mach number attainable at maximum tunnel power was increased slightly but the test section was shortened at its downstream end by use of the new diffuser-entrance-nose arrangement. The Mach number distributions of figure 23 also indicate a decrease in the uniformity of the test-section flow since the time of the

initial surveys; over a 36-inch-long region the maximum deviations from the average stream Mach numbers indicated in figure 23 were as much as 0.010 as compared with deviations of as much as 0.006 in figure 22. This deterioration of the flow was assumed to be due to the effect of discontinuities appearing in the wall-panel surfaces, as near window edges, during prolonged periods of tunnel operation when insufficient attention was given to maintenance of wall-panel smoothness.

The degree of test-section flow uniformity indicated by Mach number distributions was verified over a portion of the test region at supersonic speeds by examining schlieren pictures for the presence of stream disturbances equal to or stronger than a shock of known strength introduced into the flow. The results of the flow-uniformity check are illustrated in figure 25. A 10° included-angle cone was alined approximately parallel to the flow near the test-section center line, and schlieren pictures were made of the flow field about and ahead of the cone at stream Mach numbers of 1.035 and 1.075. The schlieren pictures were obtained for only the horizontal plane (light path through windows in panels 3 and 9) since the largest wall-surface discontinuities were known to exist on wall panel 12, and disturbances from this panel were most readily detected from horizontal schlieren surveys. The attached conical shocks were the only disturbances visible in the schlieren pictures (fig. 25) and, since these shocks were three dimensional and therefore more difficult to detect than two-dimensional disturbances, it was concluded that no abrupt disturbances of greater strength than that of the conical shock existed in the flow. (Because the conical shocks shown in figure 25 were weak, they are not very distinct in the schlieren pictures; dots have therefore been superimposed on the shock lines to emphasize their location.) The strength of the attached conical shock, expressed in terms of the Mach number decrement through the shock, is no greater than 0.004 and 0.003 at stream Mach numbers of 1.035 and 1.075, respectively (fig. 25). Mach number decrements calculated from conical-flow theory (ref. 7) are in close agreement with the two experimental points. In determining these experimental points the Mach number decrements across the cone shocks were obtained by use of oblique-shock theory (ref. 8) with shock angles measured directly from the schlieren pictures. For the stream Mach numbers and the test-section region concerned, the experimental schlieren-survey data of figure 25 appear to be consistent with the pressure-survey data in indicating the presence of no abrupt steady-flow disturbances of significant strength.

The measured angularity of conical shocks (fig. 25) offered indications of the value of the supersonic Mach number which were consistent with those indicated by pressure measurements (figs. 22 and 23) and by the angularity of weak two-dimensional disturbances from wall panels (fig. 11).

Flow calibration.—The stream flow in the slotted test section was calibrated with respect to the pressure in the chamber surrounding the slotted section, a procedure employed for smaller slotted tunnels in the investigations reported in references 1 and 6.

A typical calibration curve with the model removed from the tunnel shows the variation with test-chamber Mach number of the average Mach number over a region 30 inches in diameter and 36 inches long near the test-section center line (fig. 26). The data for this calibration were taken from the distributions of figure 22. An average value of the stream Mach number over the 30-inch-diameter region was obtained by fairing through the test points from the ten different positions of the survey tube. This faired value for the average stream Mach number varied almost linearly with, but was always smaller than, the indicated test-chamber Mach number. The Mach numbers measured at the ten survey locations did not differ from the average stream Mach number by more than 0.004 and 0.006 up to Mach numbers of 1.00 and 1.13, respectively.

In figure 27 a comparison is made of flow calibrations at the test-section center line for a region 36 inches long (from 68 to 104 inches downstream of the slot origin) with the model removed from the tunnel. The data of the comparison are taken from figure 22 (early surveys with diffuser-entrance nose A) and from figure 23 (later surveys with diffuser-entrance nose B). The agreement between the two surveys is shown to be very good for the particular flow region calibrated.

The effect of a model on the Mach number of the incoming flow upstream of the model test region was examined. The use of pressure measurements at the wall to verify the trend of the stream flow ahead of the model was considered applicable, particularly at supersonic speeds where disturbances are propagated approximately along Mach lines. This supposition was checked experimentally by comparing Mach number distributions along the slotted-section wall upstream of a wing-fuselage model (fig. 10) with wall distributions for the model-removed case. The results of this comparison for small lifting attitudes of the model (fig. 28) indicated close agreement between model-in and model-removed Mach number distributions upstream of the model location. The only discrepancy in the data of figure 28 appears immediately upstream of the model nose at a test-chamber Mach number of 1.025, where the bow wave ahead of the nose influences the model-in Mach number slightly. The evidence of figure 28 was supported by additional measurements with the same model at higher angles of attack (fig. 29). The latter data are presented to show the variation with test-chamber Mach number of the model-in and model-removed Mach numbers at the test-section wall approximately 10 inches upstream of the model-nose location. The data shown in figure 29 were obtained over a long period of time and included measurements with the wing-fuselage model at angles of attack as great as 20° and with diffuser-entrance noses A and B; the data from the many separate runs were in relatively close agreement. The combined data of figures 28 and 29 reveal generally that, for this ratio of model size to tunnel size, the pressures on the test-section wall ahead of the model were not greatly influenced (and therefore the validity of the model-removed calibration was not much affected) by the presence of the model at different lifting attitudes.

Although no quantitative comparisons are presented, it is believed from past experience in the calibration of high-speed

wind tunnels that the overall precision of calibration of a slotted test section, when the test-chamber pressure is used as a calibration reference, is superior to that of a conventional closed test section for subsonic speeds. In particular, the use of the pressure in the sealed chamber surrounding the slots as a reference pressure in calibrating the stream flow is believed to avoid the inconsistencies which may arise from the use of the static pressure indicated by a wall orifice located upstream of the minimum section.

Flow angularity.—The mean angularity of the flow in the slotted test section was measured at a center-line station 85 inches downstream of the slot origin. The measurements were limited to the vertical plane and employed the null-pressure-type instrument of figure 8 and the methods outlined earlier. A 2° included-angle wedge was first used for the flow-inclination measurements but it proved inadequate because of excessive bending near the leading edge and damage to the leading edge caused by the impact of foreign particles in the airstream. The 3° included-angle cone was less sensitive than the wedge but was superior in its relative freedom from tip bending and damage. The flow-inclination results (fig. 30), obtained from average measurements with the cone erect and inverted, indicated a mean upflow angle of approximately 0.1° which did not appear to change appreciably with Mach number. The scatter in measurements ranged up to about ±0.1° from the mean indicated angularity. Careful measurements of the angularity of wall panels 6 and 12 revealed that the geometric center line between these two panels differed from the horizontal by approximately 0.05° in the direction of the indicated upflow.

Fluctuations of the stream angularity with time were measured by means of an electrical pressure pickup in the 3° included-angle cone. The results of these measurements indicated rapid variations of about 0.4° from the mean flow angle shown in figure 30. The fluctuations were greatest at frequencies from approximately 10 to 85 cycles per second throughout the transonic speed range.

MODEL TESTING AND BOUNDARY INTERFERENCE

A preliminary investigation of boundary interference effects on pressure-distribution and drag measurements for a nonlifting body of revolution (fig. 9) in the slotted test section was conducted in order to ascertain the reliability of typical model test data obtained from the slotted test section of the Langley 8-foot transonic tunnel. This investigation involved the comparison of experimental body data from the slotted test section with essentially interference-free data from other sources and the examination of the slotted-test-section data for the presence of solid blockage and boundary-reflection effects. Experimental data from the investigation were also used in examining several flow phenomena of concern with regard to transonic testing in the slotted test section. The stream Mach numbers at which body data were obtained in the slotted test section ranged from about 0.6 to 1.136. The test Reynolds number, based on model length, ranged from approximately 9.5×10^6 to 11.0×10^6.

Flow phenomena, including shock reflections, with nonlifting body of revolution and wing-body combination at center line of slotted test section.—Some flow phenomena of interest in connection with the transonic testing of models in the slotted test section are illustrated in figures 31 and 32. These data were obtained from tests of the nonlifting body of revolution (fig. 9 (c)) and the wing-body combination (fig. 10) at the center line of the slotted test section.

At very high subsonic speeds (figs. 31 (a) to 31 (c)) the supersonic-flow expansions around the maximum-thickness region of the body of revolution (and the local shock formations associated with model-surface discontinuities and with the compression region near the base of the body) did not extend to the test-section boundary. The failure of the model-field expansions to affect significantly the Mach number distributions at the test-section wall at a stream Mach number of 0.990 (fig. 31 (c)) offered evidence as to the essential absence of boundary interference for the model size used and also indicated an alleviation of choking in the slotted test section (tests of the body in a closed test section of the same size would have resulted in choking at a stream Mach number of about 0.985).

At low supersonic speeds (figs. 31 (d) to 31 (*l*) and 32 (a) to 32 (d)) the model-field shocks and expansions are shown to impinge upon the test-section boundary at axial locations which permit the reflection of disturbances back to the surface of the model. The model nose shock (bow wave) and the expansions over the upstream portion of the model are the disturbances of concern with regard to the production of boundary interference effects on model measurements. The shock-wave reflections are illustrated (figs. 31 (d) to 31 (n) and fig. 32) by means of both schlieren pictures and model-surface and wall Mach number distributions. In these figures the lines drawn to connect the schlieren-field shocks with shock locations (maximum compression regions) at the wall do not necessarily represent accurately the actual shock curvature in either the stream or the boundary layer.

Effect of boundary interference on pressure-distribution and drag measurements for nonlifting body of revolution at center line of slotted test section.—The comparisons of figures 33 to 35 were employed to ascertain the reliability of body pressure-distribution measurements in the slotted test section and, in particular, to obtain approximate effects of boundary interference on the body pressures at supersonic speeds. The interference-free model-surface pressure distributions given in figure 33 include those obtained from theory for the basic shape of the body (fig. 9 (a)), from free-fall tests for a 120-inch-long model (fig. 9 (b)), and from tests of the wind-tunnel model (fig. 9 (c)) in the 92-inch-diameter axisymmetrical closed test section of reference 2. The closed-test-section data, which were obtained at high subsonic speeds, were corrected for blockage effects by means of relations described in reference 9. The free-fall and theoretical distributions shown in figure 33 were obtained from reference 4, which utilized linearized theory and Prandtl-Glauert adjustments for the theoretical distributions at subsonic stream Mach numbers up to 0.95 and methods of reference 10 for the distributions at Mach numbers of and larger than about 1.05. The essentially interference-free pressure distributions shown in figures 34 and 35 were obtained from tests of the wind-tunnel model in the slotted test section of the Langley 16-foot transonic tunnel.

The wind-tunnel pressure coefficients used in figures 33 to 35 were averaged from coefficients for upper and lower surfaces in order to reduce possible deviations due to model alinement errors and surface irregularities; coefficients from the Langley 8-foot transonic tunnel were also average values from a number of different runs which repeated the model pressure measurements closely.

At subcritical speeds ($M_o \leqq 0.95$) no significant effects of boundary interference on body pressures were expected, since reference 1 reported essentially zero interference for a nonlifting body in a slotted test section with a ratio of body cross-sectional area to tunnel cross-sectional area of 0.123, and the ratio was only about 0.0014 for the body and test section used in the present investigation. The close agreement expected between the pressure distributions from the slotted test section of the Langley 8-foot transonic tunnel and the various interference-free distributions was realized (figs. 33 (a), 34 (a), 34 (b), and 35), except for discrepancies in the comparisons with free-fall data in the maximum-thickness region of the body (fig. 33 (a)). These descrepancies cannot be readily explained unless the free-fall body, which was three times the size of the wind-tunnel model, differed slightly in shape from the wind-tunnel model and the basic shape in this region. Apparent discrepancies in the comparison with free-fall and theoretical pressure distributions near the base of the body (fig. 33 (a)) are to be expected since the shapes of both the basic body and the free-fall body differed from that of the wind-tunnel model in this region.

At supercritical stream Mach numbers from about 0.95 to 1.00 the agreement of the pressure-distribution measurements from the slotted test section of the Langley 8-foot transonic tunnel with those from the Langley 16-foot transonic tunnel (fig. 34 (b)) and from free-fall tests (fig. 33 (a)) was consistent with the agreement at lower speeds; this agreement attested the essential absence of boundary-interference effects on pressure measurements for the model (cross-sectional area of model only 0.14 percent of tunnel cross-sectional area) in the ⅛-open slotted test section at stream Mach numbers up to 1.00.

At very low supersonic Mach numbers ($M_o \leqq 1.025$) no appreciable effects of boundary-reflected compression waves on model-surface pressures could be detected (figs. 31 (e), 33 (b), 34 (c), and 35) but significant effects of reflected overexpansions were indicated (figs. 34 (c), 35 (b), and 35 (c)). Pressure distributions from the Langley 16-foot transonic tunnel, used as a basis for reference in figures 34 and 35, were not available at Mach number intervals close enough to define completely the variation of the interference-free pressure distribution with Mach number, nor did the data appear to be entirely free of interference effects at a Mach number of 1.019 where overexpansions (apparently due to reflected boundary disturbances similar to those described for the Langley 8-foot transonic tunnel) were indicated (figs. 34 (c) and 35 (f)). The data were sufficient, however, to provide approximate indications of boundary effects on pressure-distribution measurements for the body in the slotted test section of the Langley 8-foot transonic tunnel.

At supersonic Mach numbers slightly greater than 1.025, the effects of reflected compression shocks on model-surface pressures became significant and increased with Mach number. At Mach numbers of and greater than about 1.040, the reflected shocks were visible in schlieren pictures (figs. 31 (g) to 31 (n)) and influenced the model-surface pressures strongly (figs. 33 (b), 34 (c), and 35 (b) to 35 (f)). The model-surface pressures downstream of the region affected by the reflected compression wave were influenced by overexpansions and those upstream of the compression region were free of boundary interference. At $M \geqq 1.120$ the reflected compression was downstream of the model base (fig. 31 (n)) and no boundary interference was apparent (fig. 33 (b)). The agreement at Mach number 1.2 of interference-free pressure distributions from tests of the model in the 92-inch-diameter axisymmetrical closed test section of reference 2 with theoretical and free-fall distributions from reference 4 is consistent with that of the interference-free slotted-test-section data at lower supersonic Mach numbers (fig. 33 (b)). The close agreement of interference-free body-surface distributions from the slotted and closed test sections of the Langley 8-foot transonic tunnel with theoretical distributions (fig. 33 (b)) constitutes an experimental verification of the methods of reference 10 for computing pressure distributions on a slender body of revolution at supersonic speeds.

The maximum effects of boundary-reflected disturbances on surface pressures for the fineness-ratio-12 body of revolution in the Langley 8-foot transonic tunnel at supersonic speeds (fig. 36) were determined from maximum differences between experimental pressure coefficients from the Langley 8-foot and 16-foot transonic tunnels as shown in figure 35. The expansion components of boundary-reflected disturbances for the body tested in the ⅛-open slotted test section of the Langley 8-foot transonic tunnel were shown to affect body-surface pressures more strongly than did the compression components at stream Mach numbers less than 1.035, whereas the reverse was indicated at Mach numbers greater than 1.035. The indications of figure 36 are only approximate, however, because of the limited amount of data available from the Langley 16-foot transonic tunnel.

The effects of boundary-reflected disturbances on pressure distributions for the nonlifting body of revolution at the center line of the slotted test section of the Langley 8-foot transonic tunnel (figs. 33 to 36) were interpreted in terms of effects on body drag coefficients. In ascertaining these effects, the body drag coefficients obtained from pressure-distribution and force tests in the slotted test section of the Langley 8-foot transonic tunnel were compared with essentially interference-free data from free-fall tests (ref. 4) and from pressure-distribution tests in the Langley 16-foot transonic tunnel (slight interference effects present in the latter data measured at $M_o=1.019$ were removed, approximately, before determining the pressure drag). (See fig. 37.) The drag coefficients from pressure-distribution tests were obtained by integrating measured model-surface pressures and included skin-friction drag estimates from reference 11. The force-test body drag coefficients shown in figure 37 were obtained from unpublished experimental data for the model described in reference 12 and were corrected for sting-support tares. Estimated maximum inaccuracies of

the body drag coefficients (based on body frontal area) shown in figure 37 were approximately ± 0.016 for the data obtained from force tests in the Langley 8-foot transonic tunnel and within ± 0.010 for those obtained from free-fall tests.

Approximate boundary-interference effects on body drag measurements for the nonlifting body of revolution at the center line of the Langley 8-foot transonic tunnel slotted test section were taken as the differences between these drag measurements and the interference-free measurements (fig. 37). Correlation of these drag differences (fig. 37) with corresponding body-surface pressure distributions (figs. 33 to 35) revealed the close interrelation of the pressure-distribution and drag measurements and the dependence of the drag-coefficient changes on the effects of boundary-reflected disturbances. The indicated body drag decrements (fig. 37) at Mach numbers from 1.00 to 1.02 were apparently due to the effect of reflected overexpansions slightly upstream of the maximum-thickness region of the body, whereas drag increments at Mach numbers from 1.02 to 1.07 and drag decrements at Mach numbers from 1.07 to about 1.12 were due to the passage over the rear portion of the body of reflected overexpansions and compressions, respectively. At Mach numbers greater than about 1.12 the slight discrepancy between the free-fall data and those from force and pressure-distribution tests in the Langley 8-foot transonic tunnel could be attributed to differences in body shape or to possible inadequacies in sting-support tare corrections, but the magnitude of the indicated discrepancy is within estimated possible inaccuracies in the experimental data. The maximum effects of boundary reflections on body drag coefficients with the body at the slotted-test-section center line did not exceed about 0.04 when coefficients were based on body frontal area. Although these maximum boundary-reflection effects were not much greater than the errors of measurement normally present when the internal balance system is used for measuring model forces, they were considered sufficient to justify a brief experimental investigation of a possible means of reducing the effects.

Reduction of interference effects at supersonic speeds by testing model off center line of slotted test section.—An attempt to reduce the intensity of boundary-reflected disturbances at the model was made by testing the nonlifting body of revolution (fig. 9 (c)) at a distance of about 10.3 inches off the geometric center line of the slotted test section. Body drag coefficients obtained from pressure-distribution measurements with the body located off the test-section center line were affected less by boundary interference than were those obtained from tests of the body at the center line (see fig. 37). This reduction in interference effects on body drag can be attributed to a slight reduction in intensity (and to distribution over a greater axial distance) of boundary-reflected disturbances at the body surface, as shown by the comparison (fig. 38) of center-line and off-center body-surface Mach number distributions at a stream Mach number of 1.050 (this Mach number was used for the comparisons in order that effects of both compression and expansion components of boundary-reflected disturbances might be illustrated). The off-center location of the model appears advantageous with regard to the reduction in intensity of boundary-reflected disturbances, especially the expansion components of such disturbances, and the attendant reduction in interference effects on model drag and pressure-distribution measurements. A disadvantage of the off-center location, however, lies in the significant reduction in length of the region available for strictly interference-free supersonic testing.

Model lengths for interference-free supersonic testing at center line of slotted test section.—It has been shown that at supersonic Mach numbers the model-surface pressures upstream of the region affected by the boundary-reflected compression are free of boundary-interference effects (figs. 33 to 35) and that for a given Mach number the length of the interference-free region is greatest when the model is located at the center line of the test section (fig. 38). The axial distance L_S required for the bow wave ahead of the model to reflect from the test-section boundary and strike the surface of the model at the test-section center line is shown in figure 39. This distance, obtained from schlieren pictures and pressure measurements at stream Mach numbers from 1.04 to 1.126 and from pressure measurements at Mach numbers as low as 1.025, is expressed in terms of the distance L_M required for the reflection of Mach lines from the tunnel wall. The ratio L_S/L_M increased from a value of about 0.35 at a stream Mach number of 1.025 to about 0.81 at a Mach number of about 1.10, after which the ratio remained approximately constant except near a Mach number of 1.109 where it tended to increase slightly and then decrease as the reflected shock approached and moved downstream of the base of the model. This influence of the model tail shock on the progress of the reflected shock past the base of the model is illustrated in figures 31 (*l*) and 31 (m). An L_S/L_M value of 0.815 obtained from tests of a somewhat similar body at a stream Mach number of 1.2 in the closed nozzle of reference 2 was consistent with the ratios shown in figure 39 for Mach numbers greater than about 1.10. At the low supersonic Mach numbers of this investigation, the L_S/L_M ratio was approximately the same for both the axisymmetrical fuselage and the sweptback wing attached to the fuselage.

The distance ratios given in figure 39 neglect the effect of the model boundary layer, which permits the compression due to the incident shock to be transmitted several inches upstream of the shock location, and are therefore not strictly representative of axial distances available for interference-free supersonic testing. If the compression region is assumed to extend about 3 inches upstream of the shock location, the axial distances available for interference-free supersonic testing with the model at the center line of the slotted test section would range from about 4 inches at a Mach number of 1.025 to approximately 36 inches at a Mach number of 1.14 (fig. 40) and would not exceed 75 percent of the axial distance required for the reflection of Mach lines. At the very low supersonic Mach numbers the length of the interference-free test region is influenced to some extent by the location of the detached shock wave ahead of the model.

Location of detached shocks ahead of axisymmetrical nonlifting bodies.—Schlieren and pressure data for the body

of revolution (see fig. 31) and schlieren pictures of shocks ahead of blunt-nose (90° angle) total-pressure tubes (fig. 41) tested in the slotted section of the Langley 8-foot transonic tunnel provided experimental information concerning the location of detached shock waves ahead of axisymmetrical bodies at low-supersonic speeds. The experimental data from the Langley 8-foot transonic tunnel are compared with experimental data from other sources (refs. 4 and 13 to 15) and with approximate theory (ref. 13) in figure 42. The data used in these comparisons are expressed in terms of the ratio of shock distance ahead of the body sonic point to the body radius at the sonic point, x_{SB}/y_{SB}, a parameter used in reference 13. The sonic point for the body of revolution tested in the Langley 8-foot transonic tunnel was obtained from body-surface pressure measurements (average values from a large number of runs) at each test Mach number; the sonic point for the 90° body (total-pressure tube) tested in the Langley 8-foot transonic tunnel was assumed to occur at the shoulder of the body for all Mach numbers.

The experimental locations of the bow waves ahead of the body of revolution in the slotted test section of the Langley 8-foot transonic tunnel agreed closely with experimental data from references 4 and 13 to 15; those for the 90° body in the Langley 8-foot transonic tunnel agreed closely except at stream Mach numbers of 1.015 and 1.036 (fig. 42). The apparent discrepancies offered by these two experimental points are not due to errors in measurement; they are believed to be due to the two-dimensional nature of the bow wave ahead of the row of total-pressure tubes. (Ref. 13 shows that the ratio x_{SB}/y_{SB} is much larger for the two-dimensional case than for the axisymmetrical case.) The single bow wave existing ahead of the row of eight total-pressure tubes at the low-supersonic Mach numbers of 1.015 and 1.036 changes to individual bow waves ahead of each tube at higher Mach numbers (fig. 41).

The general agreement of the experimental data with theoretical approximations (geometric and continuity methods) from reference 13 is considered satisfactory. The experimental data appear to agree more closely with the geometric-method approximations at very low supersonic Mach numbers and with the continuity-method approximations at stream Mach numbers greater than approximately 1.10.

Applicability of boundary-reflection information from present investigation to tests of other models in slotted test section.—Although each wind-tunnel test model offers a different problem with regard to the effects of boundary-reflected disturbances, the results of the body-of-revolution tests reported earlier in this paper should prove useful in predicting disturbance phenomena and evaluating experimental data for other models.

For strictly interference-free supersonic testing the model length is dependent on the axial distance required for model disturbances to reflect from the test-section boundary back to the model surface; this distance varies with Mach number and is greatest when the model is located at the test-section center line. The shock-reflection distances shown in figure 39 and the interference-free model lengths given in figure 40 are applicable only for center-line testing of models of approximately the size and shape of the body of revolution used in this investigation; larger models of this shape or bluff bodies of the same maximum diameter will produce bow waves located farther upstream and thereby reduce the reflection distances and model lengths shown in figures 39 and 40, respectively. The approximate interference-free model length for a given axially symmetric shape can be estimated by use of figures 39 and 42, together with knowledge of the sonic-point location and the model radius at the sonic point. At very low supersonic Mach numbers the use of figure 42 to ascertain detached-shock locations ahead of axially symmetric bodies is limited to single bodies; several adjacent axially symmetric bodies located in the same plane of measurement may produce detached shocks located considerably upstream of the shock for a single body (see figs. 41 and 42).

For supersonic testing of models whose lengths permit the impingement of boundary-reflected disturbances, the effects of boundary interference on the free-air characteristics of the models are dependent on the model configurations and the model locations with respect to the test-section center line (interference effects are less for model off center line than for one on center line). The effects of boundary reflections on pressure and drag measurements for the fineness-ratio-12 body of revolution used in the present investigation are applicable only for models of approximately the same size and shape, but the described flow phenomena with the body of revolution in the slotted test section should be useful in interpreting the direction of boundary-reflection effects on test data for other models. The influence of model-attitude changes on indicated boundary-reflection effects for the body of revolution was not included in the present investigation, but approximate influences may be inferred from experimental results given in reference 16. Reference 16 also indicates that flow disturbances capable of introducing drag-coefficient changes of approximately 0.002 (drag coefficient based on wing plan-form area) may not greatly affect the lift and pitching-moment characteristics of a complete airplane model. Additional studies are needed to verify and supplement these preliminary indications of boundary-reflection effects on models at lifting attitudes in the slotted test section.

GENERAL DISCUSSION

The theory of the subsonic operation of the slotted test section has been presented in reference 1. It is of interest to consider in a qualitative manner some features of the supersonic operation. As pointed out in reference 17, the supersonic flow in a tunnel with porous walls is established by expansion through the walls. In a slotted tunnel a similar expansion must occur through the slots, but this expansion must be influenced by the boundary layer on the panels. In fact, a general knowledge of the behavior of boundary layers indicates that in the expansion the boundary layer tends to run off the panels into the slots. The effects of the slots must thus be extended over the whole periphery of the tunnel. It therefore seems that the slotted tunnel would behave more like a porous-wall tunnel than might at first be supposed. The role of the slots in controlling the expansion has already been noted.

The development of the supersonic flow in the slotted test section will now be considered in detail. At subsonic

speeds the pressure in the test chamber evidently must take a value which is some weighted average of the pressures at the slots. Moreover, in accordance with the equation of motion, as the pressures in the diffuser (including that at the diffuser entrance) are decreased, the speed in the tunnel must increase until a Mach number of 1.0 is reached at the effective minimum section, section B-B in figure 1. Consider first the case of a wall divergence of 45 minutes. With the first attainment of a Mach number of 1.0 at the minimum section, the Mach number in the slotted test section has been found to be also essentially 1.0, as is shown for a different divergence angle in figure 13; but on the curved surfaces of the panels (fig. 3 (a)) supersonic regions terminated by shocks resulting from the higher pressures in the slots must already have appeared in conformance with general flow theory. The flow within the slotted test section is thus not absolutely uniform, but consists of slightly supersonic regions terminated by shocks, which are in turn followed by slightly subsonic regions. This flow pattern can be repeated several times because in any subsonic region the pressure may be greater than that in the chamber surrounding the slots. Equalization of the pressure through the slots thus accelerates the flow, and if the panel is curved in that region or if a change in shape occurs, the flow may again become supersonic.

When the pressure at the diffuser entrance is decreased (by increasing the rotational speed of the tunnel fan) below that just necessary to produce a Mach number of 1.0 at the throat, the pressure decrease cannot be transmitted upstream through the supersonic regions in the slotted test section. This pressure decrease is, however, transmitted out through the slots in the region just upstream of the diffuser entrance. The pressure in the surrounding chamber is thus decreased and, as a result of the reaction through the upstream part of the slots, the flow in the subsonic regions is further accelerated, the shocks are moved downstream, and the supersonic regions are expanded.

This movement of the shocks downstream has been noted in schlieren observations. If the curvature and divergence of the panels are small, only a small decrease of pressure below that required for the establishment of a Mach number of 1.0 at the throat is sufficient to sweep the shocks out of the test section. In such a case one shock only may exist. With the configuration of figure 3 (a), this shock is located slightly downstream from the discontinuity in slope at the 125.6-inch station. It is evidenced in figure 6 by a rather sudden decrease in Mach number to values less than 1.0, which occurs between the 130- and 140-inch stations. At this position the shock extends across the whole central part of the flow. In all of the upstream slotted test section the stream Mach number is then greater than 1.0. At the upstream end the boundary layer flows out, so that the stream is allowed to expand, as it must do if the Mach number is to increase from the value of unity at the throat to some greater value somewhat downstream. This outward flow must evidently be balanced by an equivalent rate of mass flow into the slots near their downstream ends. Perhaps because of induced velocities due to flow through the slots, the pressures (indicated by Mach numbers in fig. 6) near the slot edges are less than those near the center of a panel, and the test chamber pressure lies generally between these two extremes.

Except for the improvement in control of the expansions obtainable by means of the slots, which has already been mentioned, the manner of operation of the slotted test section with 5-minute divergence is similar to that with 45-minute divergence. However, because with the 5-minute divergence the curved region of the panels is located at the downstream end, the shocks must first form at that end, leaving the upstream end essentially shock free, even at Mach numbers near unity. An indication of this freedom from shock disturbances was afforded by limited schlieren observations and is indicated in the Mach number distributions (figs. 13 to 20). With the 5-minute divergence of the panels the shock-disturbed Mach number range near unity is thus eliminated, and uniform test section Mach numbers continuously variable through 1.0 are possible.

The conditions at the downstream end of the slotted section will now be considered. In this region, for the configurations discussed in this report, the air flow which has been extruded from the upstream part of the slots must be taken back into the tunnel stream. Because of the turbulent mixing with the air in the chamber surrounding the slots, this extruded air has lost most of its kinetic energy; but once this air has reentered the slots, it is again accelerated by mixing with the main stream. This mixing process is believed to be accelerated by vorticity generated by inflow over the slot edges.

The mixing is known to be an inefficient process and must in any case entail a power loss; but even greater power losses may occur if, because of the intake of this low-energy air, the diffuser flow is spoiled. Conditions are necessarily particularly critical near the diffuser entrance, both because of the inflow of the low-energy air and because in this region the kinetic energy of the main stream is large. Because of the mixing (ejector principle) some diffusion would occur in this region even if the expansion angle of the diffuser were zero. Indeed, the mixing is so strong that, as may be seen from figures 13 to 20, the diffusion starts even slightly upstream of the diffuser entrance noses.

Because of space limitations the original expansion angle at the upstream end of the diffuser was made greater than was considered desirable, and when the panels were reversed this angle was increased still more, to 3°45′, as shown in figure 3 (b). In the region of the diffuser entrance noses the effective expansion is somewhat less than this value because the upper surfaces of the noses fall outside the panel surfaces (fig. 3). At some sacrifice of test-section length, nose shape B (fig. 4 (b)), which extended farther upstream, furnished a short region of essentially constant effective cross-sectional area at the beginning of the diffuser. Such a length of essentially constant or only slightly varying diffuser area is believed to be desirable in order to provide a mixing region without too great diffusion, but no investigations have been conducted to determine the proper length or divergence of such a region for minimum power.

The need for a length of diffuser with small or zero expansion near the diffuser entrance is accentuated by the presence of the shock. In reference 2 it was shown that in

such a region the boundary layer behind a shock terminating the test region at a Mach number of 1.2 recovered rapidly without separation. In a diverging channel, on the other hand, such a shock might easily lead to separation. The shocks indicated at the diffuser entrance in figures 13 to 20 appear to be oblique rather than normal shocks, since the greater disturbance occurs at the center and that at the wall is spread out and does not decrease the indicated Mach number below unity. The use of a region of zero expansion at the diffuser entrance should spread these disturbances still farther and may very well effect their practical elimination.

The shock at the diffuser entrance is similar to one which might exist ahead of a nose inlet. Because the high-speed flow is limited to a jet, however, it should be possible to draw the shock down into the diffuser, but in this case the power required would almost certainly be greater than if the shock were close to the diffuser entrance. The most favorable configuration, for minimum power, is believed to be that for which the shock stands just inside an essentially zero-divergence region at the diffuser entrance or has been practically eliminated in the mixing region.

The minimum diffuser entrance cross-sectional area constitutes, in effect, a second throat. If this second throat is too small the flow will be choked and the Mach number attainable will be limited. Because of the thick boundary layer formed by the inflow through the slots, the required area of the second throat is greater than would be necessary for a closed nozzle with the same size of first minimum. With increase in supersonic Mach number the required area of the second throat increases on account of both the increase in entropy through the shocks and the increasing flow through the slots. With the configuration of figure 3 (b), a diffuser minimum area 13 percent greater than the first throat area was sufficient to permit the attainment of a Mach number of 1.14. With the reduction in slot area and the provision of an essentially constant-area mixing region provided by nose B, the required area at the second minimum was reduced to a value 9 percent greater than that at the first. Because of the thick boundary layer, choking is not sharp at the second minimum; but after a Mach number of 1.0 has been reached in the main stream, the volume flow can still be increased by acceleration of the boundary layer, though the cost in power rapidly becomes excessive.

Because of the larger minimum diffuser area required for the supersonic flow, the diffuser entrance area is greater than that required for the subsonic flow. Since the flow attaches to the diffuser entrance noses, diffusion, and consequently negative Mach number gradient, occurs upstream from the noses. This effect was sufficiently severe in the case of nose shape B to require the provision of flaps which, when open, permitted the entrained flow to pass over the noses and thus prevented attachment of the main flow. Moreover, inasmuch as the diffuser entrance area affects the diffusion, physical considerations would suggest that the power required is also affected. Tests carried out in the Langley 24-inch tunnel have shown this to be the case. An increase of the diffuser minimum cross section appreciably beyond the size necessary for the required Mach number results in an increase in the power required. An increase in noise and vibration is also believed to be likely. It is suggested that, in any future slotted tunnel installation similar to that discussed herein, the effective diffuser entrance area be made adjustable by means of radially adjustable diffuser entrance noses.

It was thought that the heavy boundary layer due to the inflow into the slots might spoil the diffuser, but an extensive investigation by means of tufts failed to reveal any separation, though separation may have existed on the diffuser entrance noses. Because of the large amount of kinetic energy in that region, the possibility of significant power loss is greater near the diffuser entrance than farther downstream.

An examination of power data for varying slot area showed that, as might be expected, the power required for a given Mach number decreases as the slot area decreases. Power consumption is therefore also less if the diffuser entrance nose is as far upstream as possible. This effect may be expected to become relatively less important as the Mach number is increased, because the increasing required outflow through the upstream part of the slots and the corresponding inflow at the downstream ends is only weakly dependent on the slot area. It also appears likely that with increasing inflow of this low-energy air the essentially constant-area mixing region required for its acceleration might have to be increased in order to avoid spoiling the diffuser flow. Economy of power might indeed, at higher Mach numbers, require that this low-energy air be pumped to approximately stream total pressure by means of a separate compressor rather than by means of turbulent mixing in the diffuser. The use of a separate compressor, however, might affect the use of the tank pressure as a reference pressure for determining Mach number.

The power absorption per square foot of throat area in the Langley 8-foot transonic tunnel is shown in figure 43. These data were taken from a number of different runs, as indicated in the figure. The power data have been adjusted to the same stagnation pressure and temperatures through the assumption that, for constant geometry and Mach number, power is proportional to $p_t\sqrt{T_t}$, where p_t is the stagnation pressure and T_t is the absolute value of the stagnation temperature. The power for the slotted tunnel is compared with that for the Langley 8-foot transonic tunnel with slots closed, that for the plaster nozzle of reference 2, and that for a closed-tunnel estimate based on reference 18. The reduction in power due to the installation of diffuser entrance nose B (fig. 4 (b)) is seen from a comparison of the power for this nose with that for nose A (fig. 4 (a)). A more detailed investigation of the power losses is given in reference 3.

CONCLUDING REMARKS

The Langley 8-foot high-speed tunnel was converted to transonic operation and the characteristics of the transonic flow in the slotted test section were investigated. The results of flow surveys with various slot shapes, and with and without a typical model in the slotted test section, warrant the following conclusions:

1. As a result of the investigation of the flow characteristics of the tunnel with various slot shapes, a configuration

which produced nearly uniform supersonic flow has been devised.

2. With this configuration the Mach number was continuously variable up to the greatest value, approximately 1.14, permitted by the power available; the quality of the flow was entirely satisfactory for testing purposes and compared favorably with that in the best two-dimensional solid supersonic nozzles. Deviations from the average stream Mach number in a model test region 36 inches long and 30 inches in diameter generally increased with Mach number but did not exceed approximately 0.006 at stream Mach numbers up to 1.13, provided the tunnel wall surfaces were kept sufficiently smooth.

3. The Mach number distribution was found to be affected by the detailed slot shape if the divergence angle between the panels and the center line of the test section was sufficiently small.

4. The power required at a given Mach number was considerably in excess of that necessary for a closed tunnel at the same Mach number.

5. The ratio of the test-chamber pressure to the stream total pressure provided a reliable index of the test-section Mach number independent of model configuration or attitude.

6. The direction of the airstream agreed within the limits of experimental error (0.1°) with the geometric center line of the test section.

7. The use of slots to reduce choking limitations at stream Mach numbers near 1.0, reported earlier for small tunnels, was substantiated by tests of a 3.33-inch-diameter body of revolution in the approximately 88-inch-diameter slotted test section.

8. Interference effects due to boundary-reflected disturbances were present in pressure-distribution and drag measurements for a 33.5-inch-long nonlifting body of revolution with a fineness ratio of 12 in the slotted test section at low supersonic speeds; the effects were reduced by testing the body off the test-section center line in order to avoid focusing of the reflected disturbance waves. No boundary interference was present at the higher supersonic speeds attained.

9. The model length for interference-free supersonic testing increased with Mach number but did not exceed about 75 percent of the axial distance required for reflection of Mach lines.

10. Experimental locations of bow waves ahead of axially symmetric bodies were in satisfactory agreement with theoretical locations predicted by the approximate methods of NACA TN 1921.

11. An experimental verification of the method of NACA TN 1768 for predicting pressure distributions over slender bodies of revolution at supersonic speeds is afforded by the close agreement of theoretical pressure distributions for a fineness-ratio-12 body of revolution with interference-free distributions measured in the Langley 8-foot transonic tunnel.

Langley Aeronautical Laboratory,
National Advisory Committee for Aeronautics,
Langley Field, Va., *July 3, 1958.*

REFERENCES

1. Wright, Ray H., and Ward, Vernon G.: NACA Transonic Wind-Tunnel Test Sections. NACA Rep. 1231, 1955. (Supersedes NACA RM L8J06.)
2. Ritchie, Virgil S., Wright, Ray H., and Tulin, Marshall P.: An 8-Foot Axisymmetrical Fixed Nozzle for Subsonic Mach Numbers up to 0.99 and for a Supersonic Mach Number of 1.2. NACA RM L50A03a, 1950.
3. Whitcomb, Richard T., Carmel, Melvin M., and Morgan, Francis G., Jr.: An Investigation of the Stream-Tube Power Losses and an Improvement of the Diffuser-Entrance Nose in the Langley 8-Foot Transonic Tunnel. NACA RM L52E20, 1952.
4. Thompson, Jim Rogers: Measurements of the Drag and Pressure Distribution on a Body of Revolution Throughout Transition From Subsonic to Supersonic Speeds. NACA RM L9J27, 1950.
5. Loving, Donald L., and Estabrooks, Bruce B.: Transonic-Wing Investigation in the Langley 8-Foot High-Speed Tunnel at High Subsonic Mach Numbers and at a Mach Number of 1.2—Analysis of Pressure Distribution of Wing-Fuselage Configuration Having a Wing of 45° Sweepback, Aspect Ratio 4, Taper Ratio 0.6, and NACA 65A006 Airfoil Section. NACA RM L51F07, 1951.
6. Ward, Vernon G., Whitcomb, Charles F., and Pearson, Merwin D.: An NACA Transonic Test Section With Tapered Slots Tested at Mach Numbers to 1.26. NACA RM L50B14, 1950.
7. Staff of the Computing Section, Center of Analysis (Under Direction of Zdeněk Kopal): Tables of Supersonic Flow Around Cones. Tech. Rep. No. 1 (NOrd Contract No. 9169), M.I.T., 1947.
8. Neice, Mary M.: Tables and Charts of Flow Parameters Across Oblique Shocks. NACA TN 1673, 1948.
9. Herriot, John G.: Blockage Corrections for Three-Dimensional-Flow Closed-Throat Wind Tunnels, With Consideration of the Effect of Compressibility. NACA Rep. 995, 1950. (Supersedes NACA RM A7B28.)
10. Thompson, Jim Rogers: A Rapid Graphical Method for Computing the Pressure Distribution at Supersonic Speeds on a Slender Arbitrary Body of Revolution. NACA TN 1768, 1949.
11. Young, A. D.: The Calculation of the Total and Skin Friction Drags of Bodies of Revolution at Zero Incidence. R. & M. No. 1874, British A.R.C., 1939.
12. Osborne, Robert S.: A Transonic-Wing Investigation in the Langley 8-Foot High-Speed Tunnel at High Subsonic Mach Numbers and at a Mach Number of 1.2—Wing-Fuselage Configuration Having a Wing of 45° Sweepback, Aspect Ratio 4, Taper Ratio 0.6, and NACA 65A006 Airfoil Section. NACA RM L50H08, 1950.
13. Moeckel, W. E.: Approximate Method for Predicting Form and Location of Detached Shock Waves Ahead of Plane or Axially Symmetric Bodies. NACA TN 1921, 1949.
14. Heberle, Juergen W., Wood, George P., and Gooderum, Paul B.: Data on Shape and Location of Detached Shock Waves on Cones and Spheres. NACA TN 2000, 1950.
15. Laitone, Edmund V., and Pardee, Otway O'M.: Location of Detached Shock Wave in Front of a Body Moving at Supersonic Speeds. NACA RM A7B10, 1947.
16. Ritchie, Virgil S.: Effects of Certain Flow Nonuniformities on Lift, Drag, and Pitching Moment for a Transonic-Airplane Model Investigated at a Mach Number of 1.2 in a Nozzle of Circular Cross Section. NACA RM L9E20a, 1949.
17. Nelson, William J., and Klevatt, Paul L.: Preliminary Investigation of Constant-Geometry, Variable Mach Number, Supersonic Tunnel With Porous Walls. NACA RM L50B01, 1950.
18. Goethert, Bernhard: Power Requirements and Maximum Reynolds Number in Transonic Wind Tunnels Having a Maximum Mach Number of 2.0. AAF TR No. 5564, Air Materiel Command, Army Air Forces, Mar. 25, 1947.

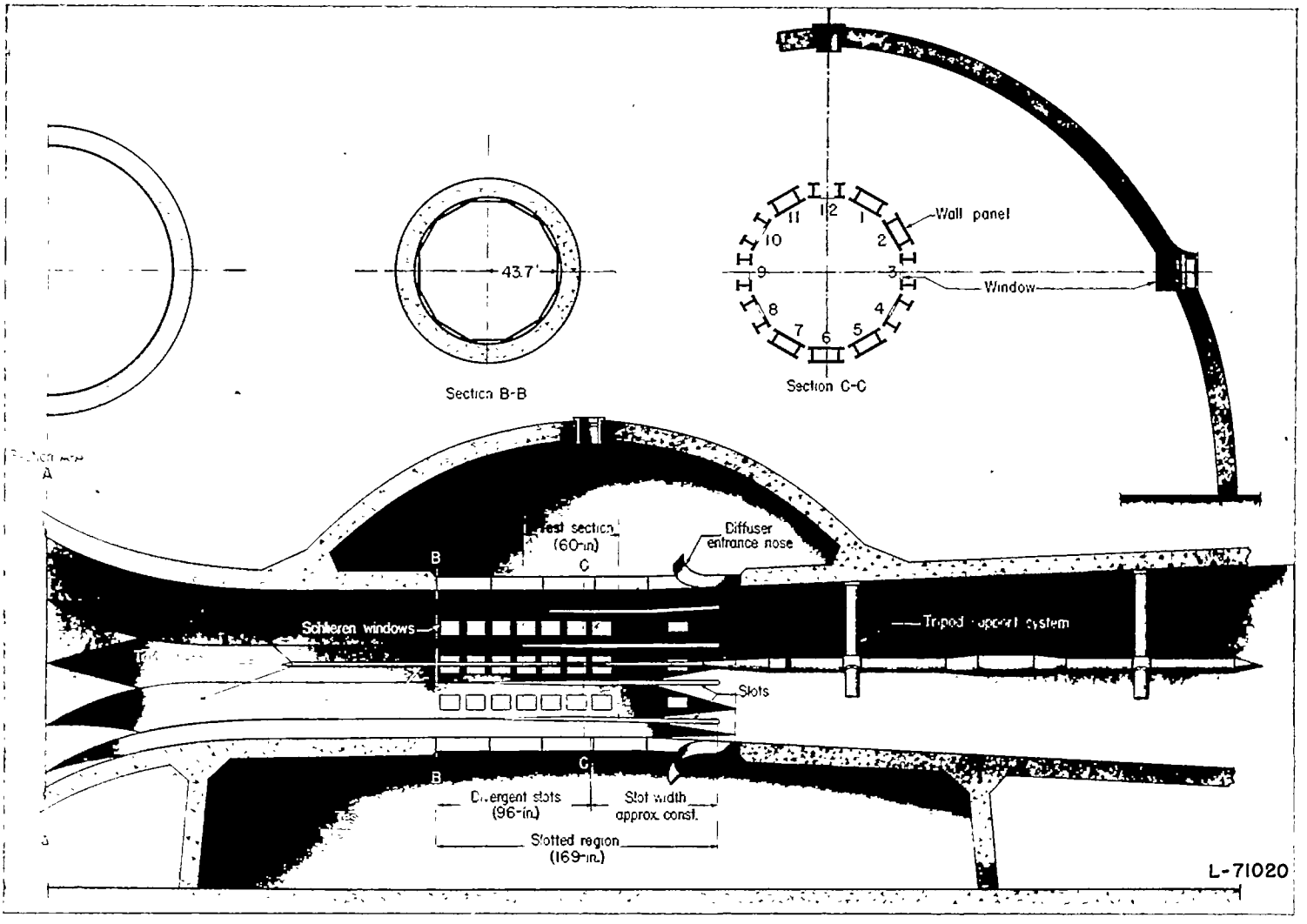

FIGURE 1.—Views of throat region of Langley 8-foot transonic tunnel showing slotted test section, cylindrical survey tube, and support system.

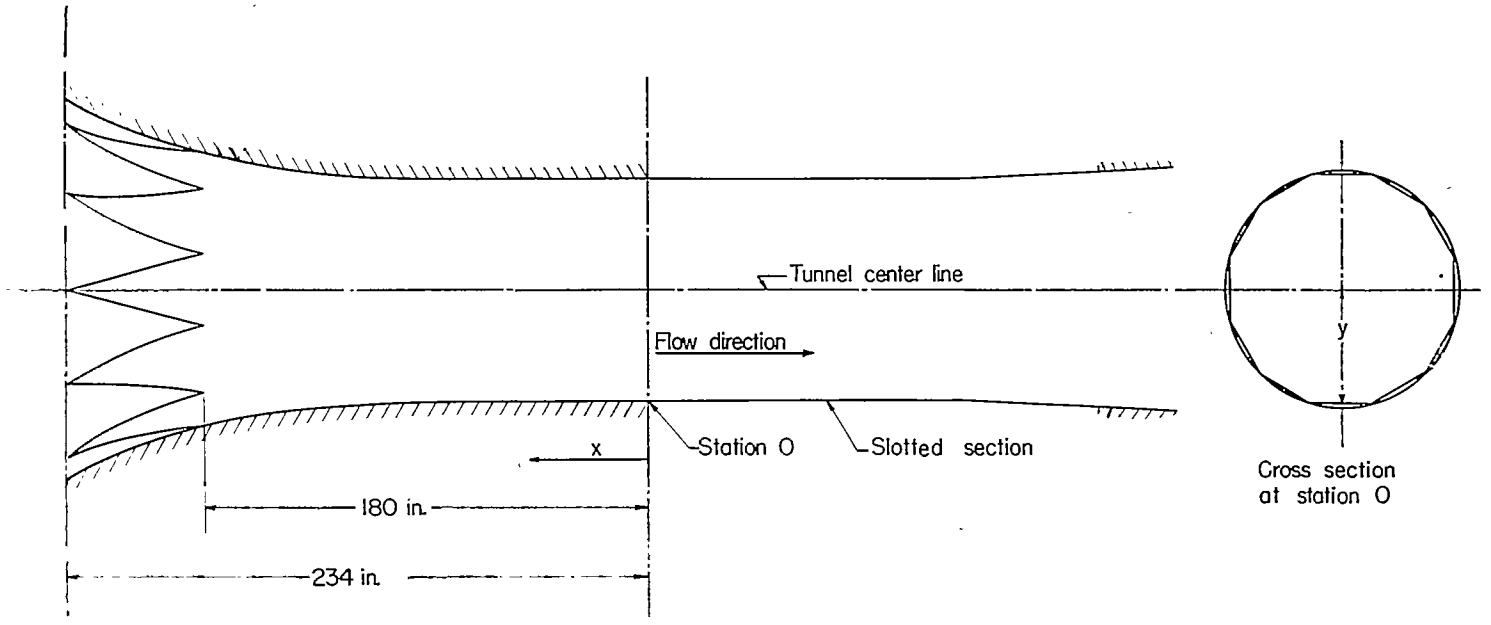

x (in.)	y (in.)	x (in.)	y (in.)	x (in.)	y (in.)	x (in.)	y (in.)
0	43.700	24	43.668	48	43.685	140	47.593
2	43.697	26	43.666	50	43.692	150	48.882
4	43.694	28	43.665	55	43.715	160	50.459
6	43.691	30	43.664	60	43.748	170	52.365
8	43.688	32	43.663	65	43.793	180	54.641
10	43.685	34	43.663	70	43.851	190	57.333
12	43.682	36	43.664	80	44.018	200	60.488
14	43.679	38	43.665	90	44.266	210	64.480
16	43.677	40	43.667	100	44.618	220	69.200
18	43.674	42	43.670	110	45.099	228	73.680
20	43.672	44	43.674	120	45.735	230	74.860
22	43.670	46	43.679	130	46.555	234	77.188

x=Distance upstream of station O
y=Distance from tunnel center line to center of panel

FIGURE 2.—Coordinates of approach to slotted region of tunnel throat.

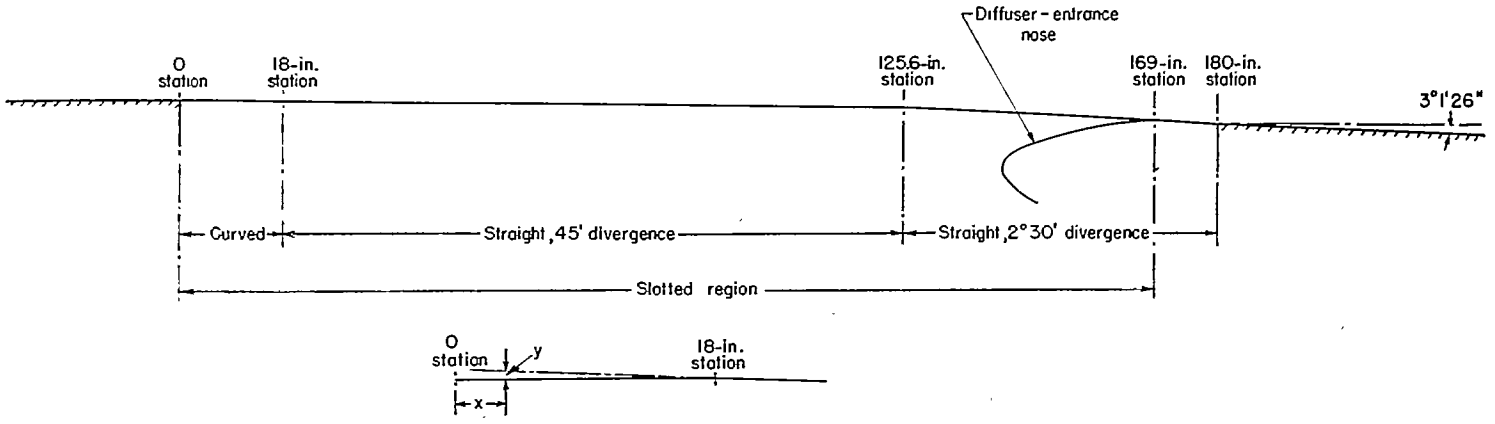

Coordinates of curved region

x (in)	y (in)
0	0.105
2	.083
4	.064
6	.047
8	.033
10	.020
12	.012
14	.006
16	.001
18	0

(a)

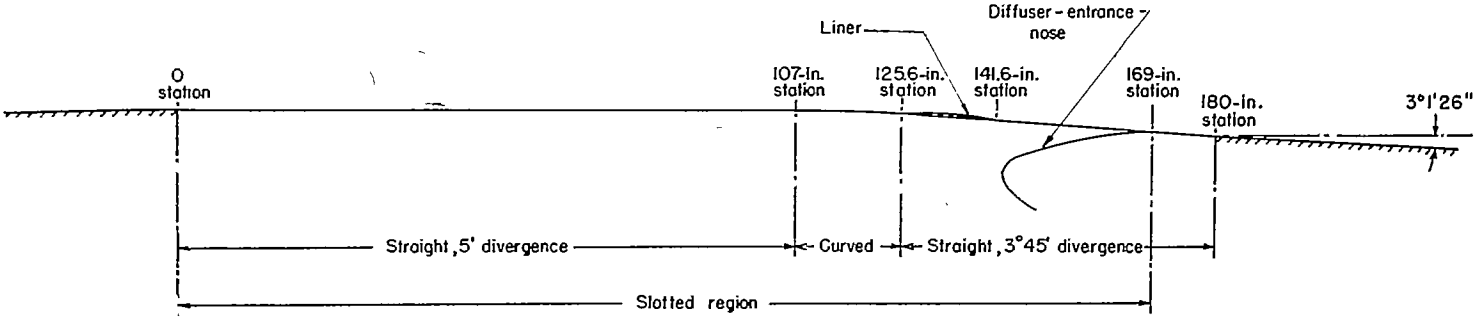

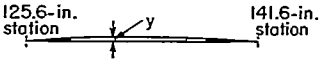

Coordinates for liner

x (in)	y (in)
125.6	0
128.0	.0132
130.0	.204
132.0	.242
134.0	.250
136.0	.240
138.0	.200
141.6	.030

(b)

(a) Original wall-panel arrangement with 45-minute divergence in test section.
(b) Reversed wall panels with 5-minute divergence in test section.

FIGURE 3.—Tunnel throat geometry including diffuser-entrance nose shape and wall divergence

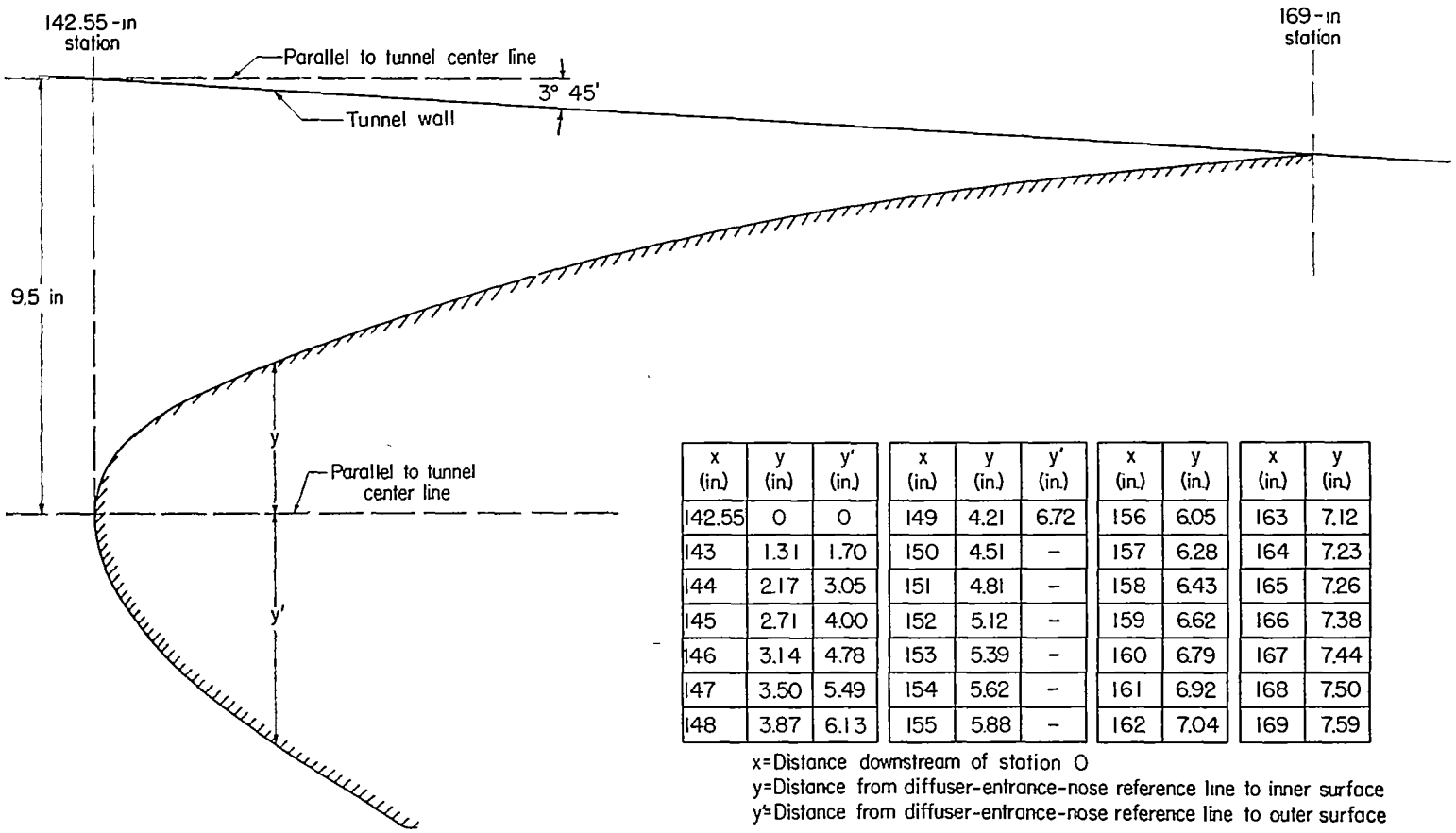

x (in.)	y (in.)	y' (in.)	x (in.)	y (in.)	y' (in.)	x (in.)	y (in.)	x (in.)	y (in.)
142.55	0	0	149	4.21	6.72	156	6.05	163	7.12
143	1.31	1.70	150	4.51	–	157	6.28	164	7.23
144	2.17	3.05	151	4.81	–	158	6.43	165	7.26
145	2.71	4.00	152	5.12	–	159	6.62	166	7.38
146	3.14	4.78	153	5.39	–	160	6.79	167	7.44
147	3.50	5.49	154	5.62	–	161	6.92	168	7.50
148	3.87	6.13	155	5.88	–	162	7.04	169	7.59

x=Distance downstream of station 0
y=Distance from diffuser-entrance-nose reference line to inner surface
y'=Distance from diffuser-entrance-nose reference line to outer surface

(a) Shape A.

FIGURE 4.—Coordinates of diffuser-entrance nose shapes.

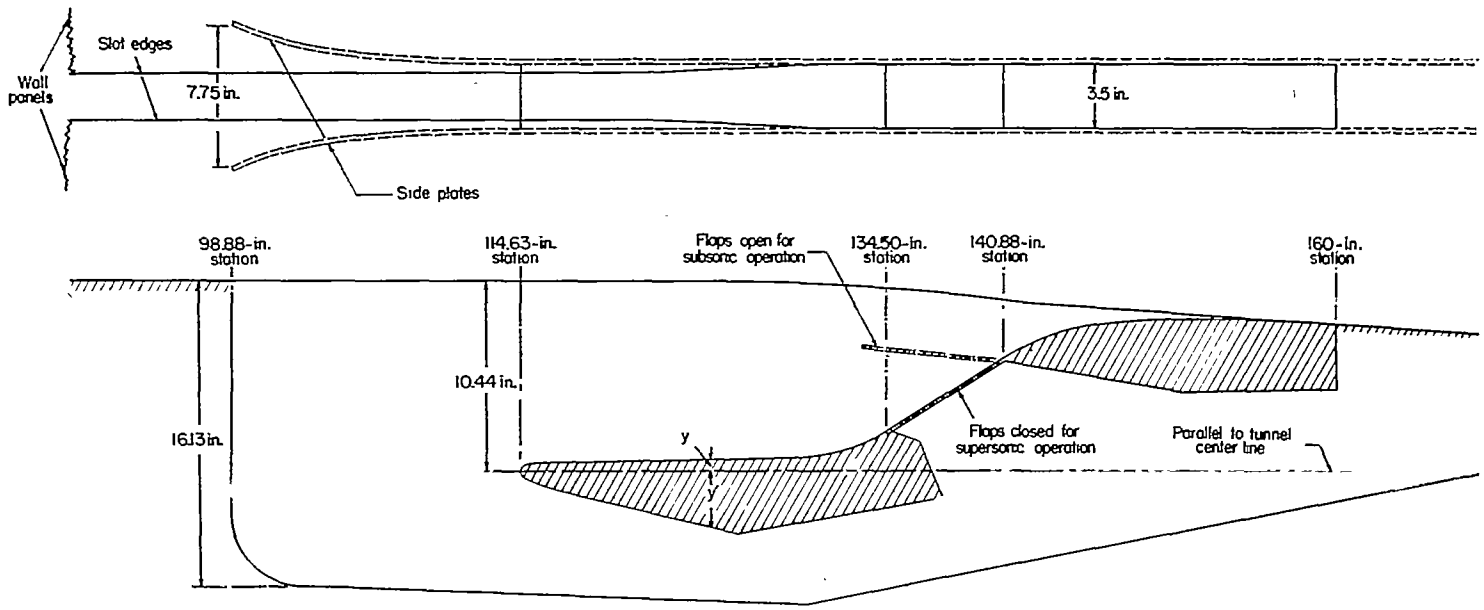

x (in.)	y (in.)	y' (in.)	x (in.)	y (in.)	y' (in.)	x (in.)	y (in.)
114.63	0	0	126	.65	3.33	146	800
115	.42	.47	128	.71	3.82	148	820
115.50	.47	.67	130	.82	–	150	829
116	.48	.85	132	1.07	–	152	831
118	.52	1.36	134.50	2.12	–	154	830
120	.55	1.86	140.88	6.30	–	156	828
122	.59	2.33	142	6.66	–	158	815
124	.62	2.83	144	7.58	–	160	803

x = Distance downstream of station 0
y = Distance from diffuser-entrance-nose reference line to inner surface
y' = Distance from diffuser-entrance-nose reference line to outer surface

(b) Shape B.

FIGURE 4.—Concluded.

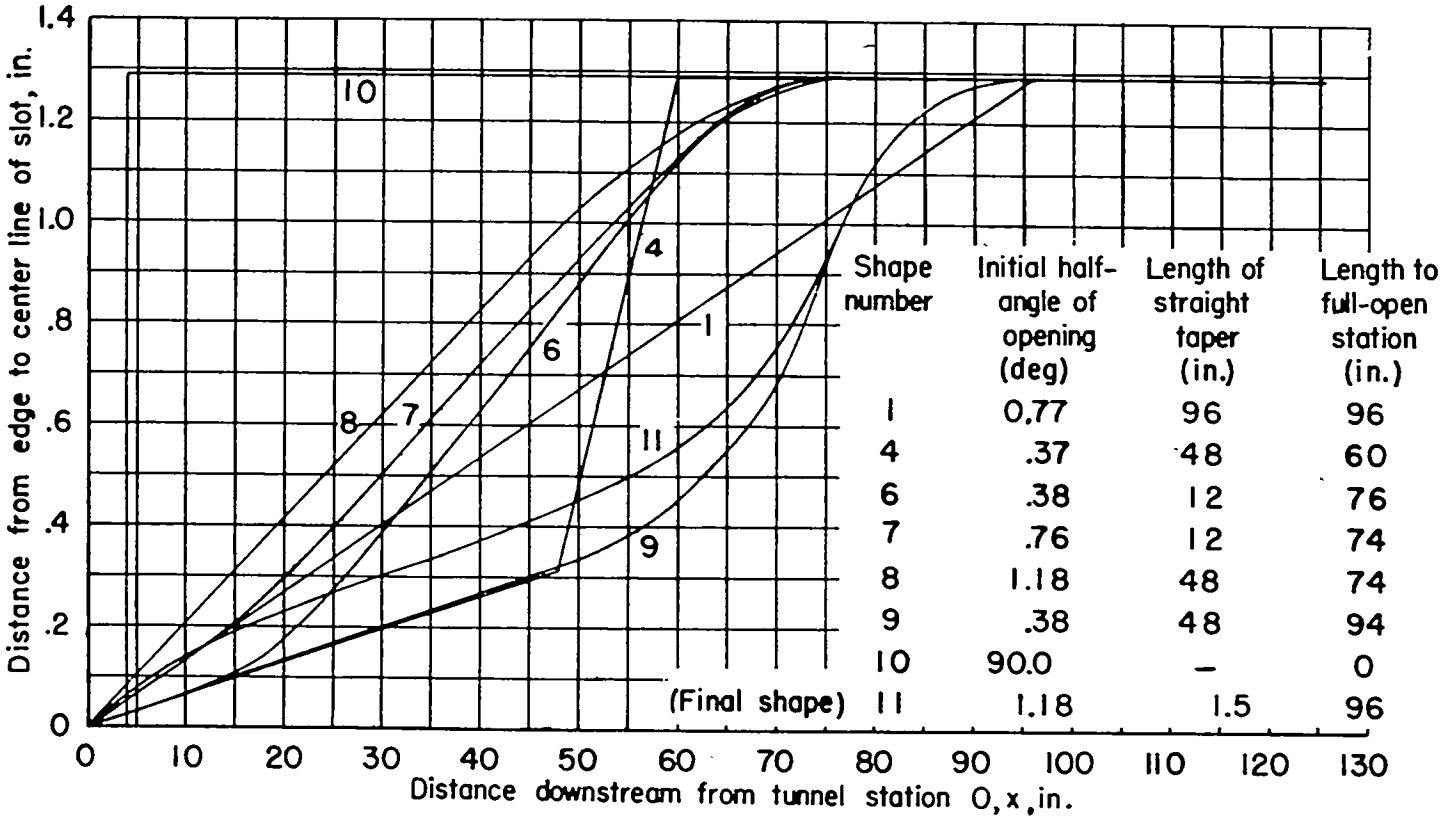

FIGURE 5.—Various slot shapes investigated in the Langley 8-foot high-speed tunnel with 5-minute wall-panel divergence in test section.

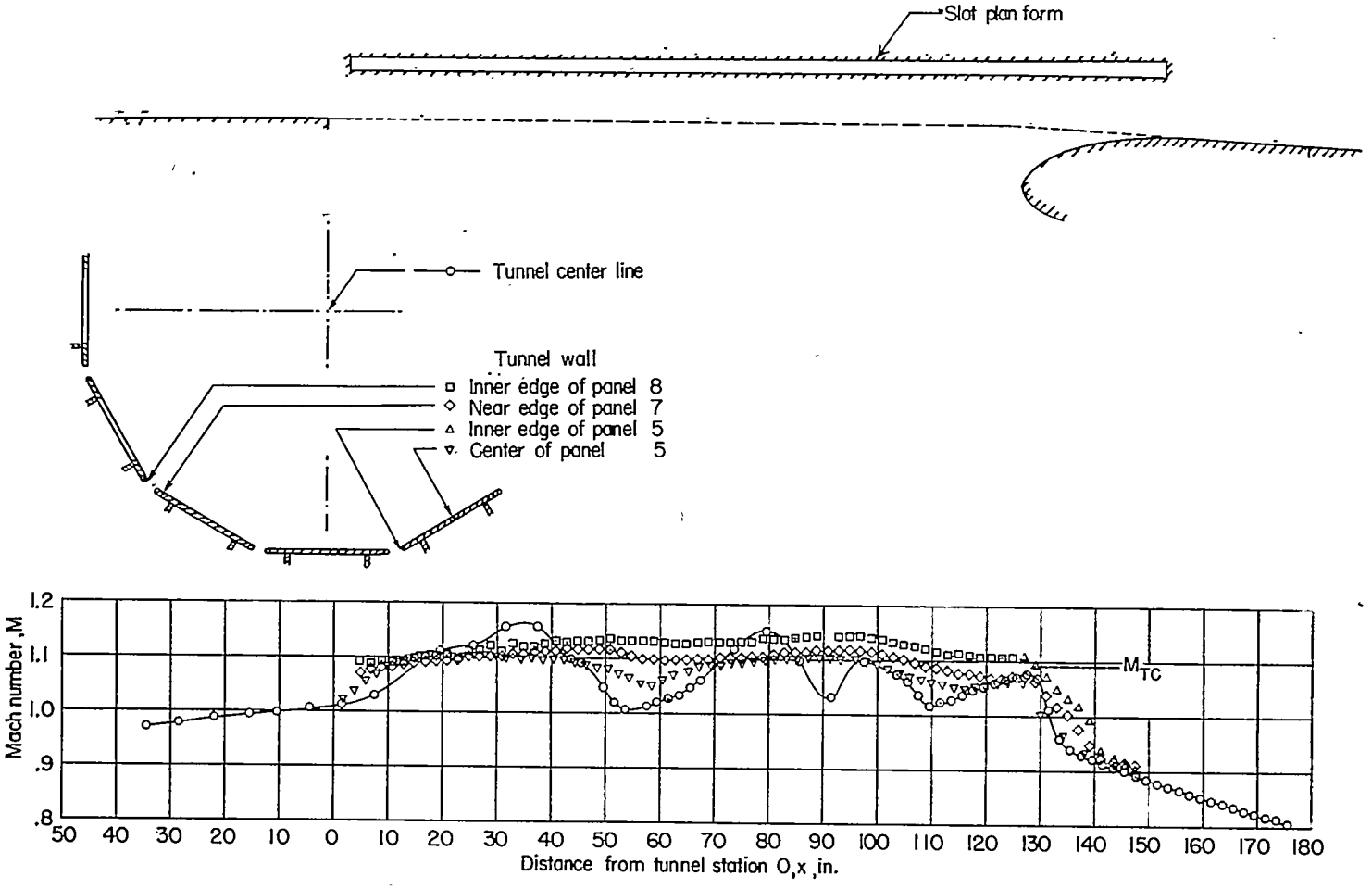

FIGURE 6.—Comparison of Mach number distributions measured axially along tunnel center line with those measured along center and edges of wall panels. Nose A; slot shape 10 (rectangular); 45-minute divergence of wall panels in test section; $M_{TC}=1.092$.

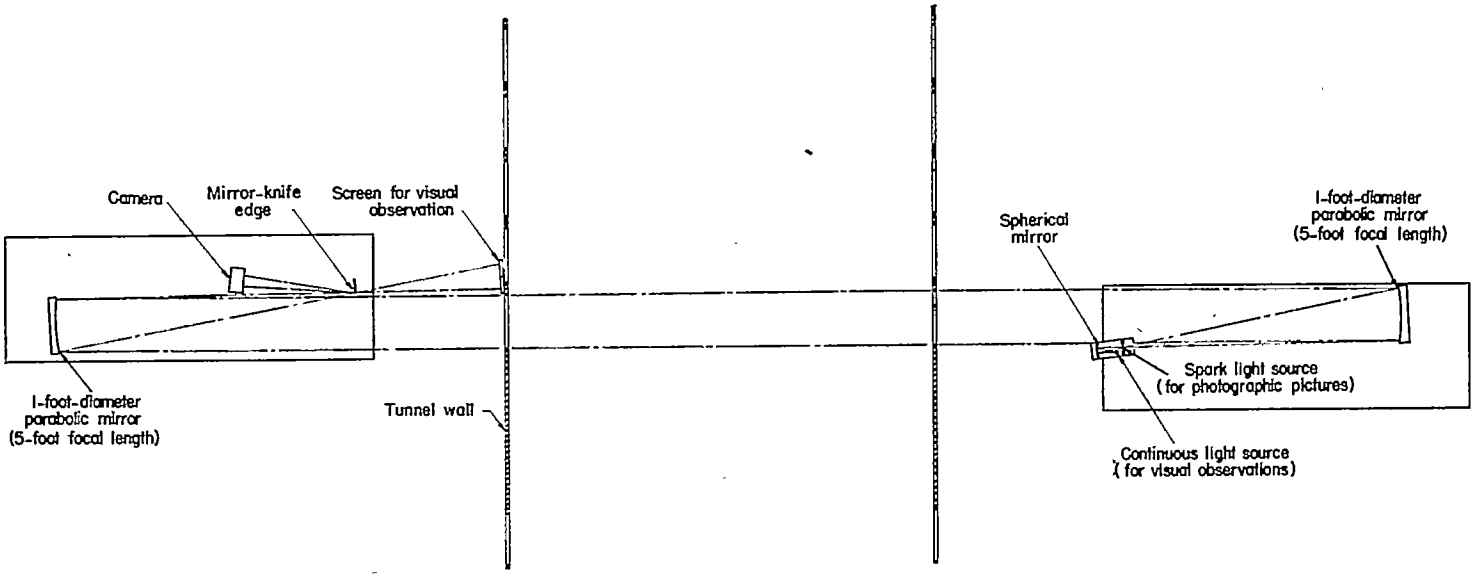

FIGURE 7.—Temporary schlieren system used in connection with slotted-test-section flow surveys.

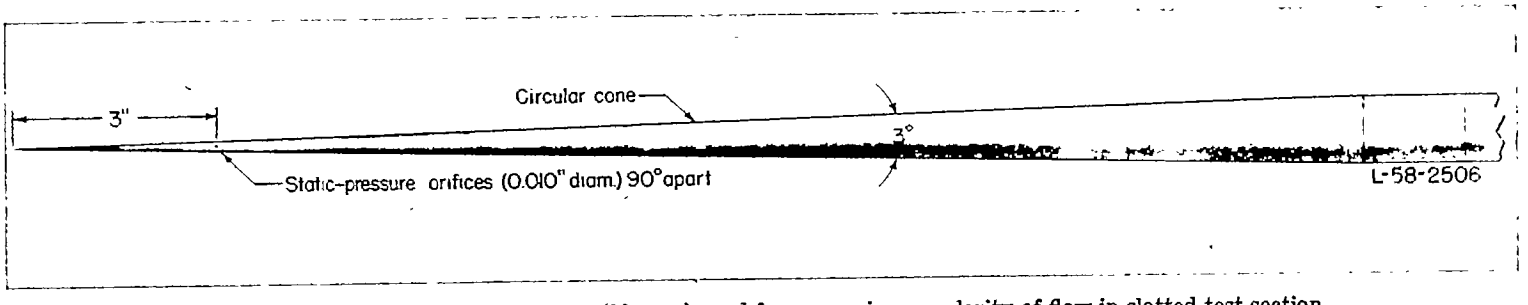

FIGURE 8.—Null-pressure-type instrument (3° cone) used for measuring angularity of flow in slotted test section.

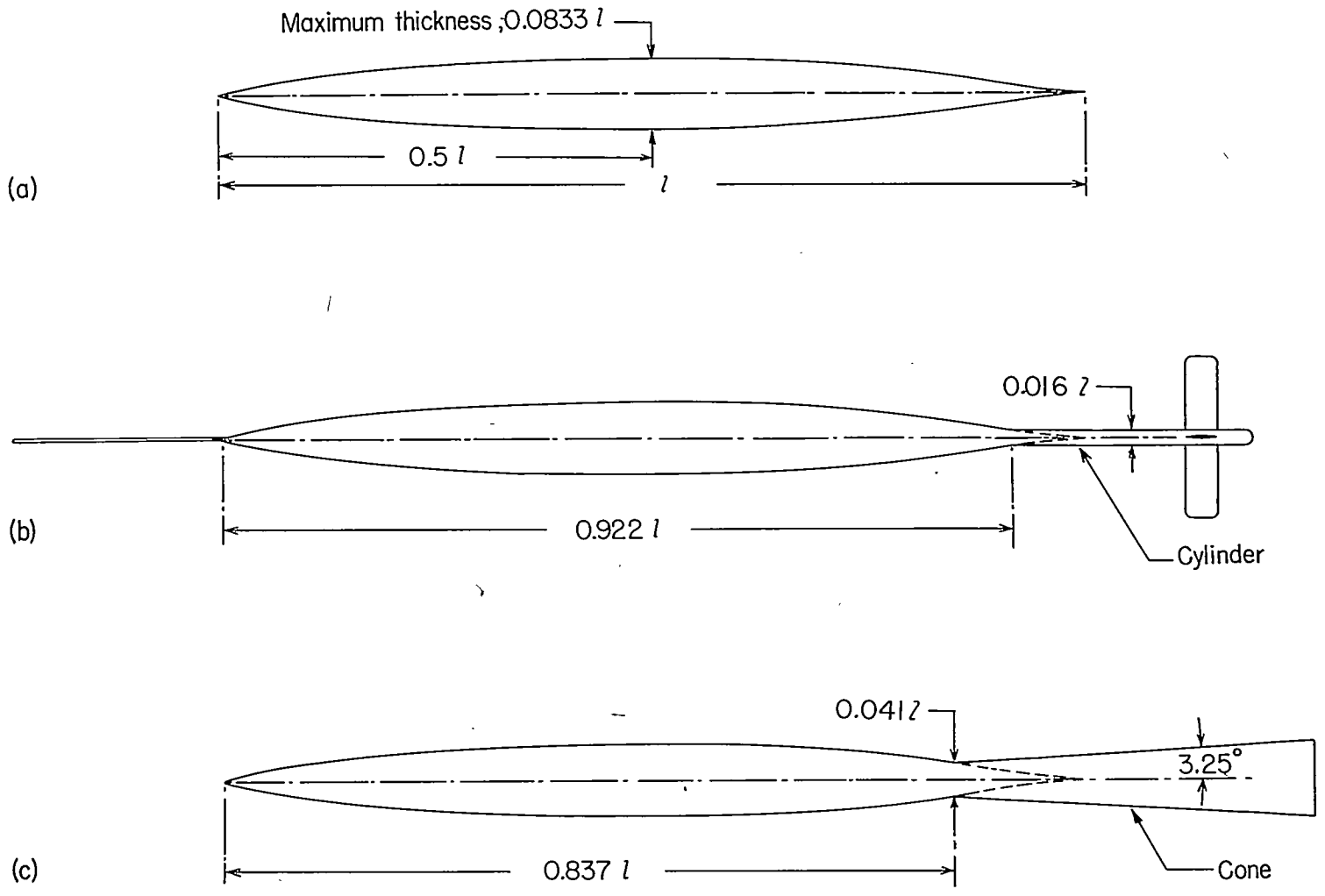

(a) Basic body shape.
(b) Free-fall body.
(c) Wind-tunnel model.

FIGURE 9.—Body of revolution used for comparison of body-surface pressure distributions obtained from wind-tunnel tests with those from free-fall tests and theory.

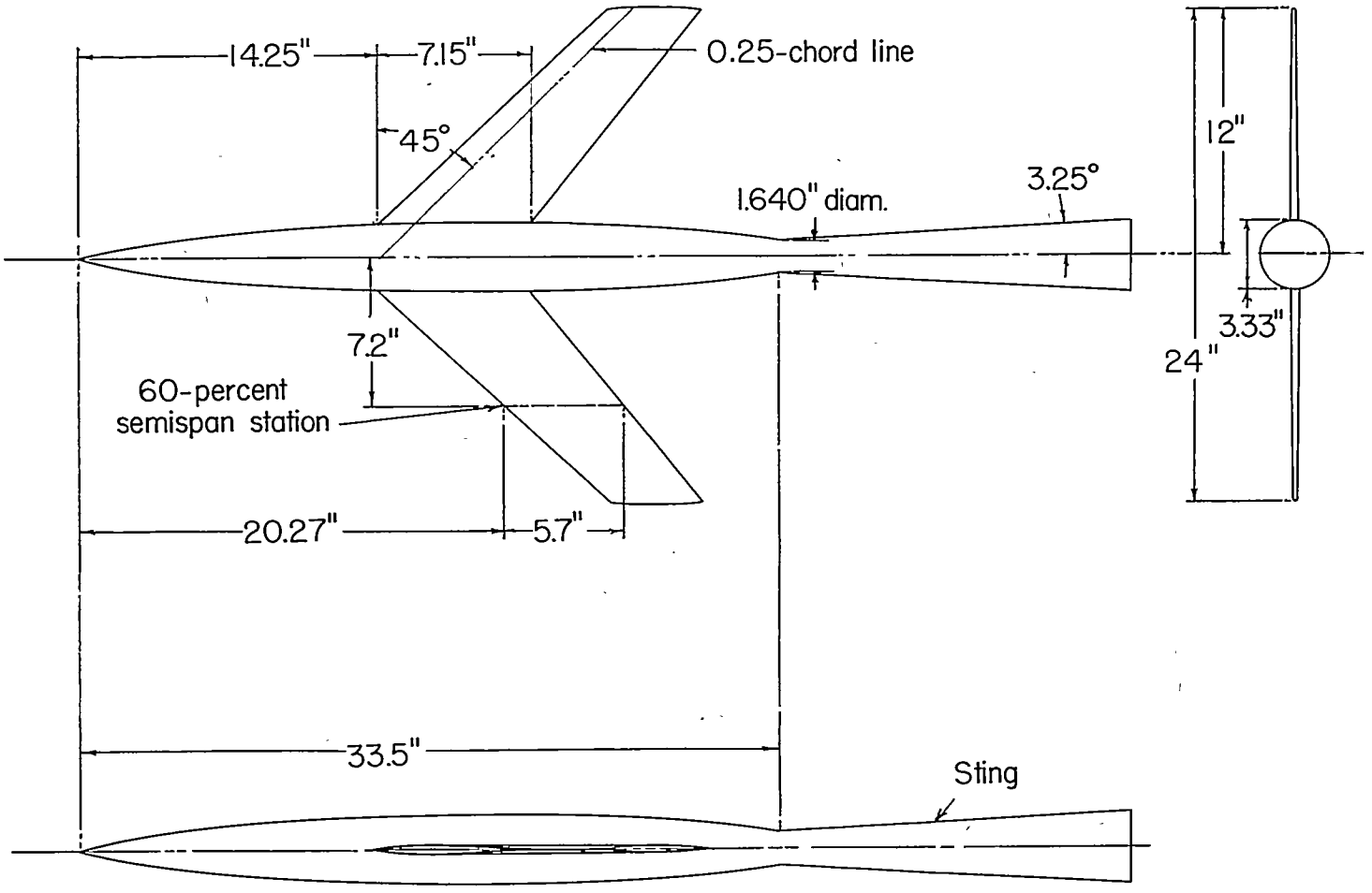

FIGURE 10.—Transonic-airplane model investigated in connection with flow surveys in slotted test section.

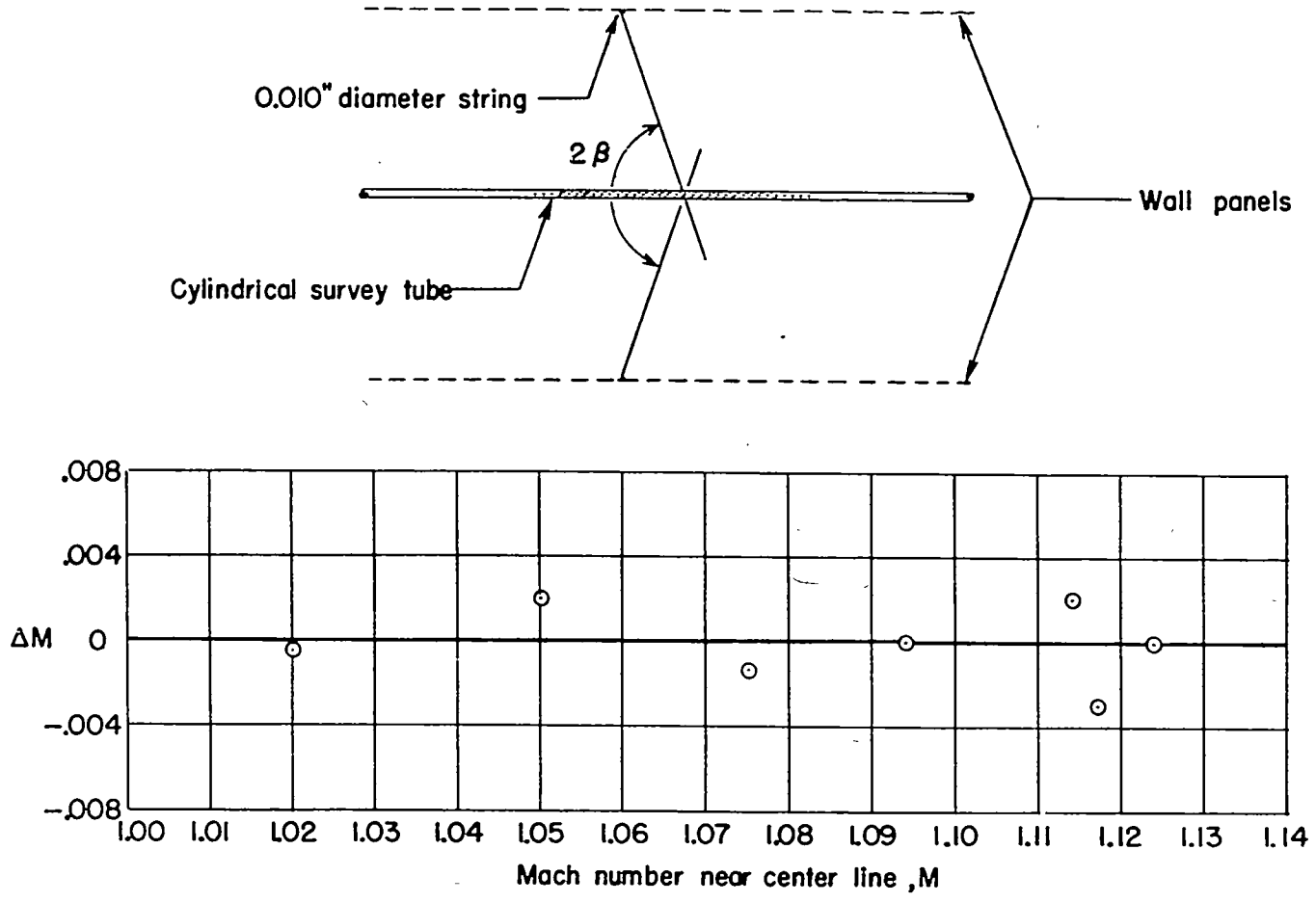

FIGURE 11.—Agreement of flow Mach numbers obtained from pressure measurements at test-section center line with those indicated by measured angularity of weak shocks produced by 0.010-inch-diameter strings fastened to wall panels. ΔM is the Mach number from pressure measurements minus the Mach number indicated by shock angles.

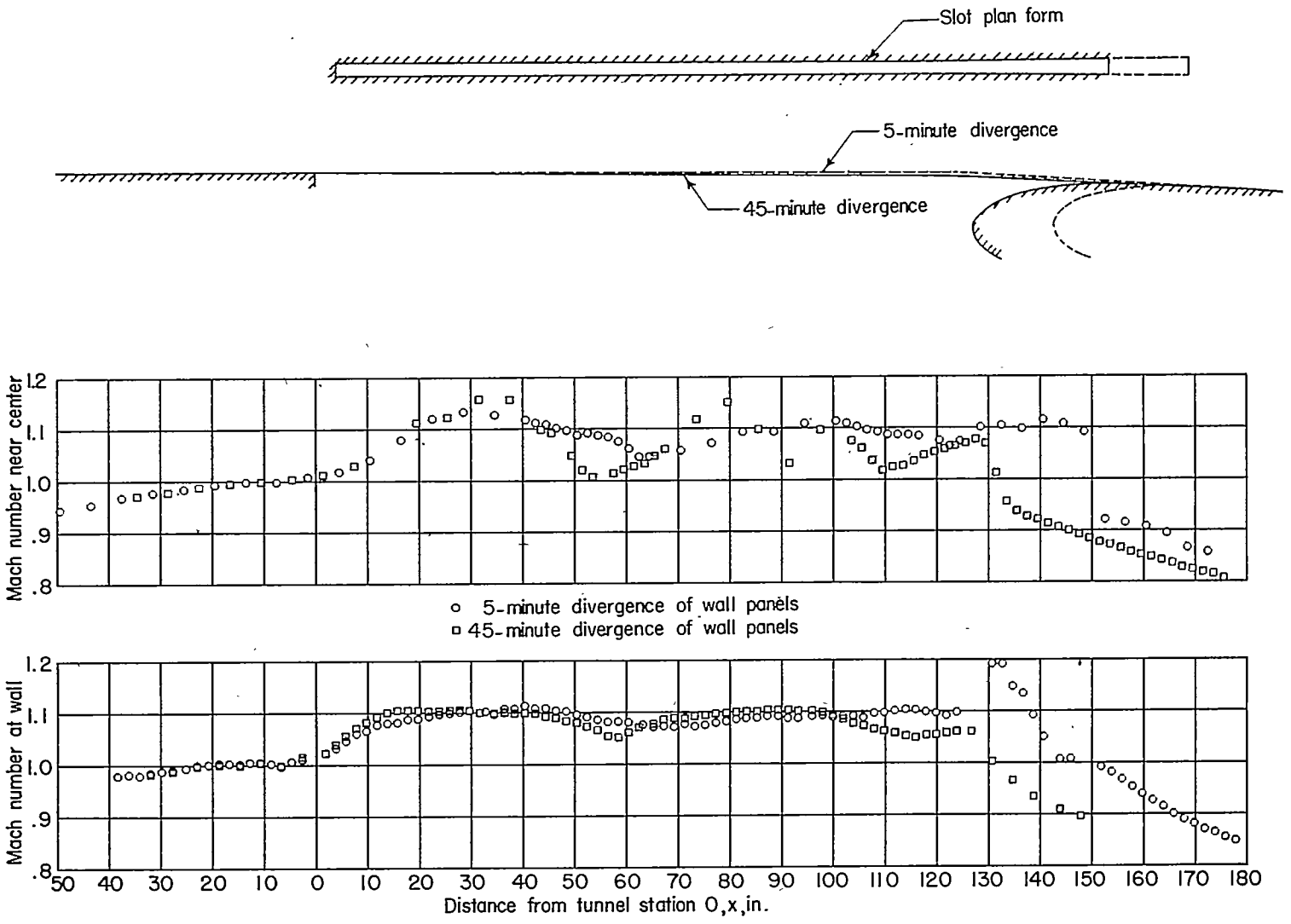

FIGURE 12.—Comparison of Mach number distributions axially along center line and wall of the slotted throat with 5-minute and 45-minute divergence of test-section wall panels. Slot shape 10; $M_{TC}=1.093$.

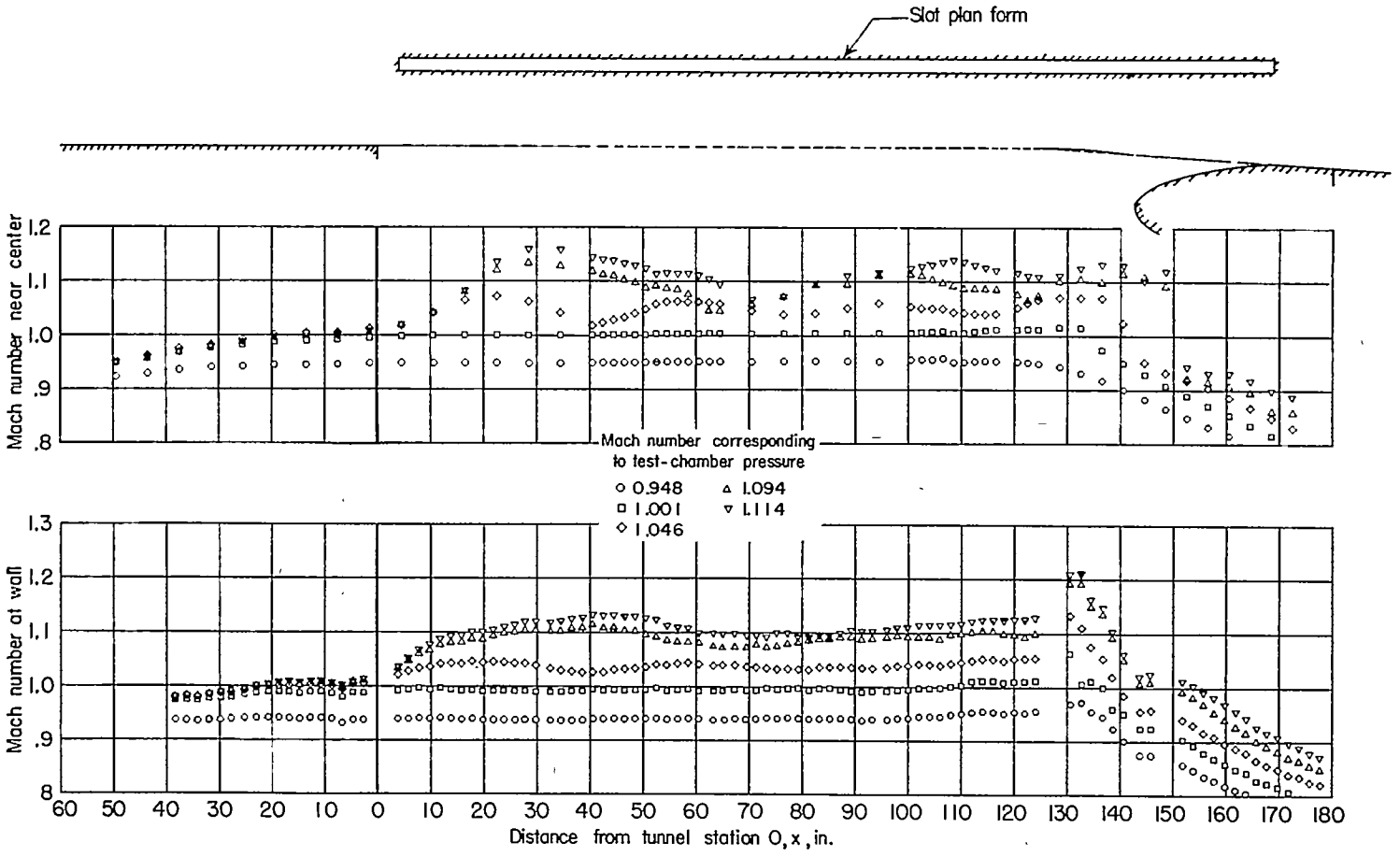

FIGURE 13.—Mach number distributions axially along center line and wall of the slotted throat with 5-minute divergence of test-section wall panels. Slot shape 10.

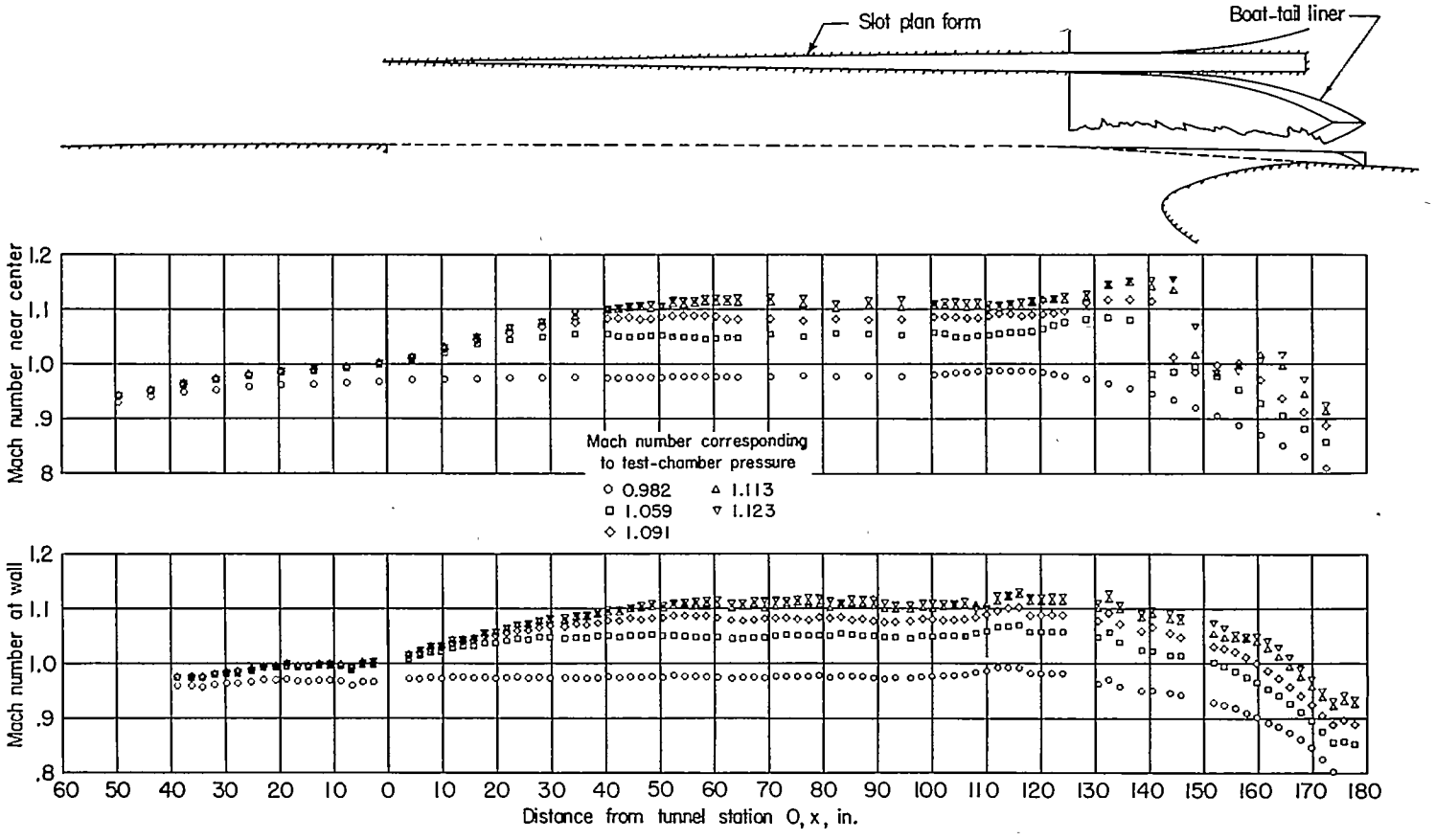

FIGURE 14.—Mach number distributions axially along center line and wall of the slotted throat with 5-minute divergence of test-section wall panels. Slot shape 1.

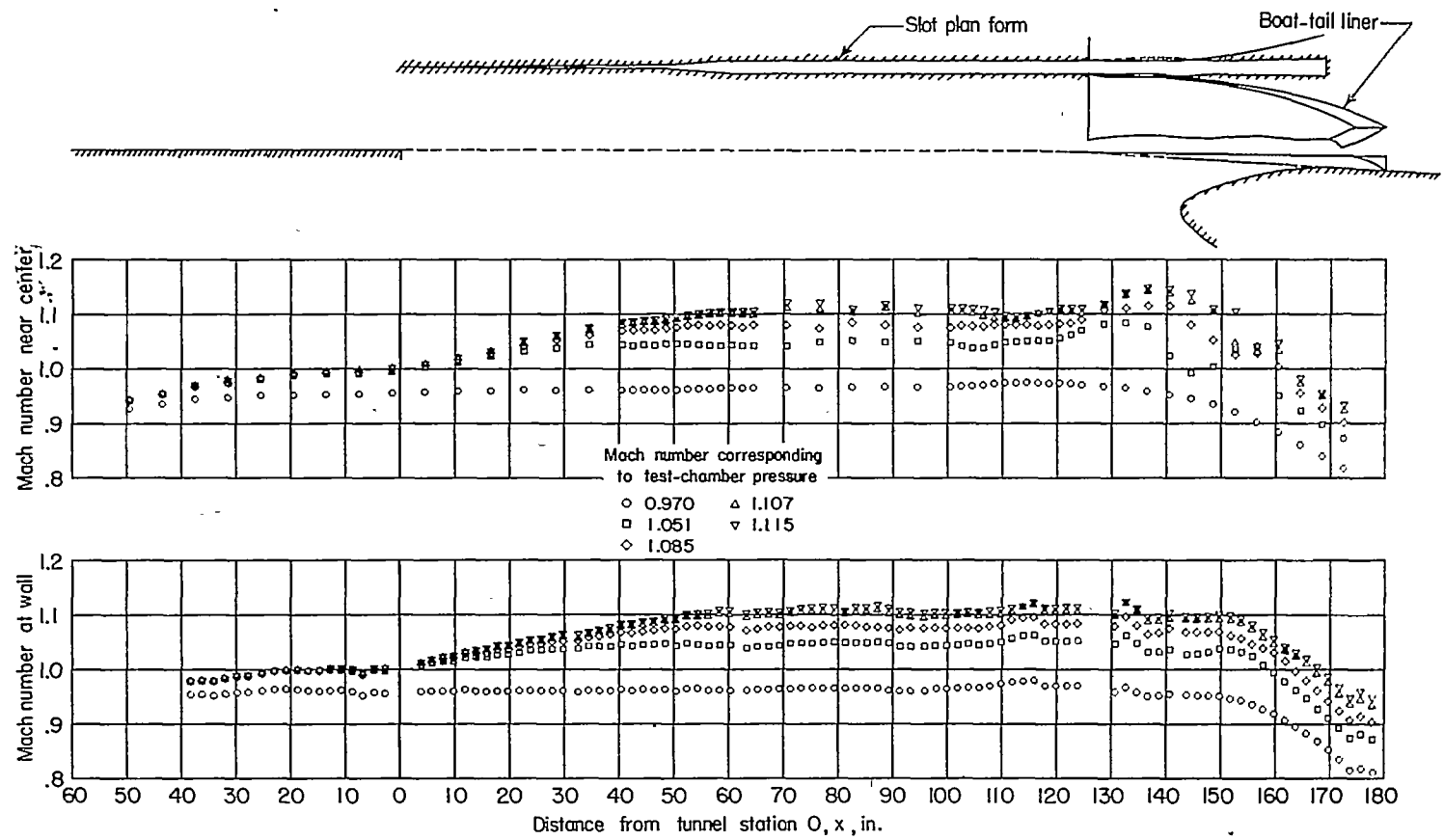

FIGURE 15.—Mach number distributions axially along center line and wall of the slotted throat with 5-minute divergence of test-section wall panels. Slot shape 4.

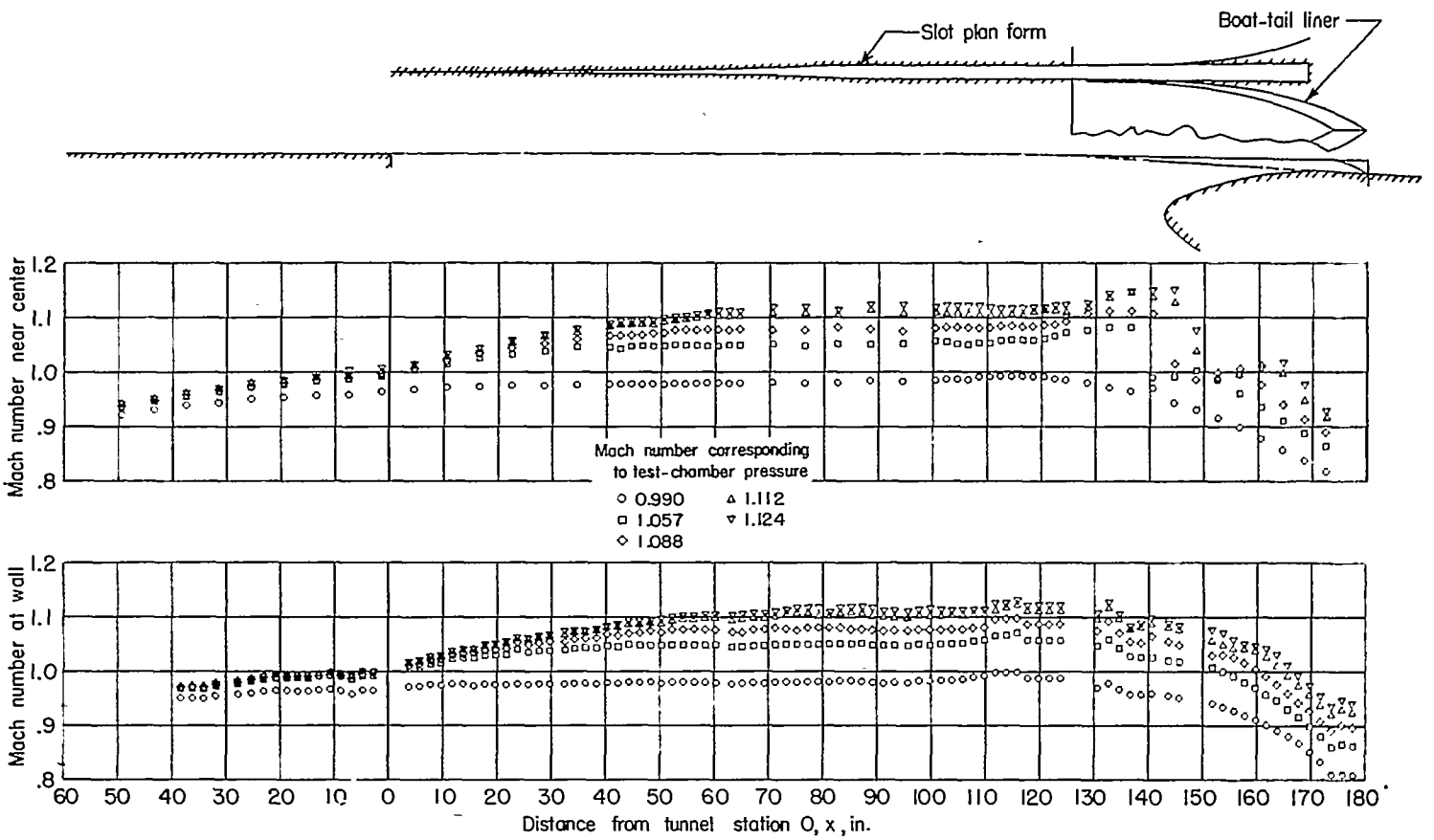

FIGURE 16.—Mach number distributions axially along center line and wall of the slotted throat with 5-minute divergence of test-section wall panels. Slot shape 9.

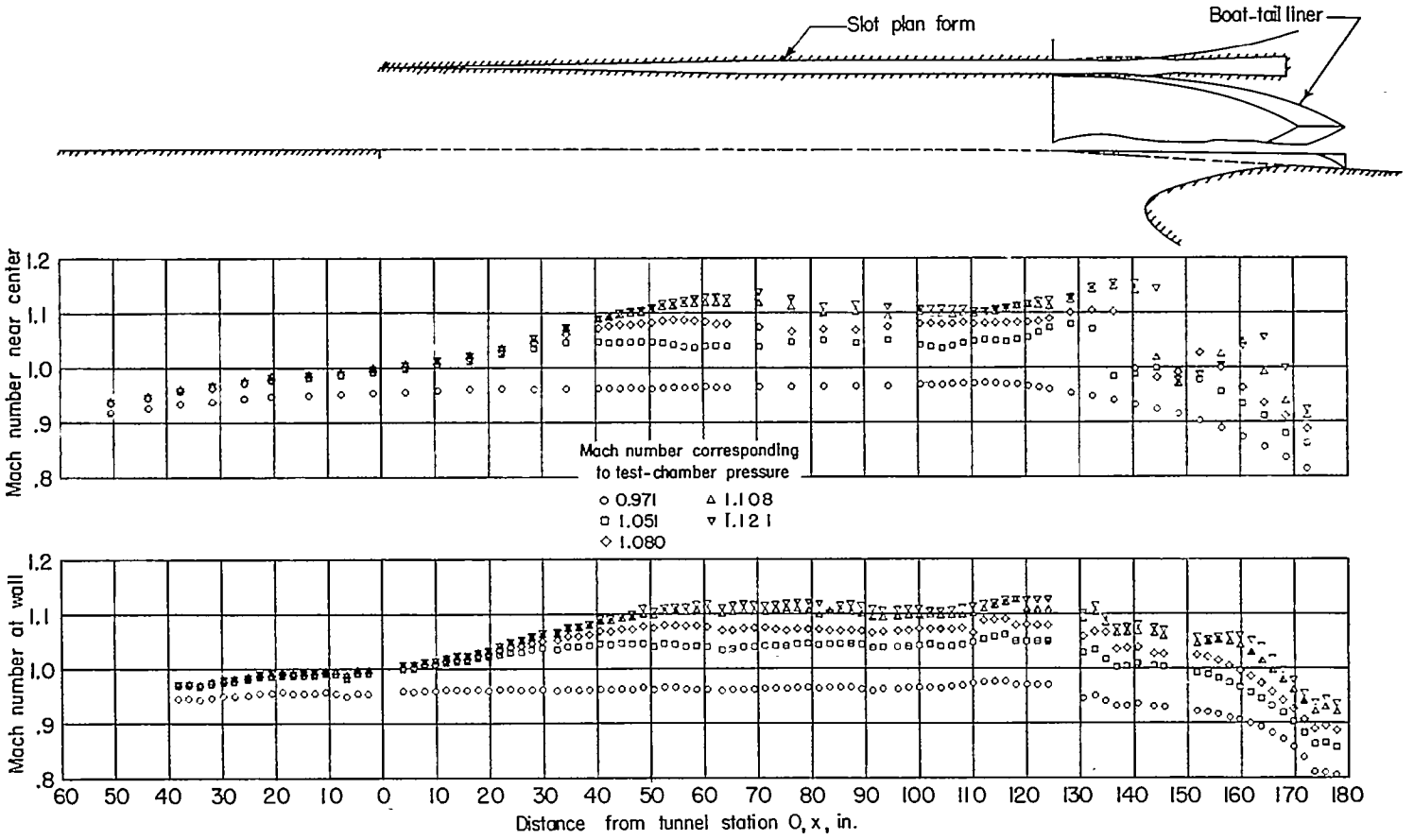

FIGURE 17.—Mach number distributions axially along center line and wall of the slotted throat with 5-minute divergence of test-section wall panels. Slot shape 6.

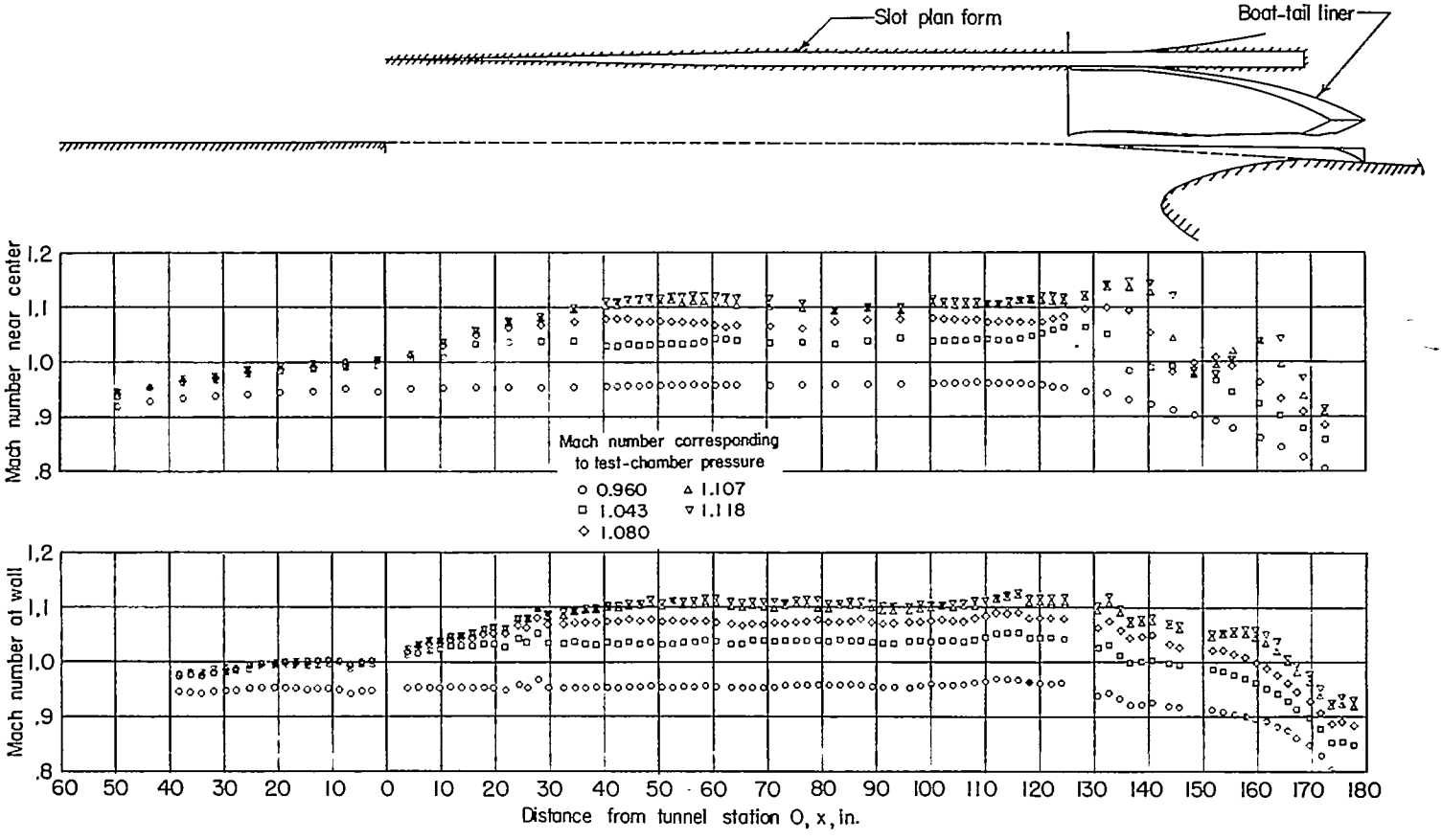

FIGURE 18.—Mach number distributions axially along center line and wall of the slotted throat with 5-minute divergence of test-section wall panels. Slot shape 7.

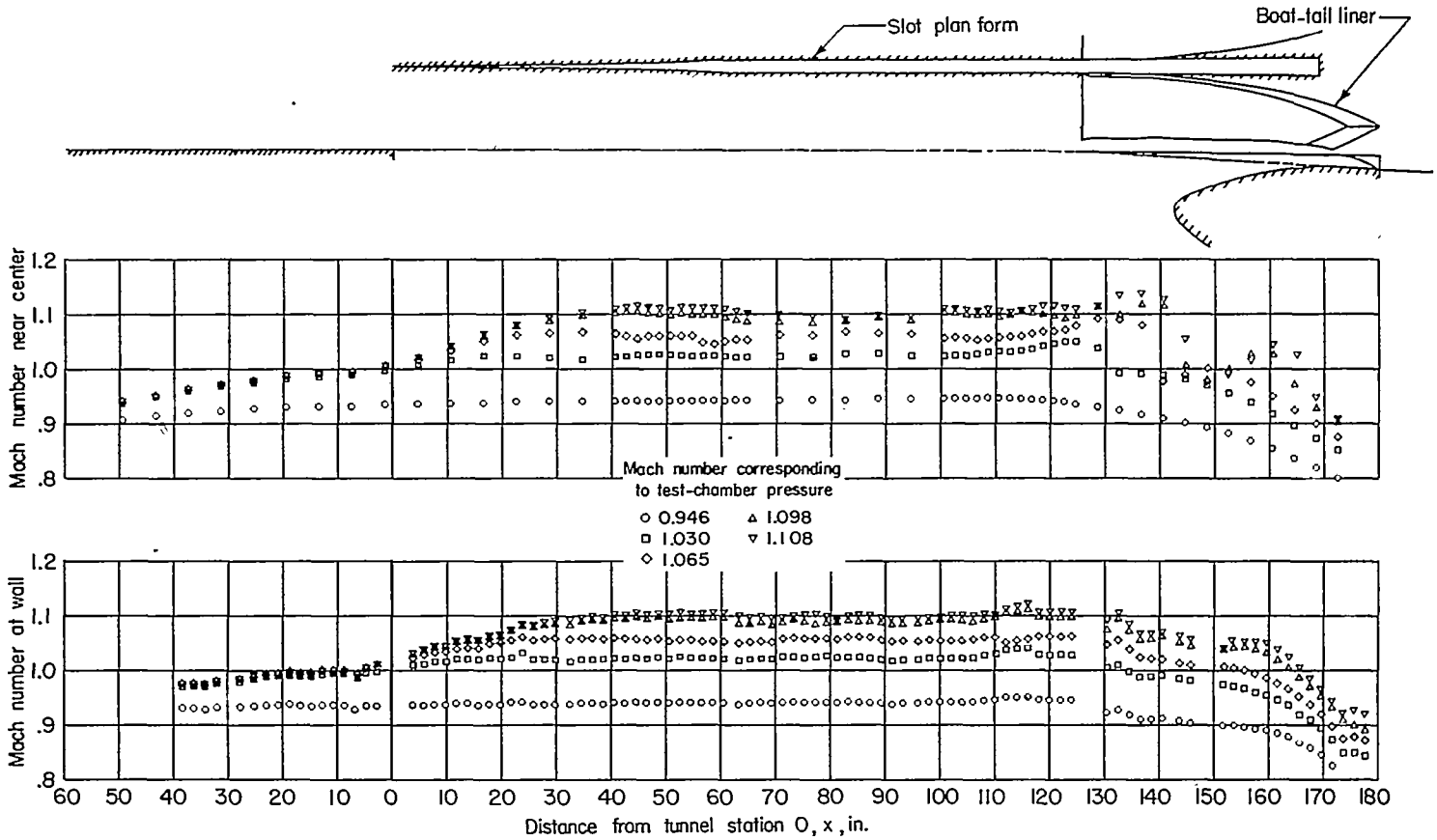

FIGURE 19.—Mach number distributions axially along center line and wall of the slotted throat with 5-minute divergence of test-section wall panels. Slot shape 8.

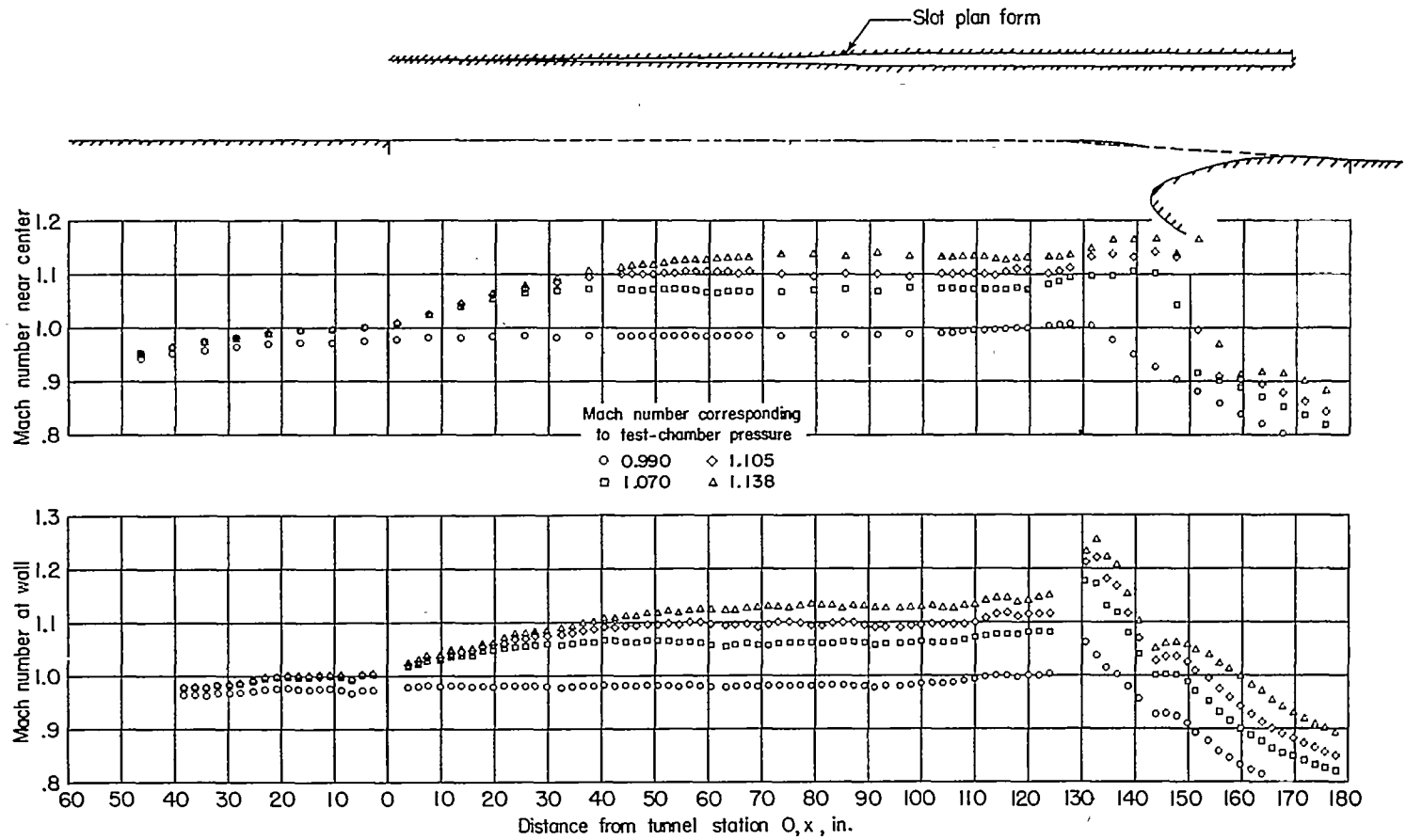

FIGURE 20.—Mach number distributions axially along center line and wall of the slotted throat with 5-minute divergence of test-section wall panels. Slot shape 11.

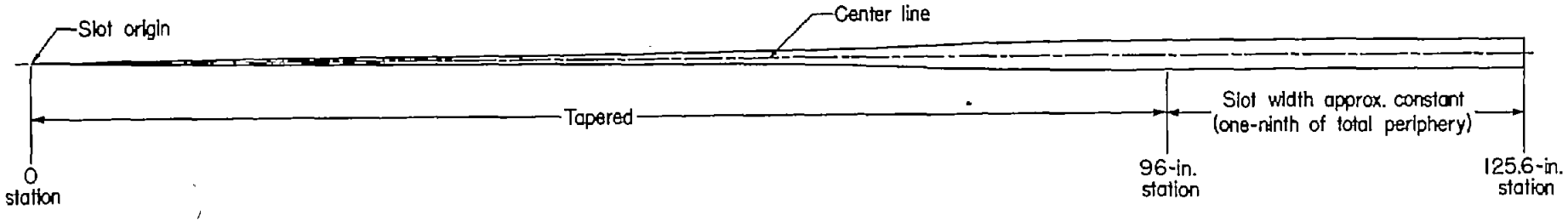

x (in.)	y (in.)	x (in.)	y (in.)	x (in.)	y (in.)	x (in.)	y (in.)	x (in.)	y (in.)
0	0	20	.233	40	.371	60	.556	80	1.120
2	.037	22	.250	42	.386	62	.585	82	1.170
4	.068	24	.263	44	.403	64	.618	84	1.210
6	.098	26	.278	46	.418	66	.656	86	1.240
8	.122	28	.290	48	.433	68	.700	88	1.260
10	.144	30	.303	50	.451	70	.751	90	1.273
12	.165	32	.316	52	.469	72	.812	92	1.281
14	.185	34	.329	54	.486	74	.882	94	1.288
16	.202	36	.343	56	.508	76	.969	96	1.290
18	.219	38	.356	58	.530	78	1.060	125.6	1.291

x = Distance downstream of slot origin
y = Distance from slot edge to center line

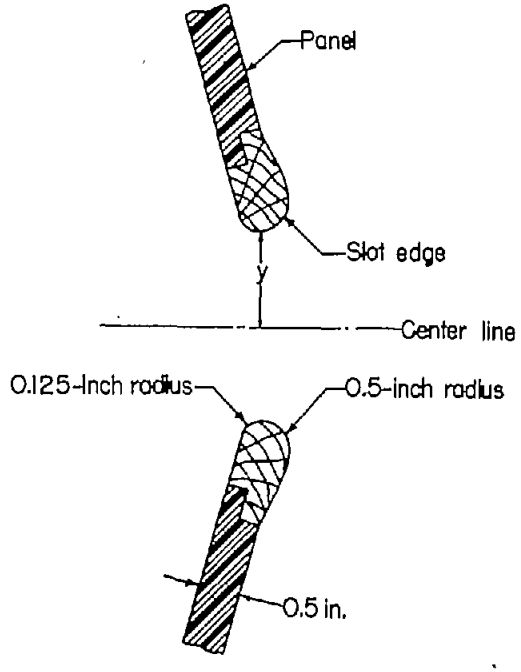

FIGURE 21.—Coordinates of final slot shape developed for use in the Langley 8-foot transonic tunnel.

620687—60——96

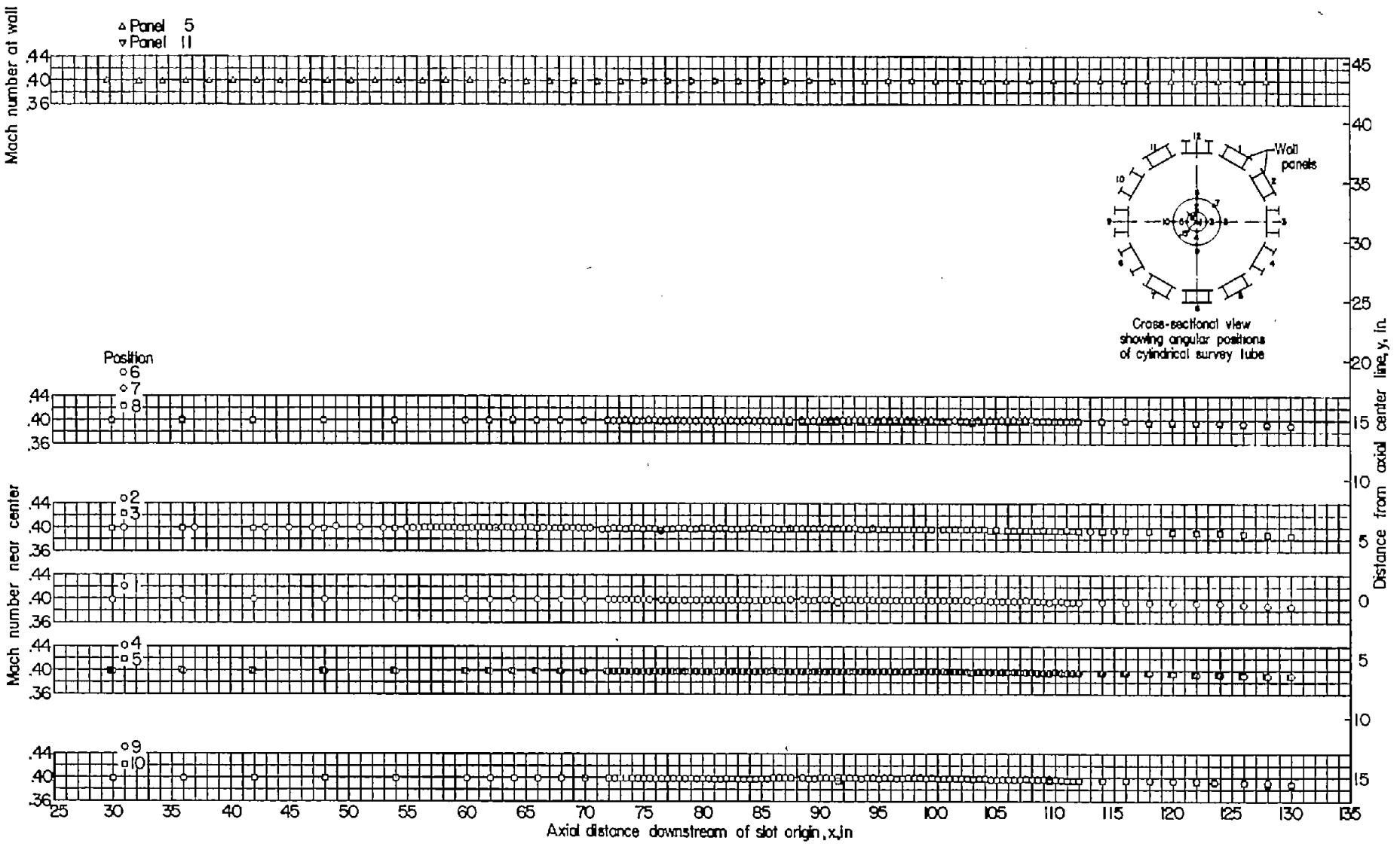

(a) $M_{TO}=0.40$.

FIGURE 22.—Basic flow-survey charts showing Mach number distributions axially along wall and near center line of slotted test section with model removed. Diffuser-entrance nose A. Slot shape 11.

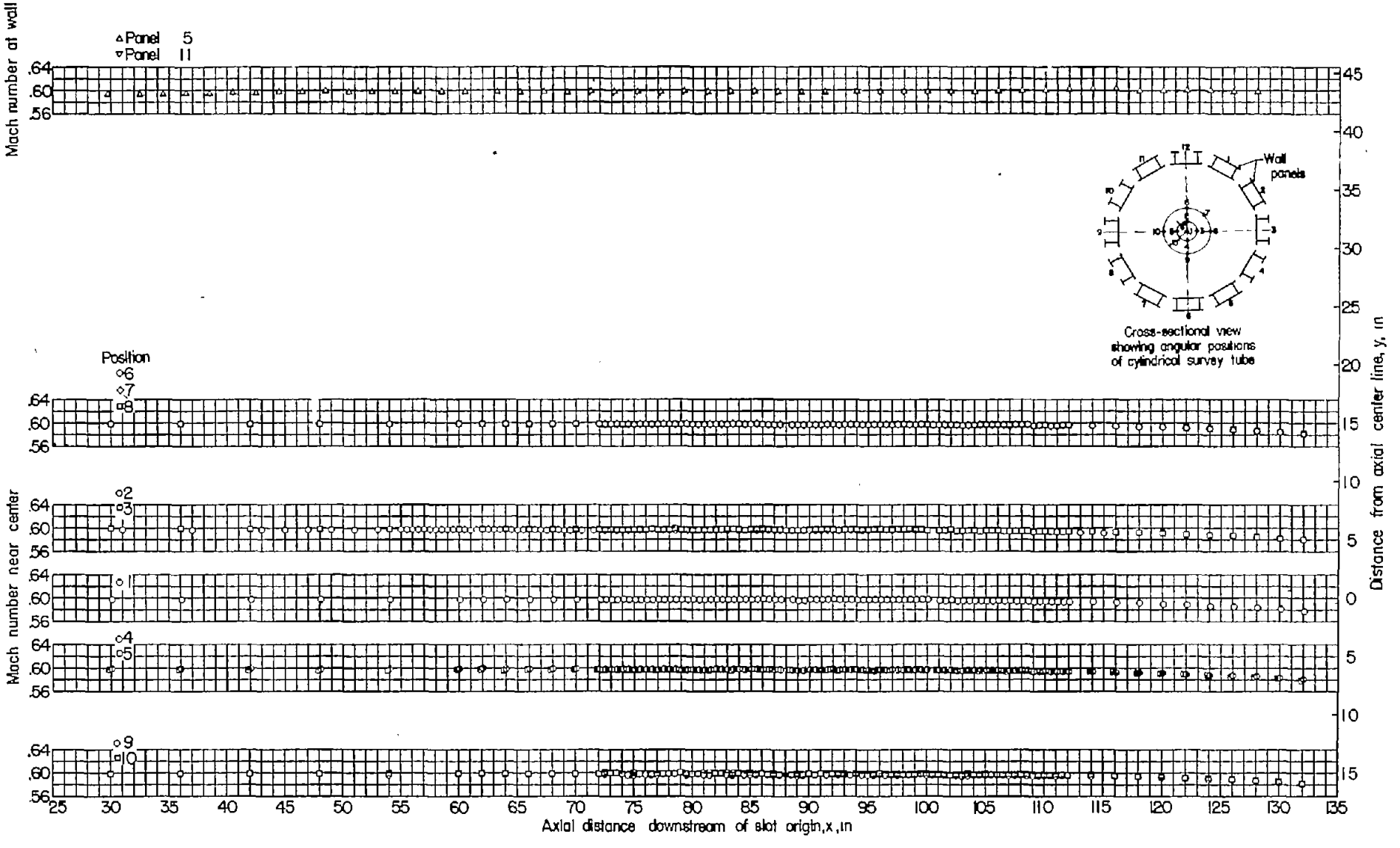

(b) $M_{TO}=0.60$.

FIGURE 22.—Continued.

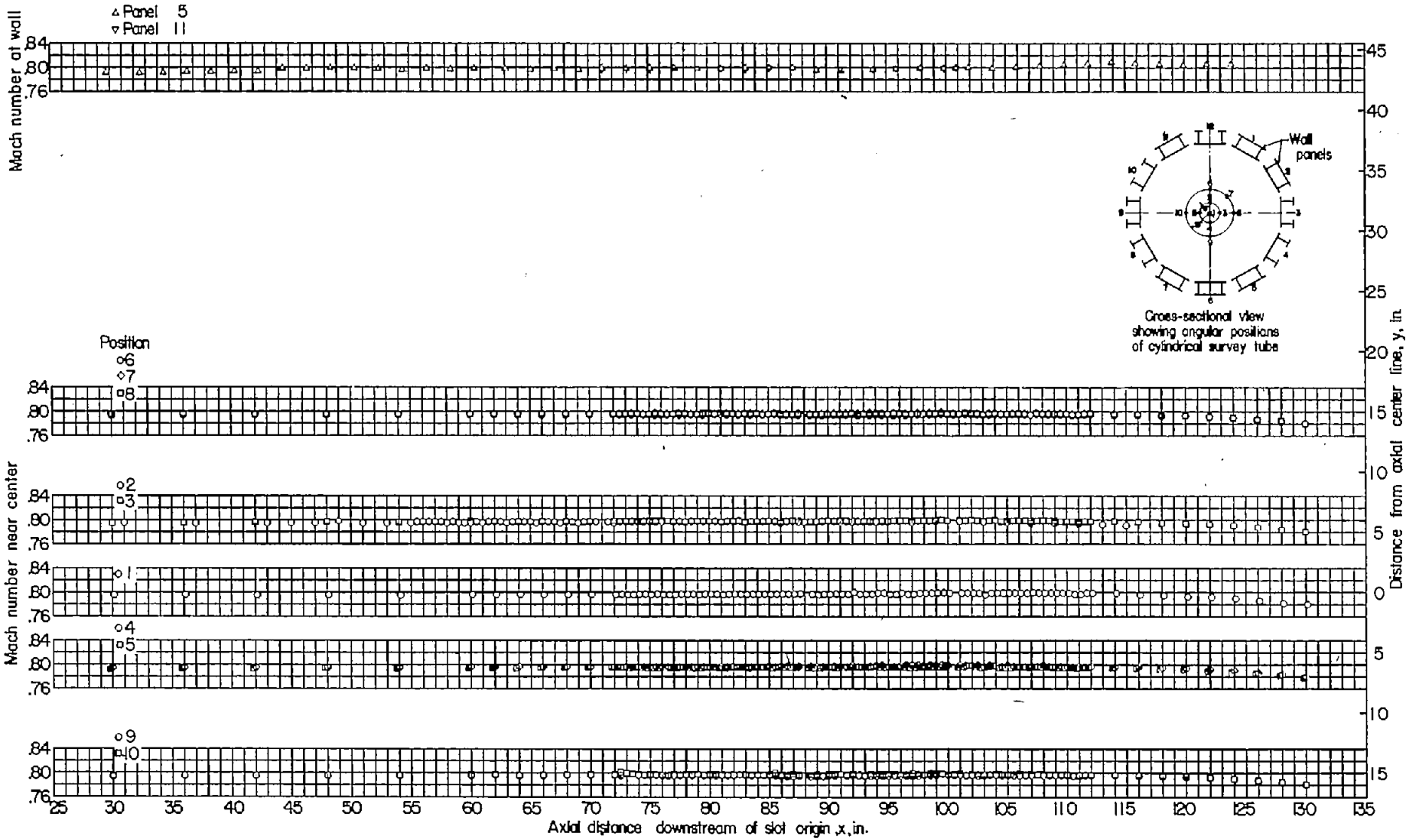

(c) $M_{TC}=0.80$.

FIGURE 22.—Continued.

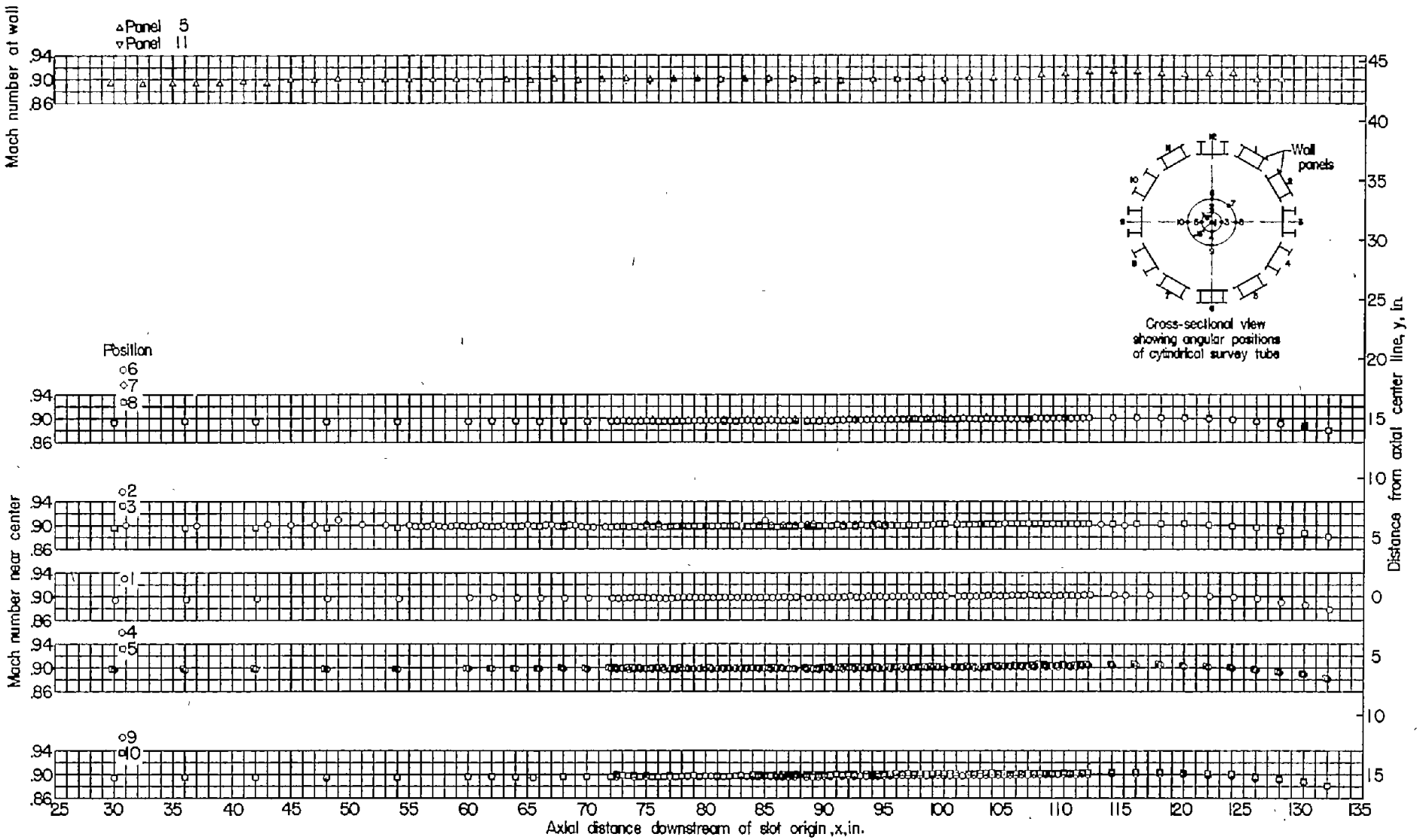

(d) $M_{TO}=0.90$.

FIGURE 22.—Continued.

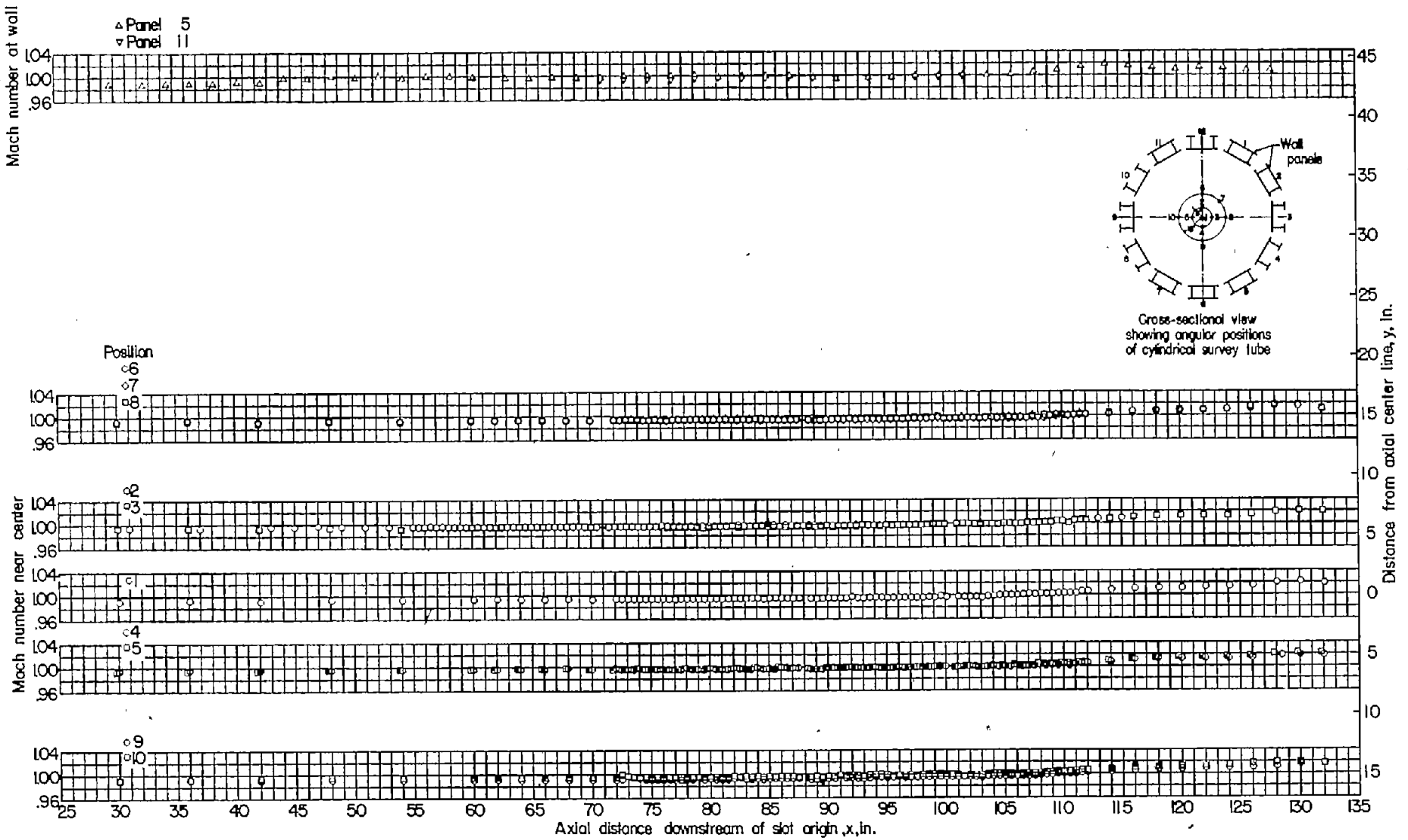

(e) $M_{T0}=1.00$.

FIGURE 22.—Continued.

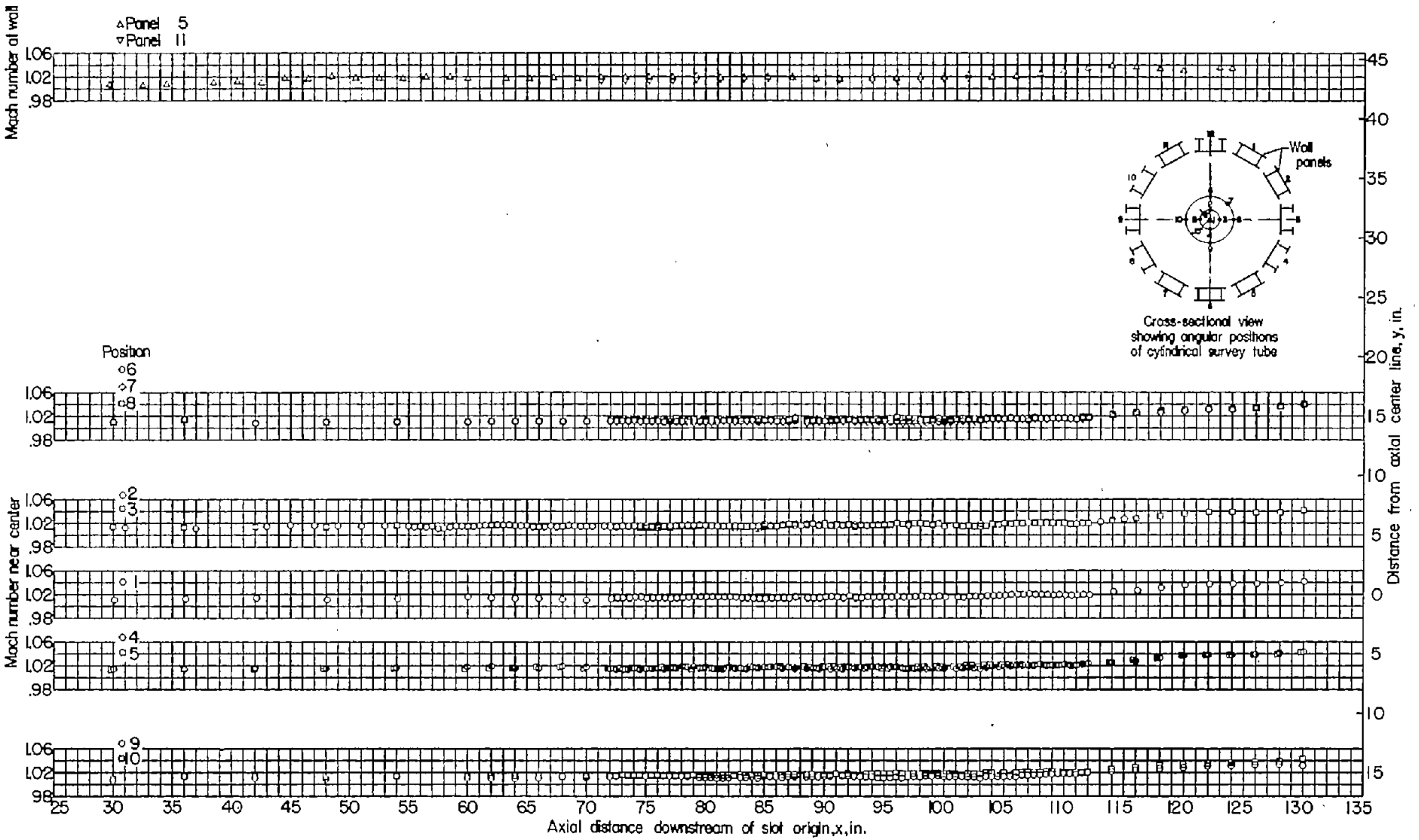

(f) $M_{TC}=1.02$.

FIGURE 22.—Continued.

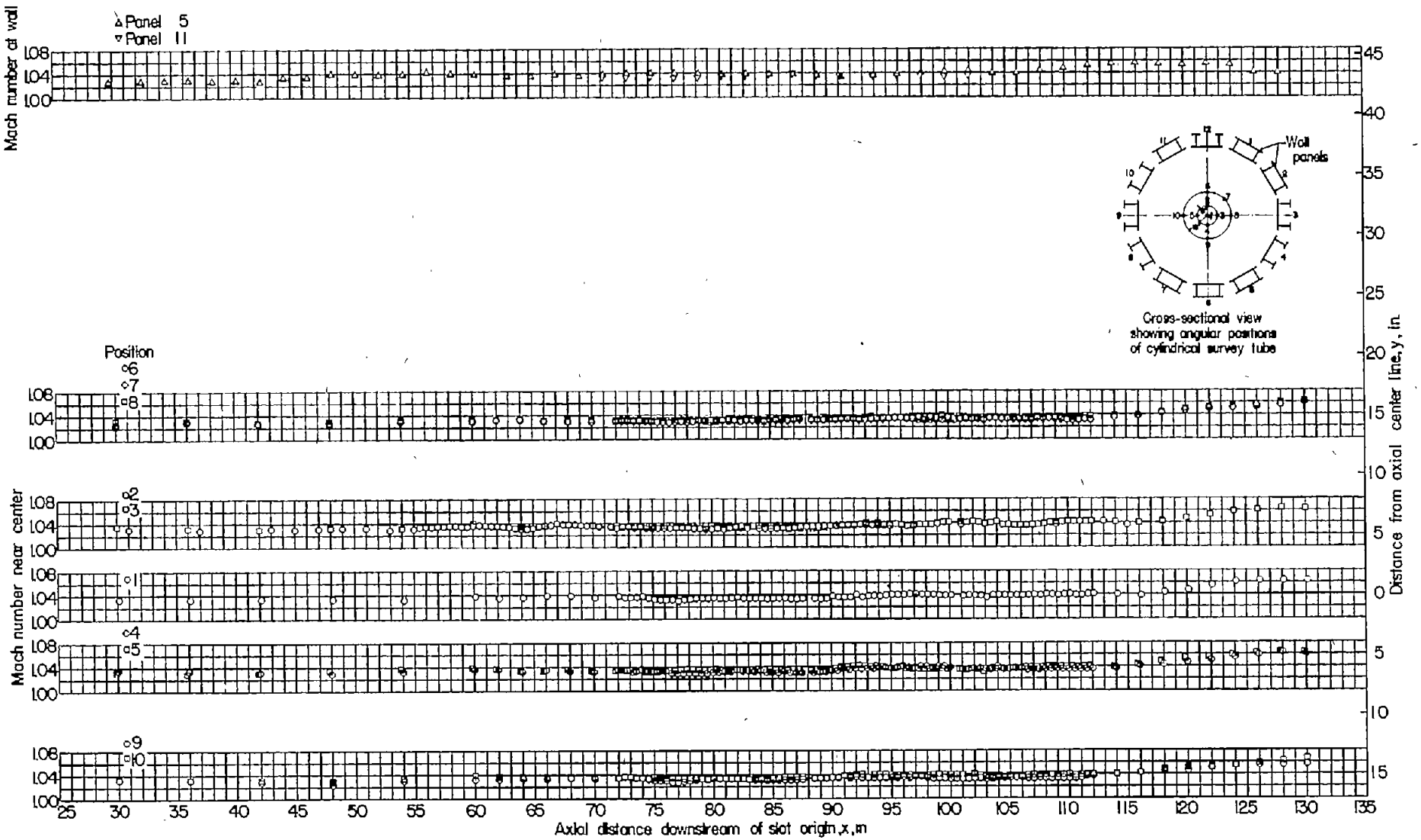

(g) $M_{TC}=1.04$.

FIGURE 22.—Continued.

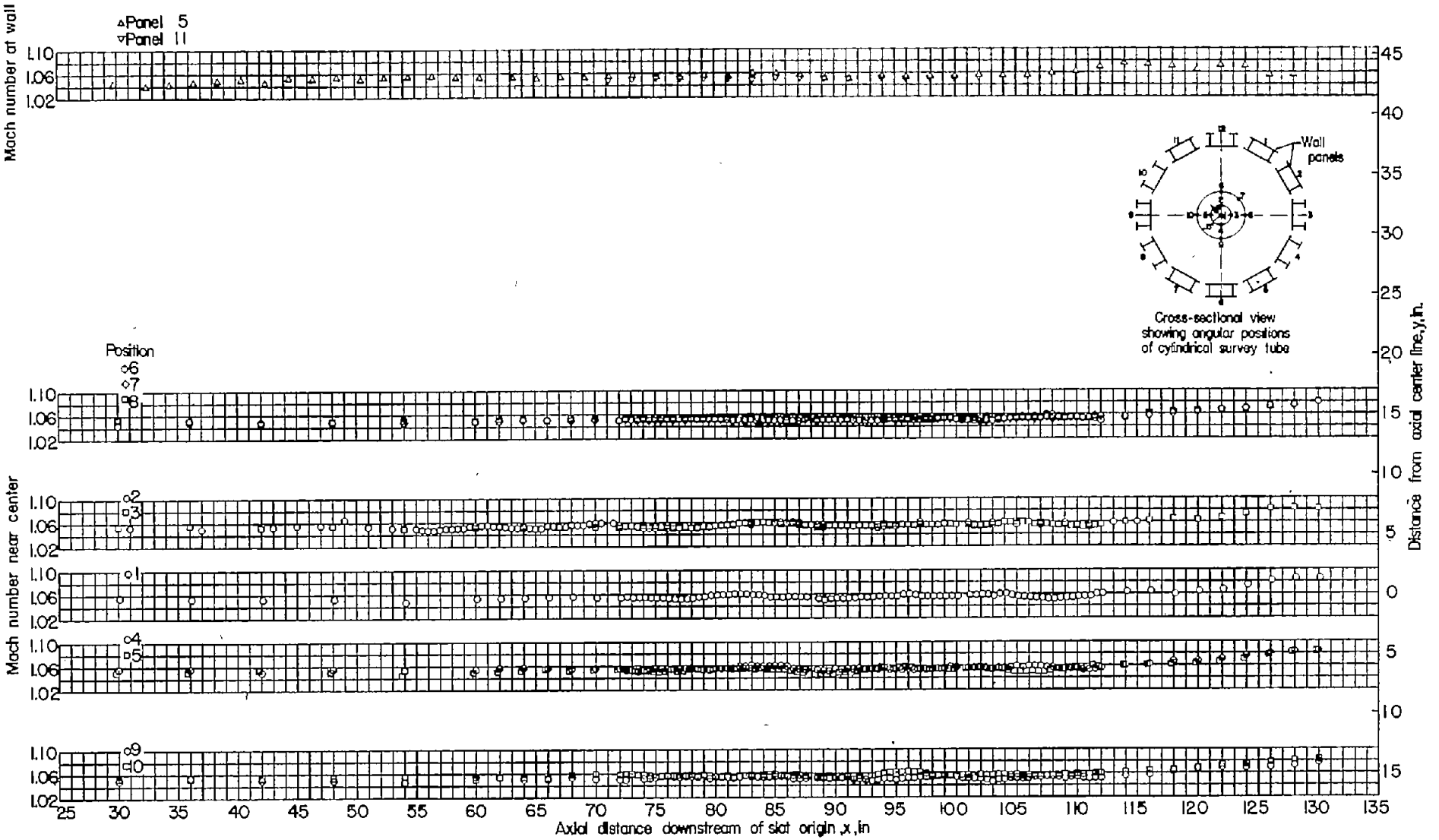

(h) $M_{TC}=1.06$.

FIGURE 22.—Continued.

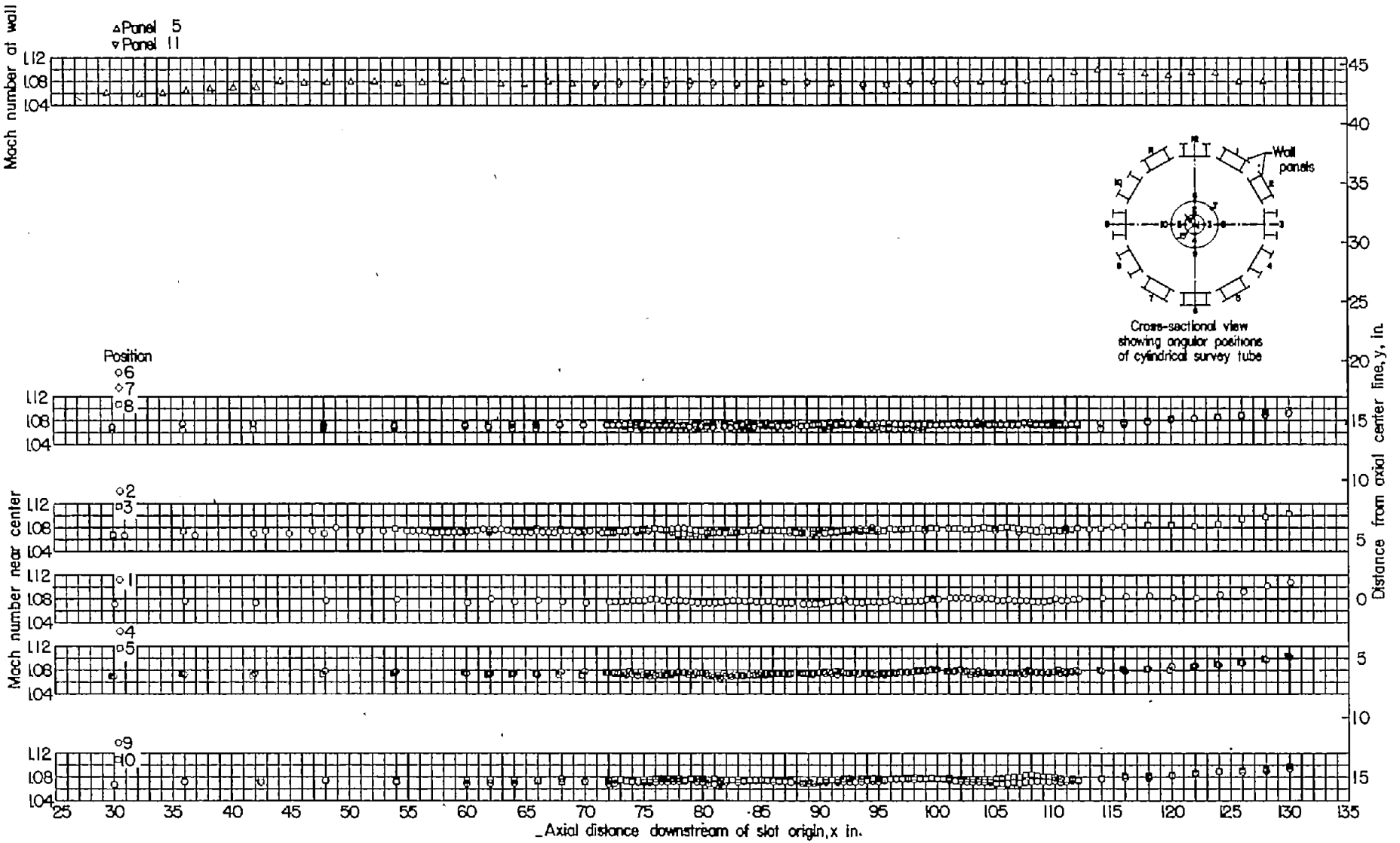

(l) $M_{TO}=1.08$.

FIGURE 22.—Continued.

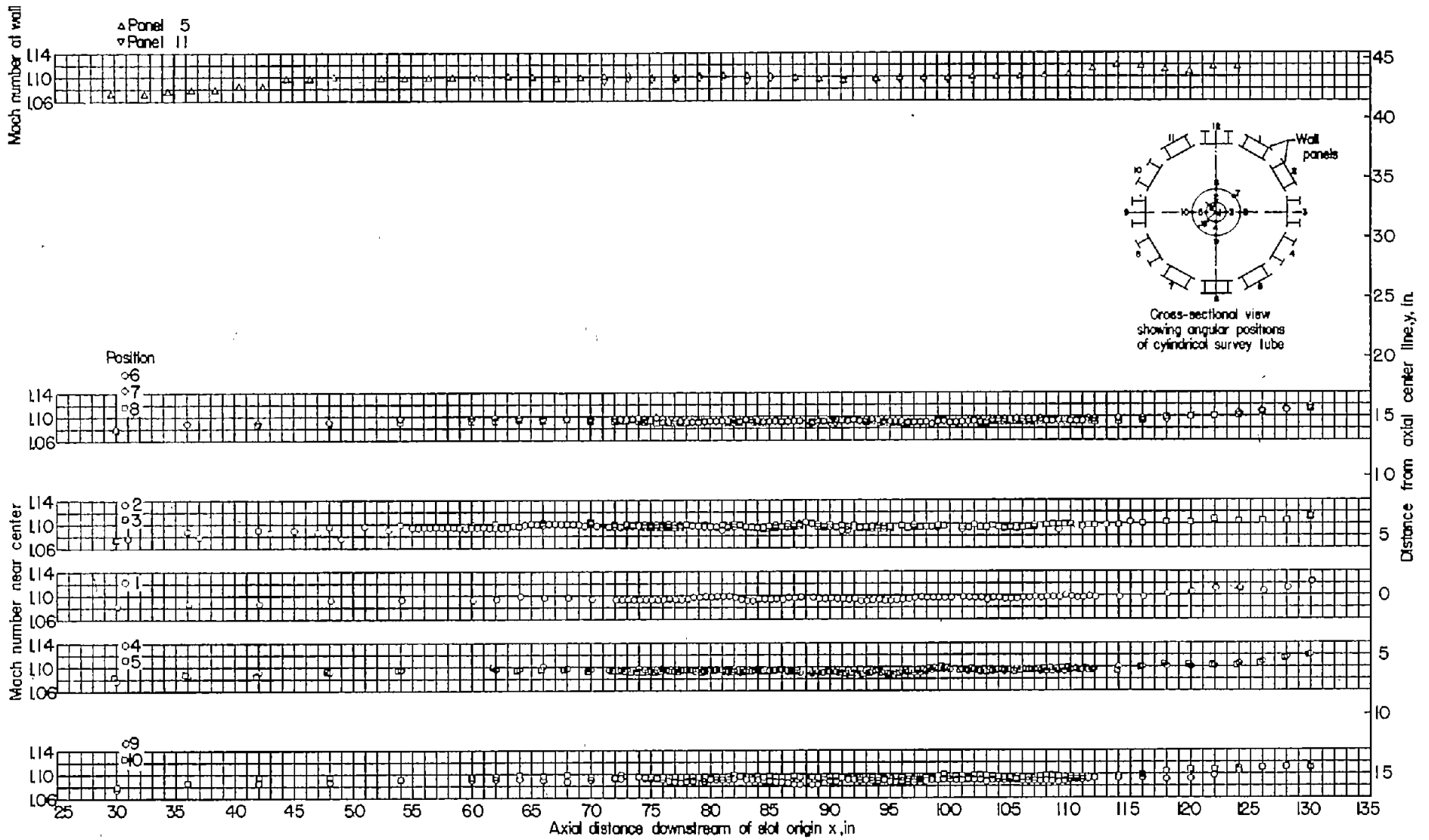

(j) M_{TU}=1.10.

FIGURE 22.—Continued.

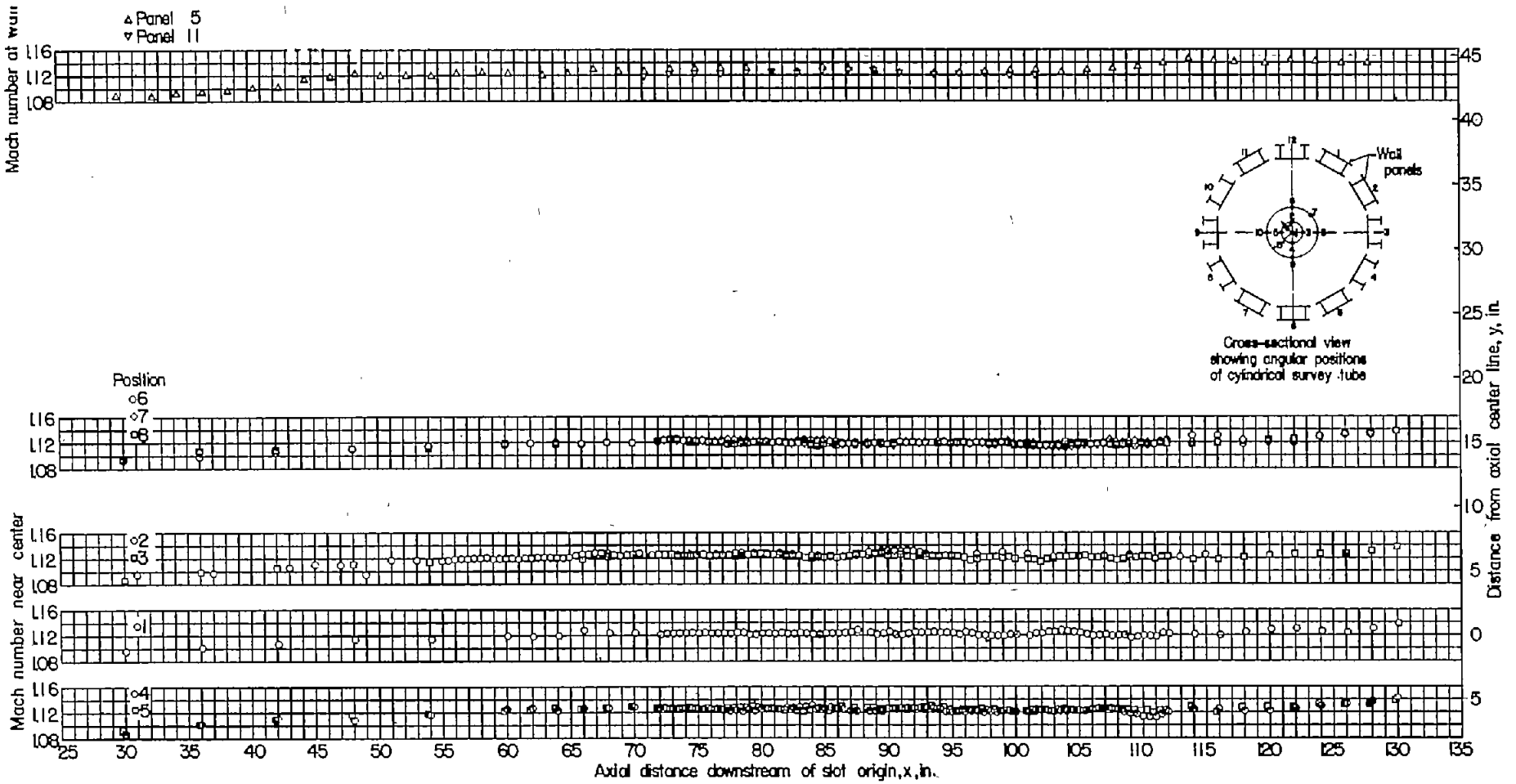

(k) $M_{TC}=1.13$.

FIGURE 22.—Concluded.

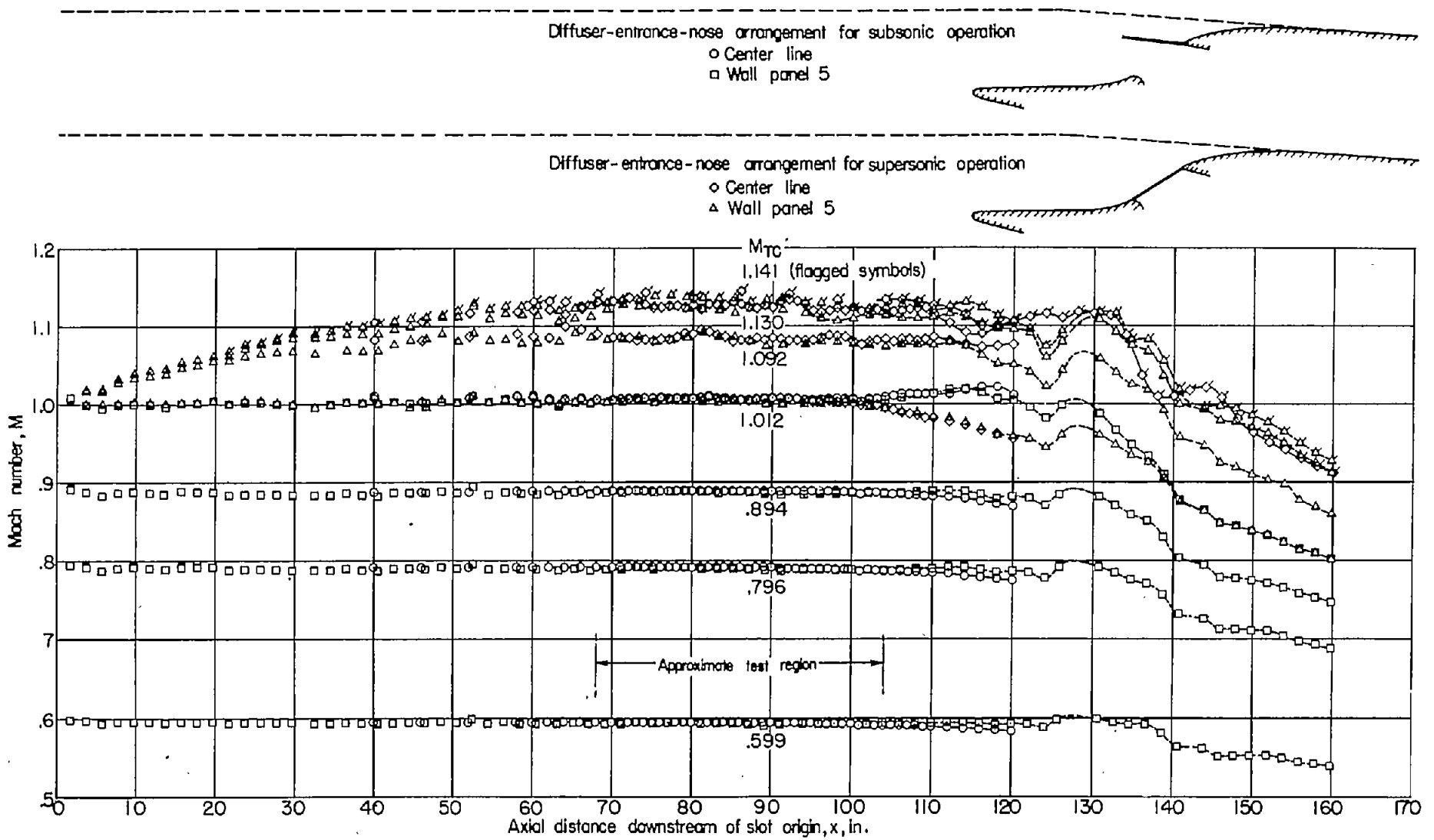

FIGURE 23.—Mach number distributions measured axially along center line and wall of slotted test section with a diffuser-entrance nose arrangement for reduction of tunnel power requirements and attainment of higher Mach number. Model removed; diffuser-entrance nose B; slot shape 11.

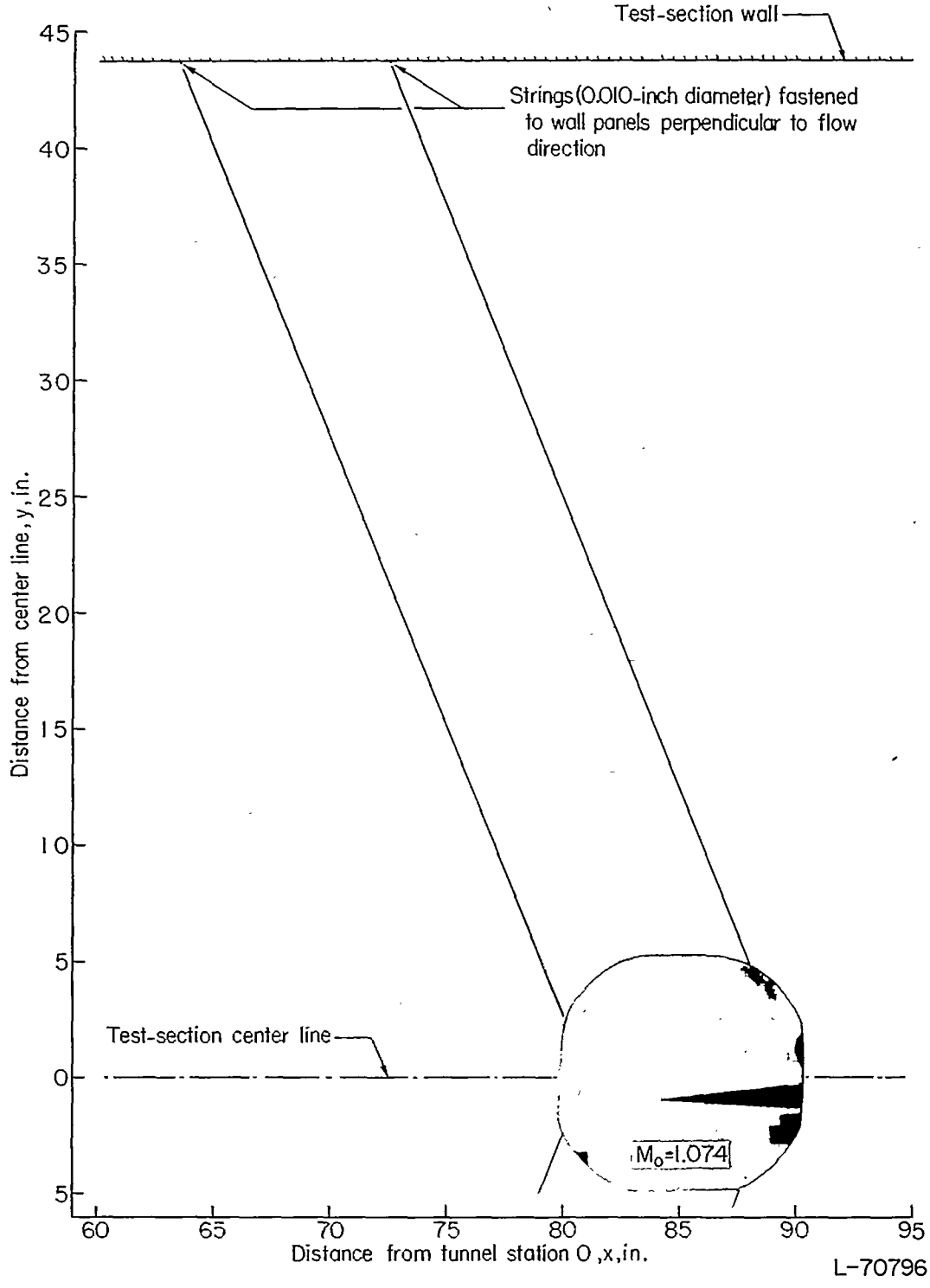

FIGURE 24.—Schlieren picture illustrating the propagation of weak disturbances in supersonic flow in the slotted test section. M_o=1.074.

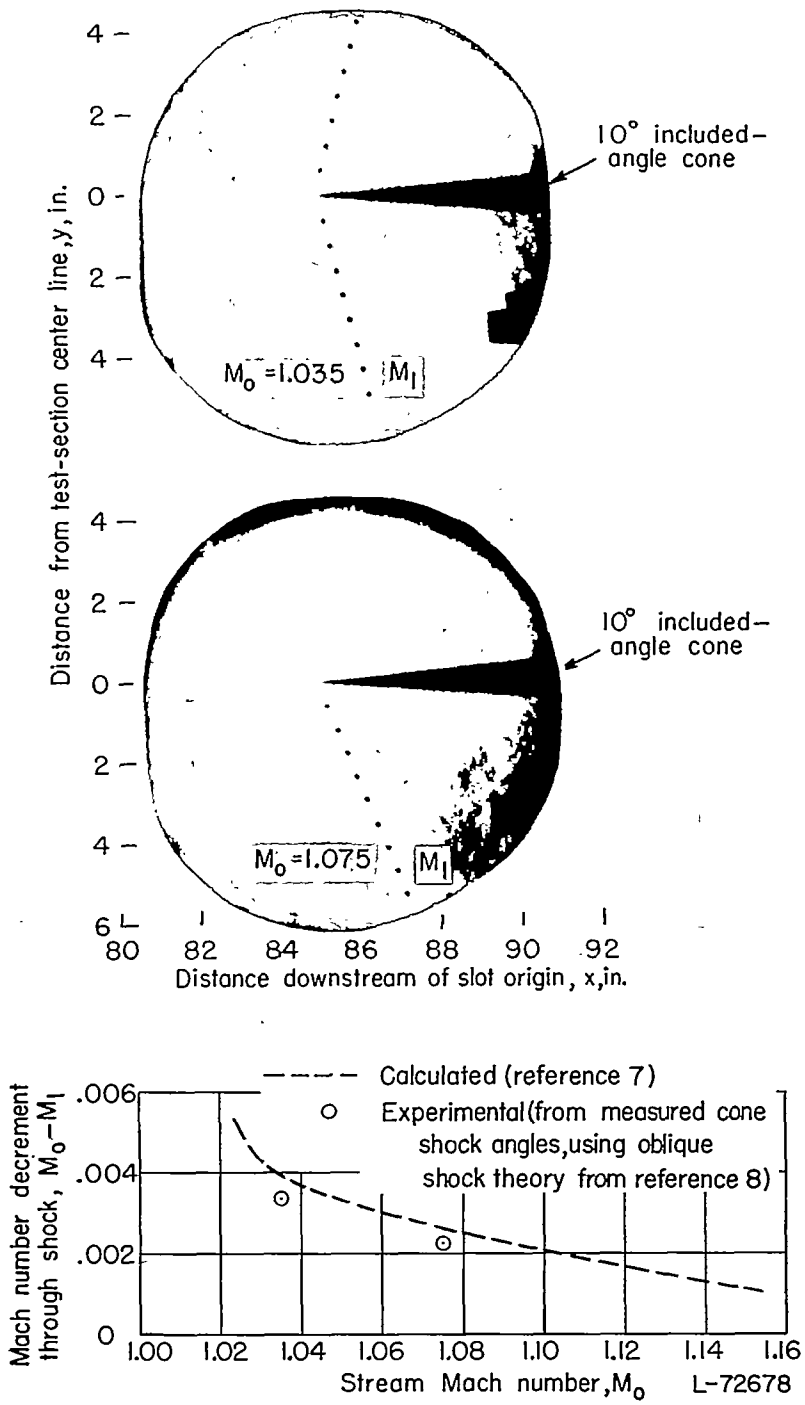

FIGURE 25.—An illustration of the degree of flow uniformity in a region of the slotted test section. Shock waves of known strength (produced by a 10° included-angle cone at zero angle) are used as the flow-uniformity criterion. Diffuser-entrance nose A.

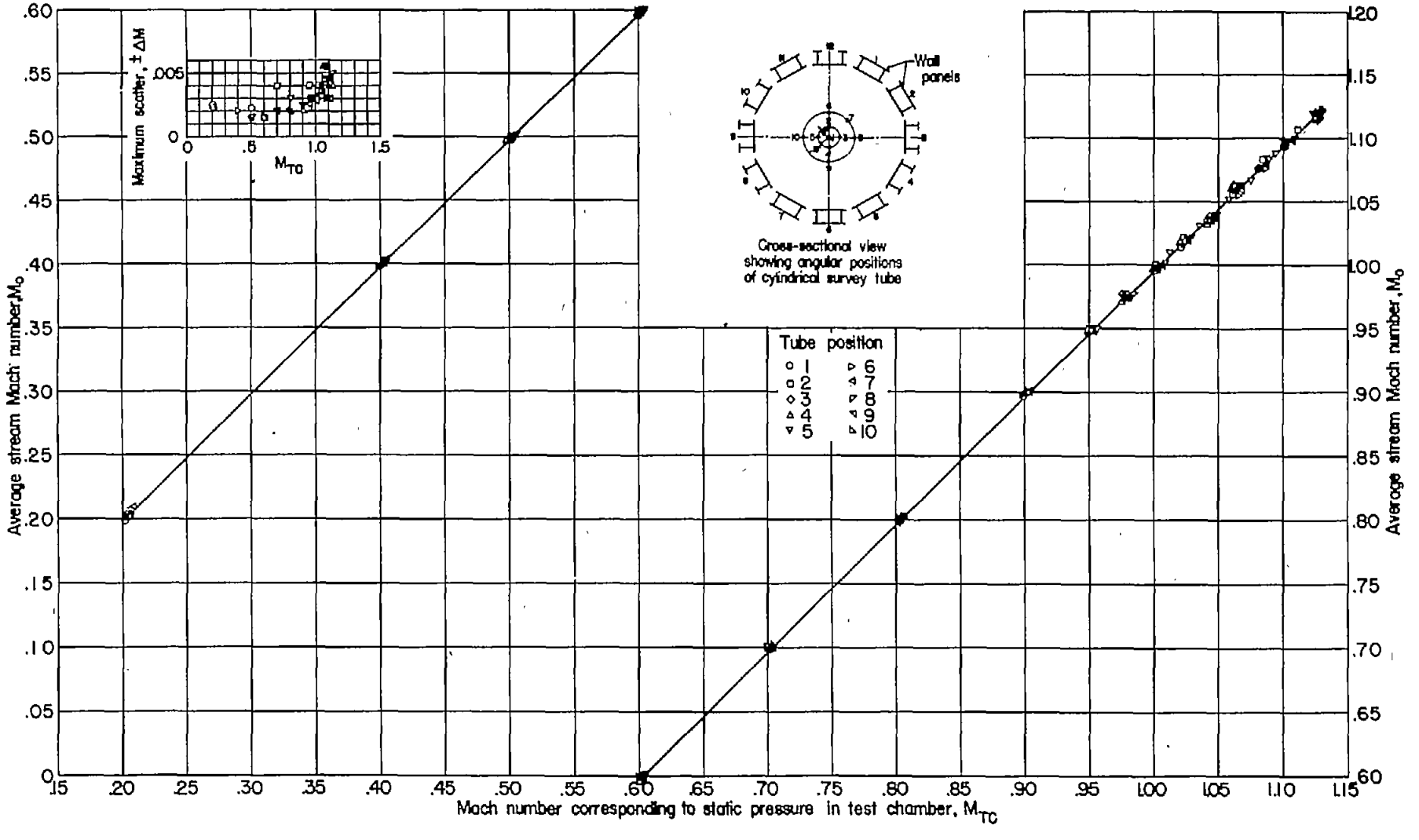

FIGURE 26.—Typical calibration curve showing the variation with test-chamber Mach number of the average Mach number over a test region 36 inches long and 30 inches in diameter near the center line of the slotted test section with diffuser-entrance nose A. Model removed; slot shape 11.

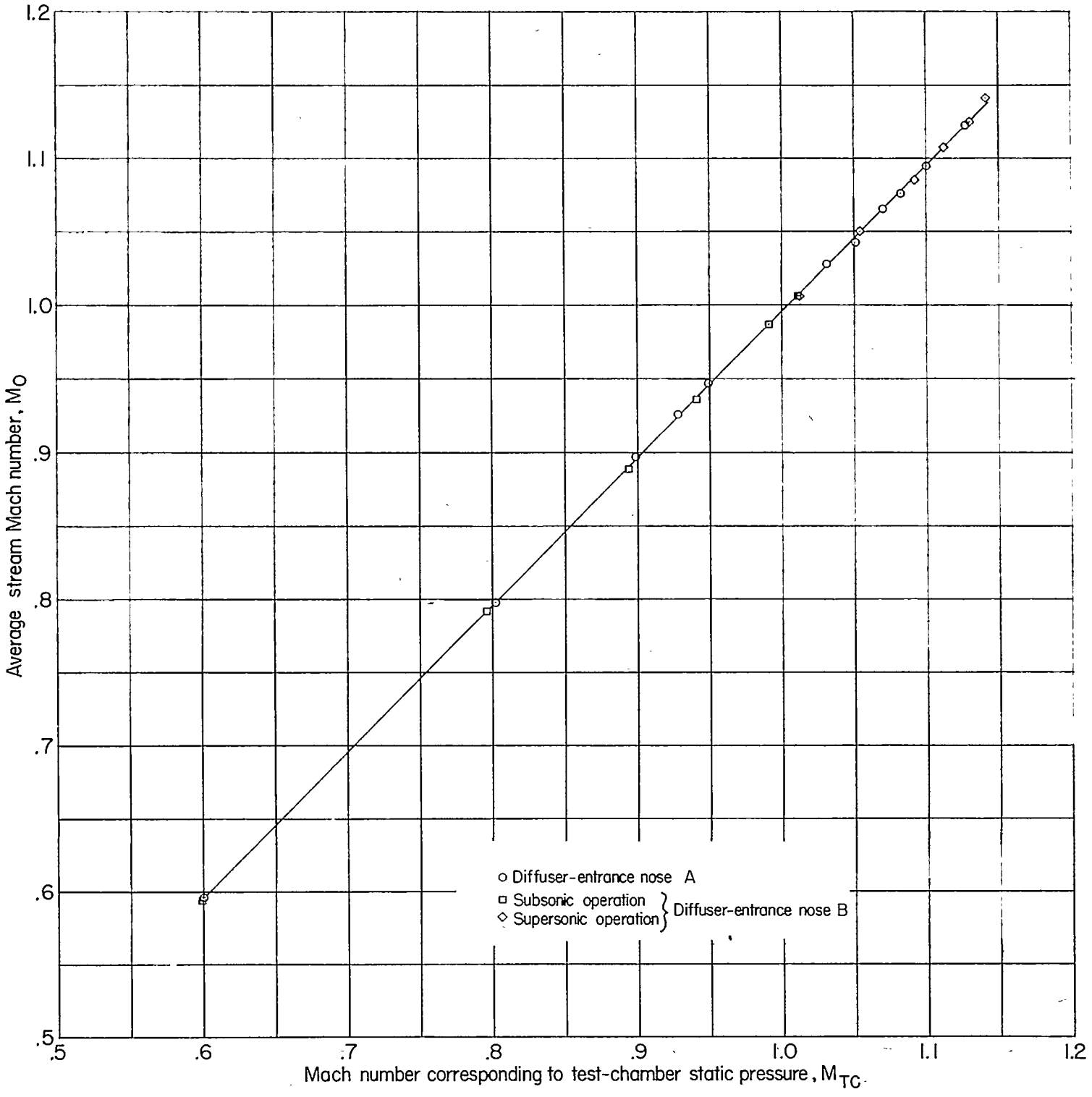

FIGURE 27.—Agreement of calibrations of the average Mach number over a 36-inch-long region at the center line of the slotted test section with diffuser-entrance noses A and B. Model removed; slot shape 11. Maximum deviations in Mach number for surveys with nose A and nose B are within 0.006 and 0.010, respectively.

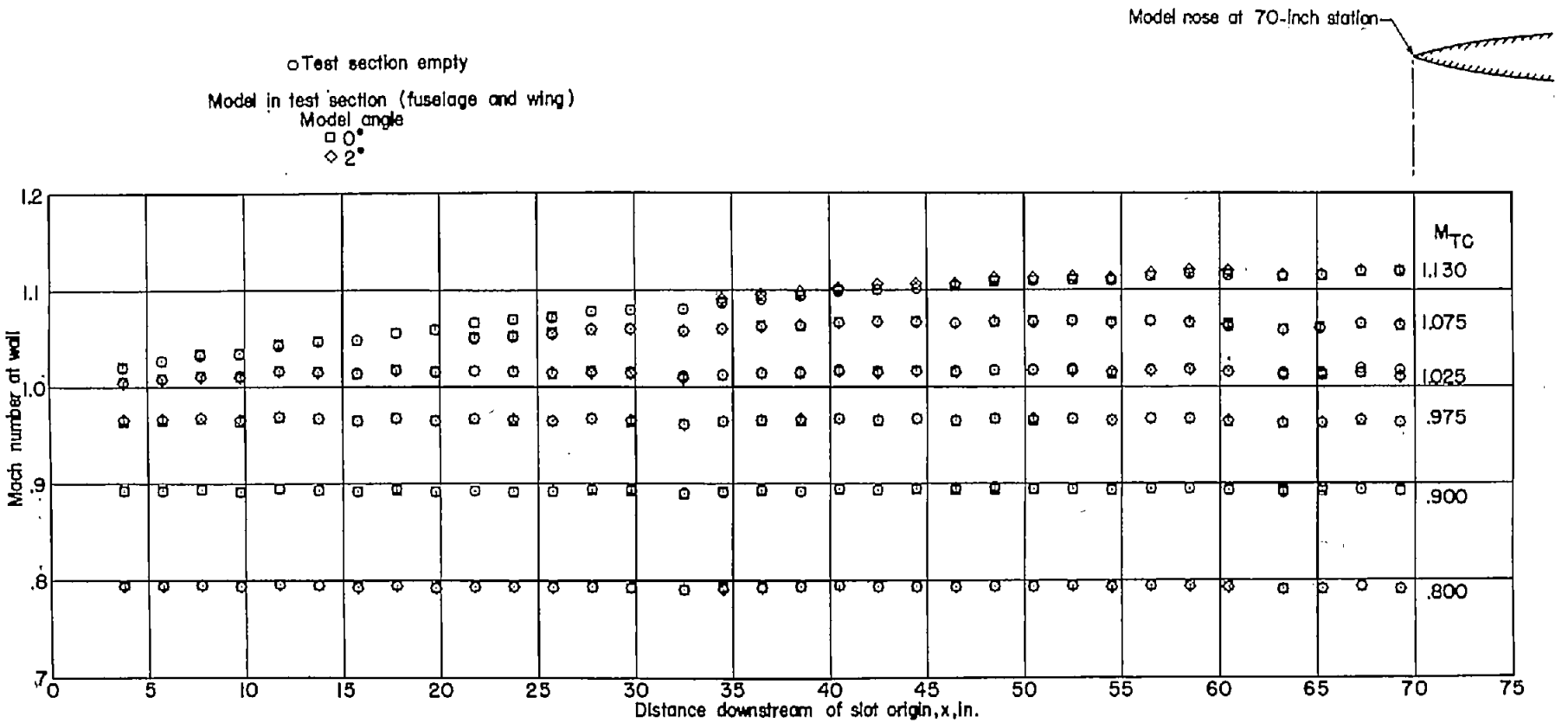

FIGURE 28.—Agreement of Mach number distributions axially along wall of slotted test section upstream of model location with model in and model removed. Diffuser-entrance nose A; slot shape 11.

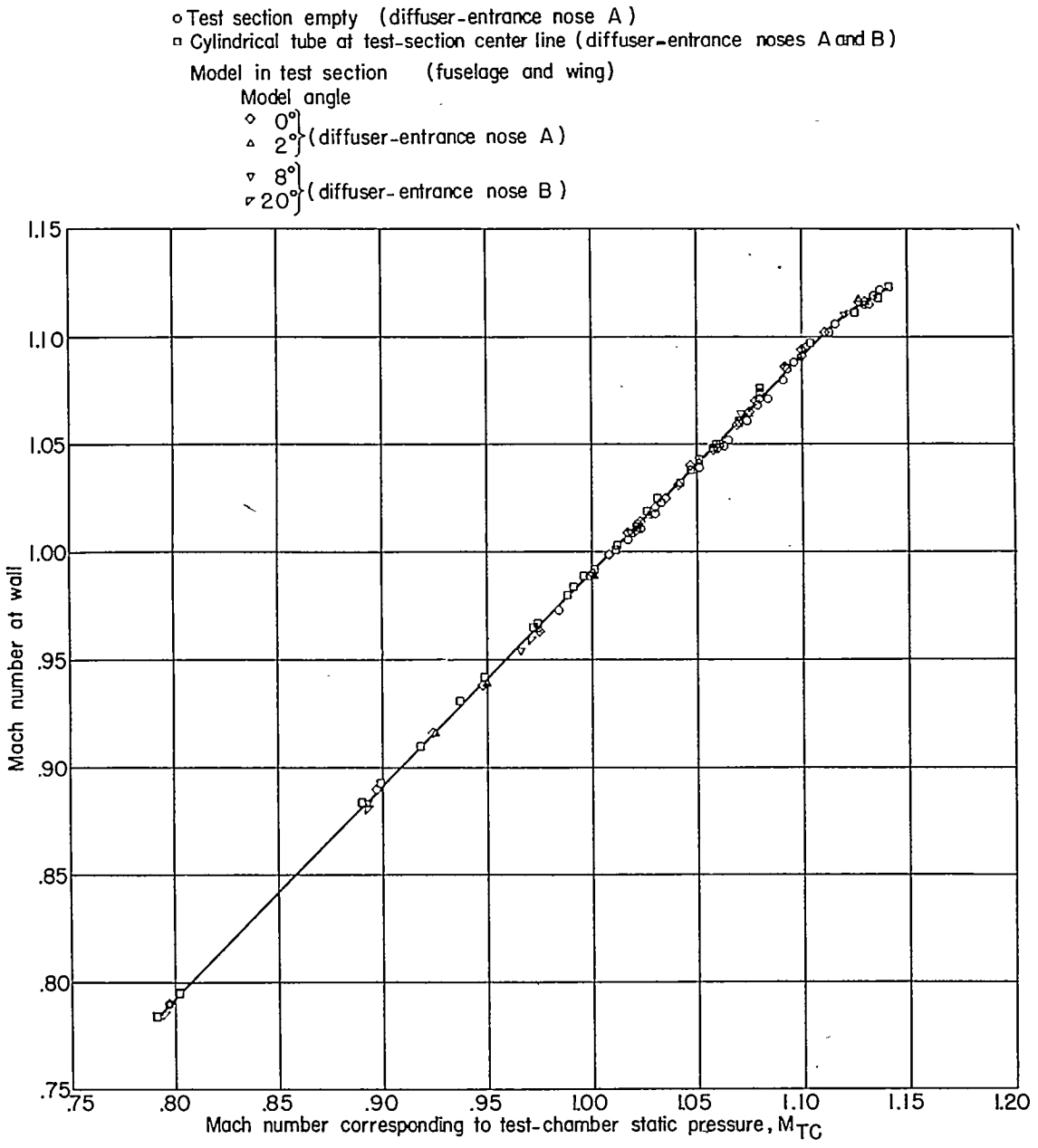

FIGURE 29.—Variation with test-chamber Mach number of Mach numbers measured on tunnel wall approximately 10 inches upstream of model nose (model at different angles of attack) and Mach numbers measured at the same axial station with model removed. Slot shape 11.

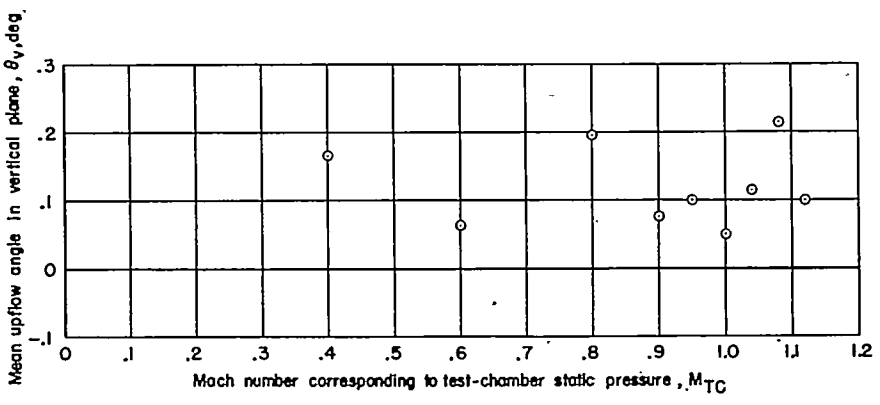

FIGURE 30.—Flow angularity in vertical plane, indicated by null-pressure cone-surface measurements at test-section center line 85 inches downstream of slot origin. Slot shape 11.

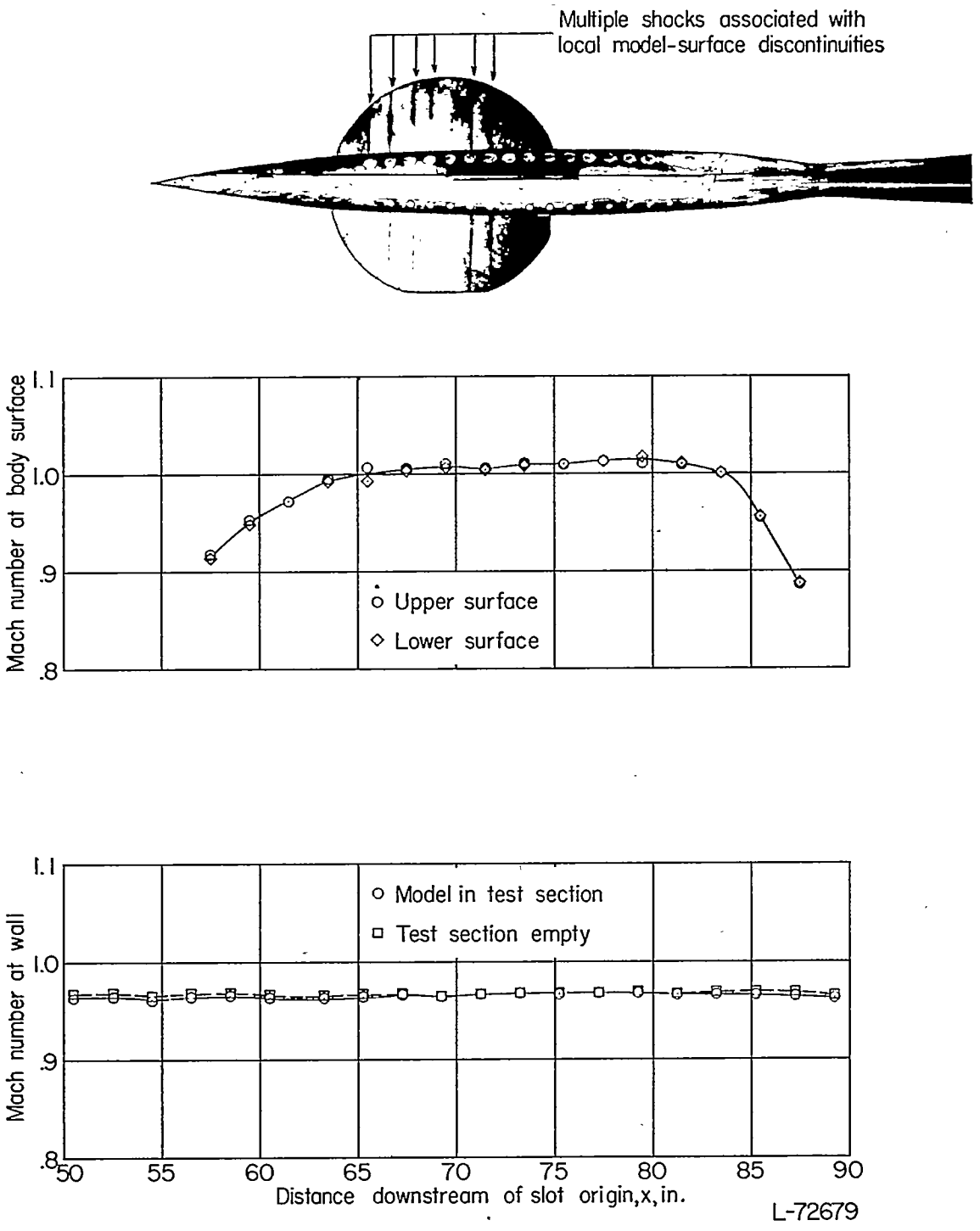

(a) $M_o=0.970$.

FIGURE 31.—Shock formations and reflections at transonic speeds with body-of-revolution model at center line of slotted test section. $\alpha=0°$; diffuser-entrance nose A; slot shape 11.

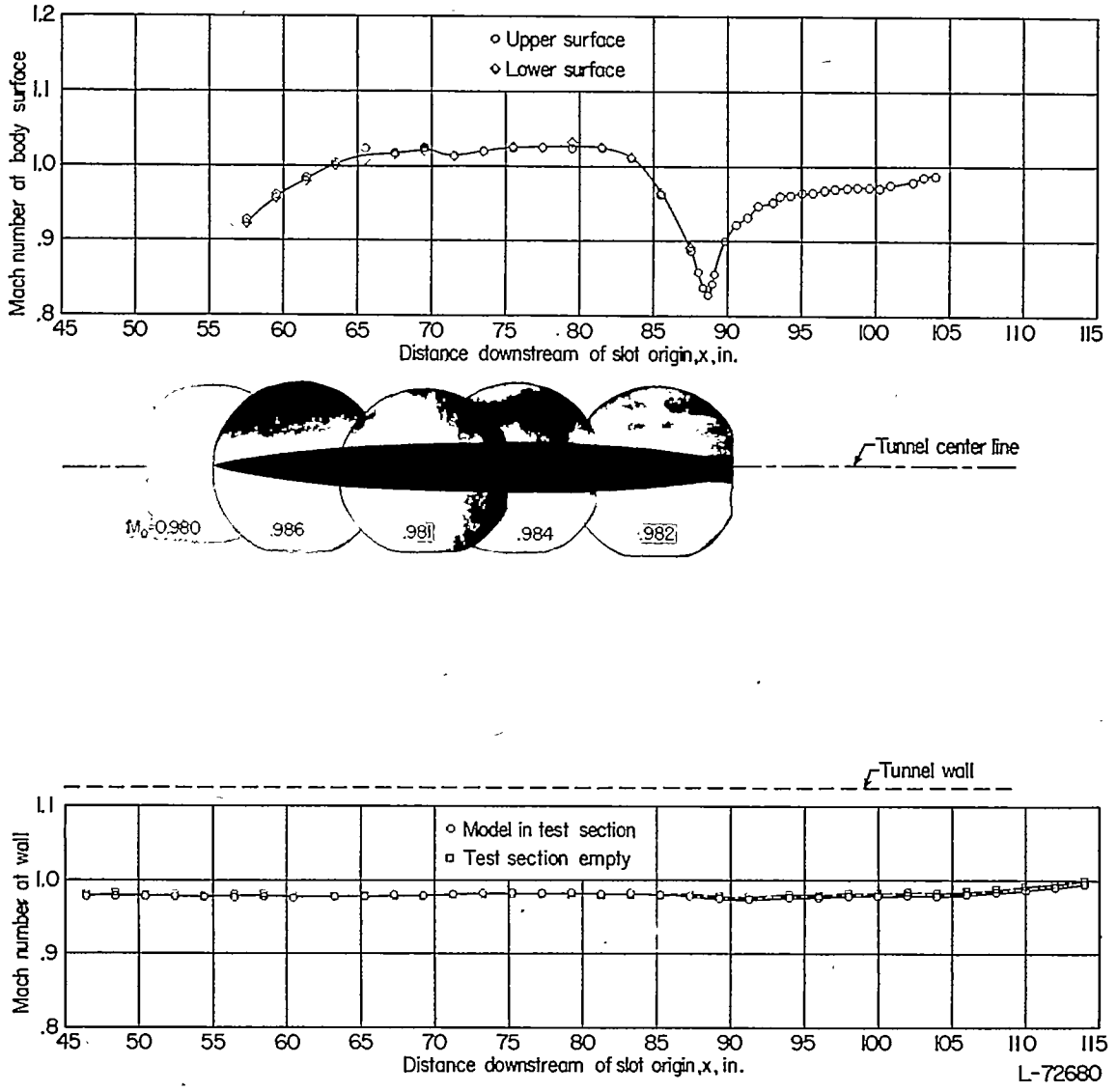

(b) $M_o=0.980$.

FIGURE 31.—Continued.

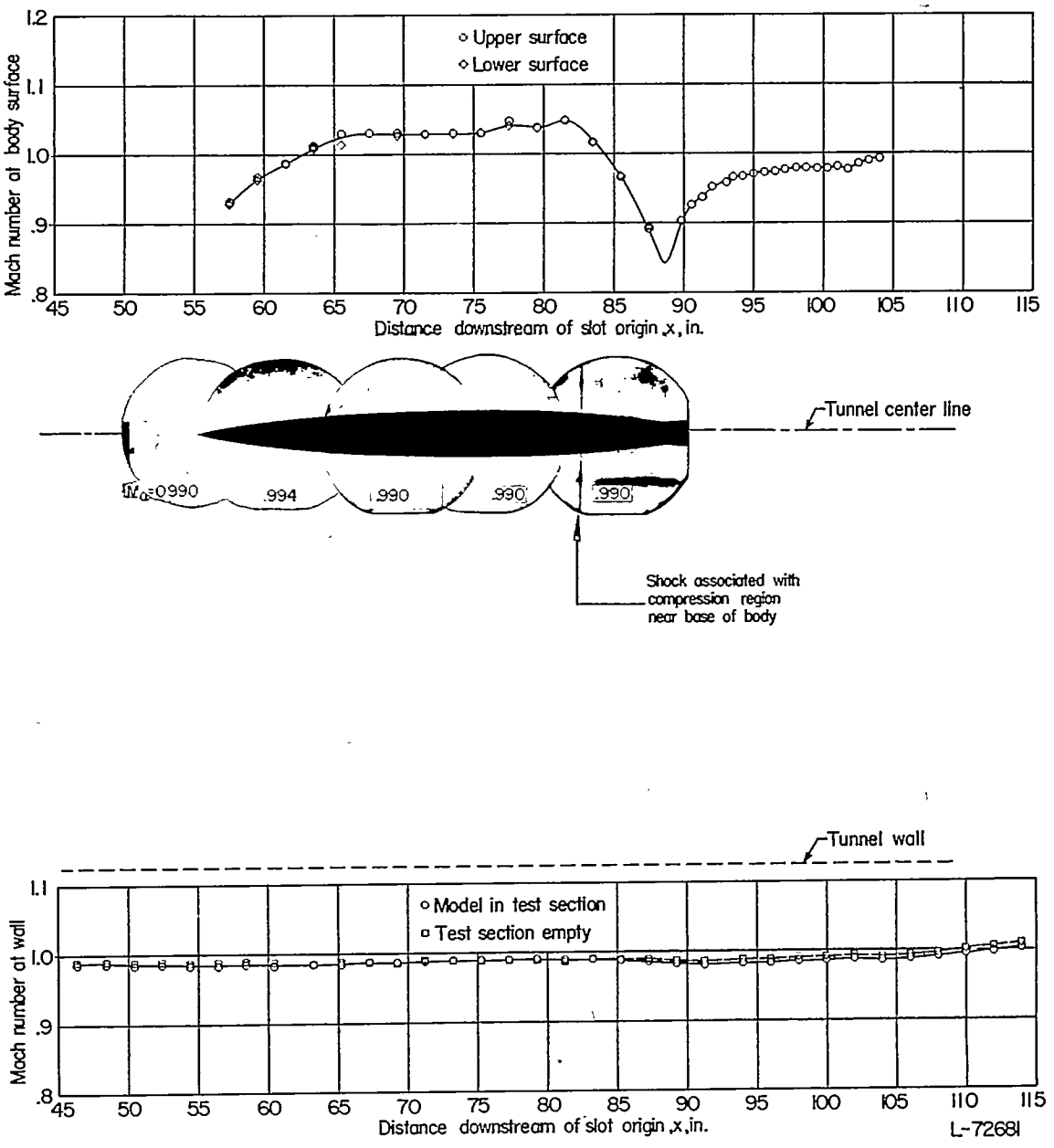

(c) M_0=0.990.

FIGURE 31.—Continued.

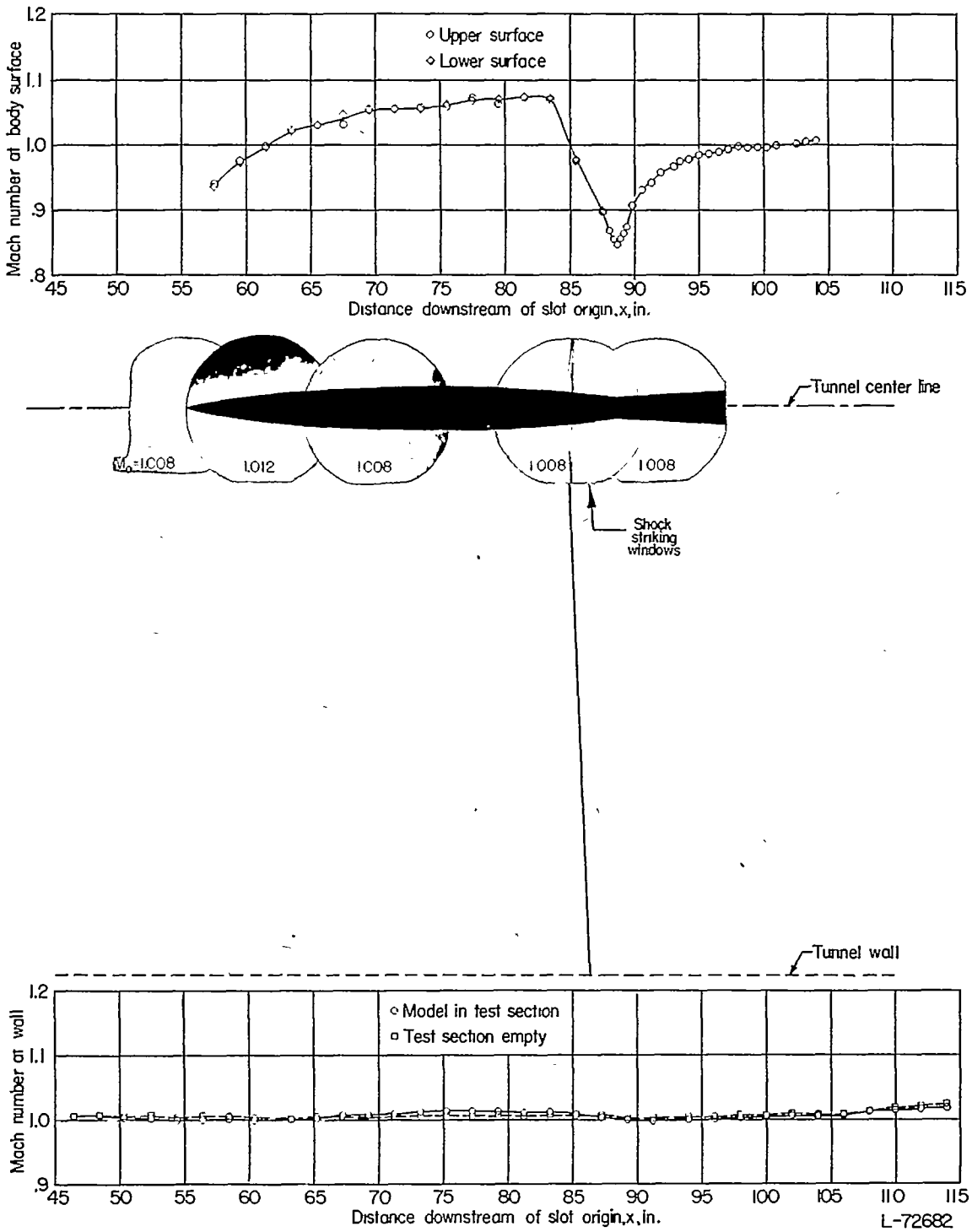

(d) M_o=1.008.

FIGURE 31.—Continued.

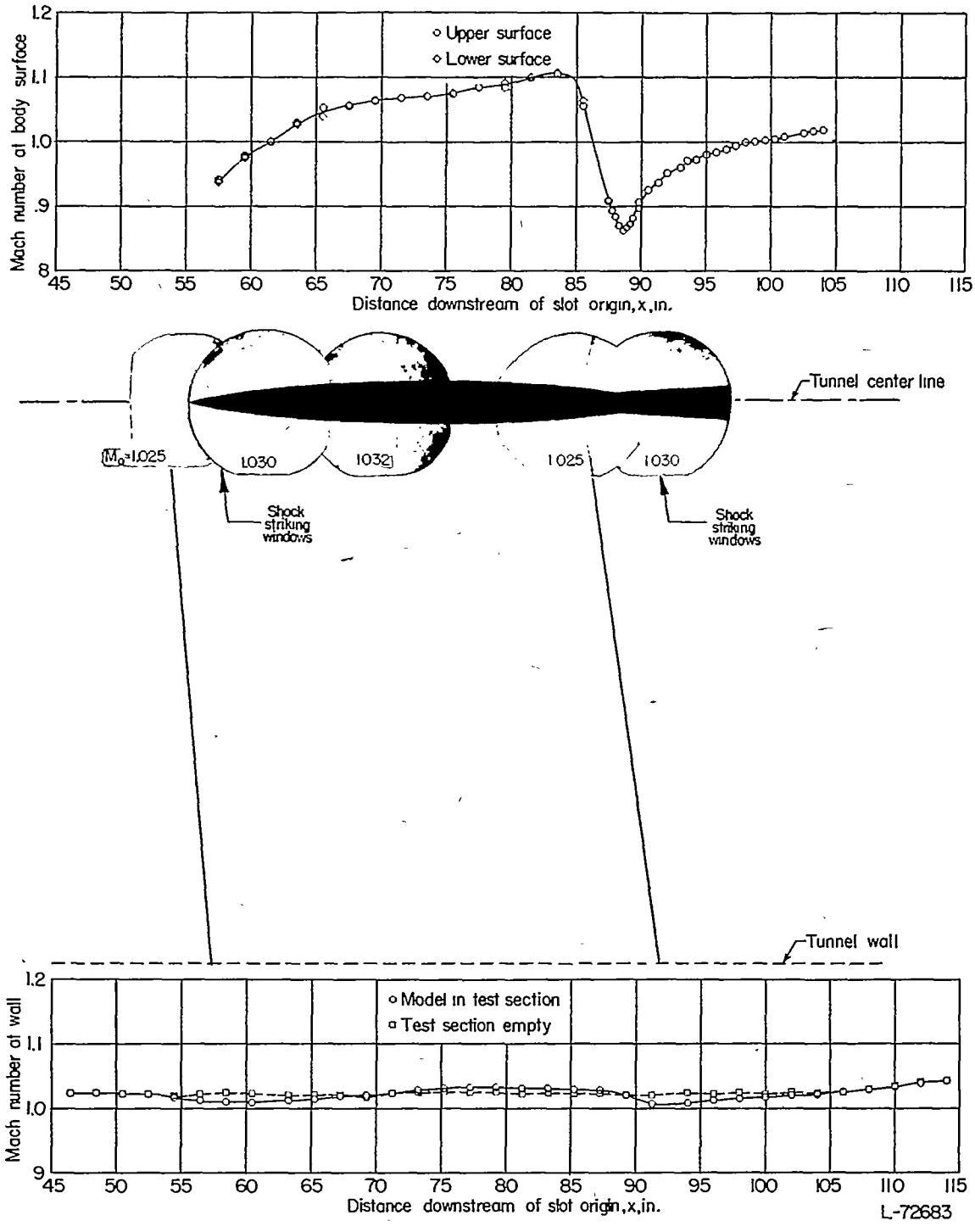

(e) M_o=1.025.

FIGURE 31.—Continued.

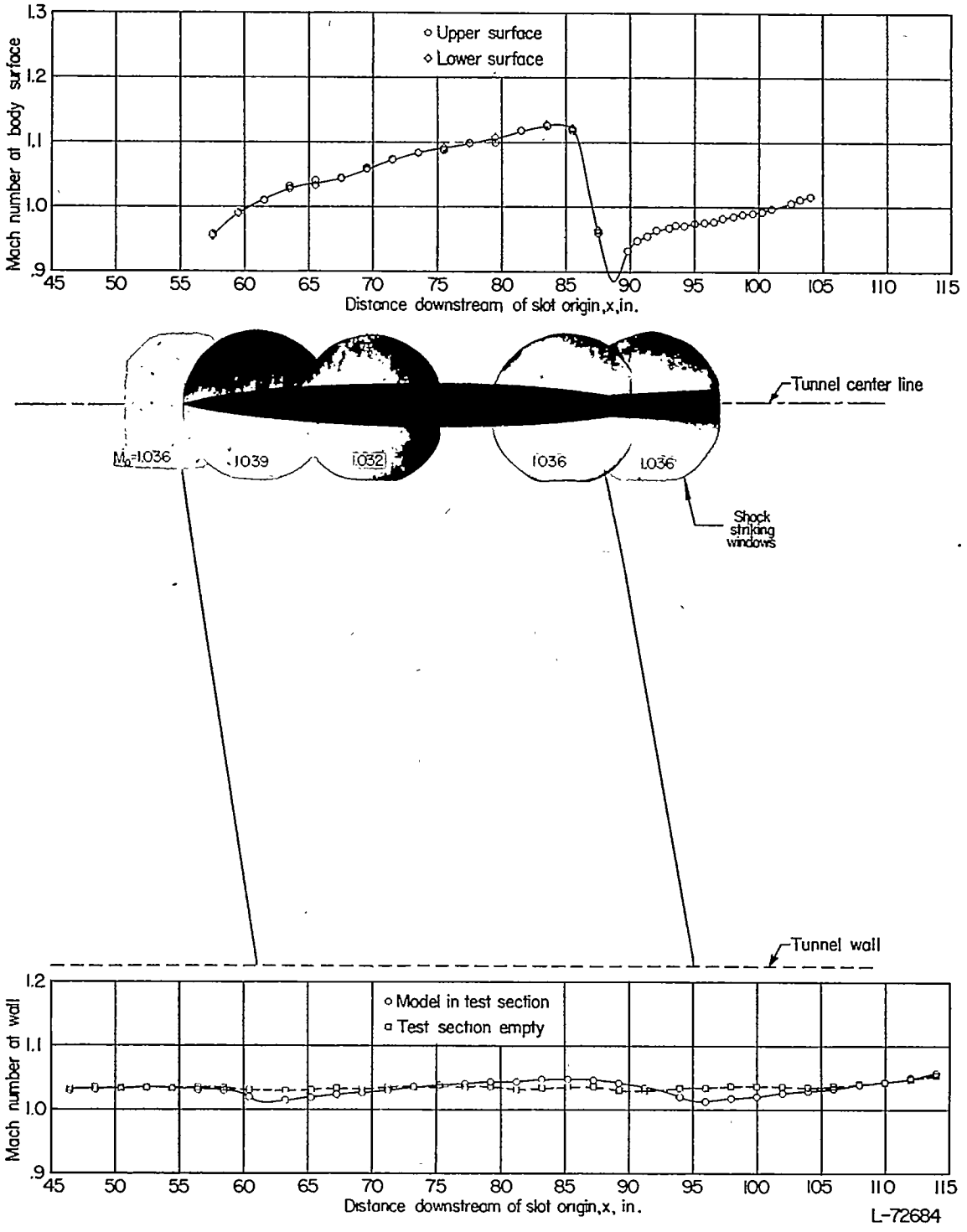

(f) M_o=1.036.

FIGURE 31.—Continued.

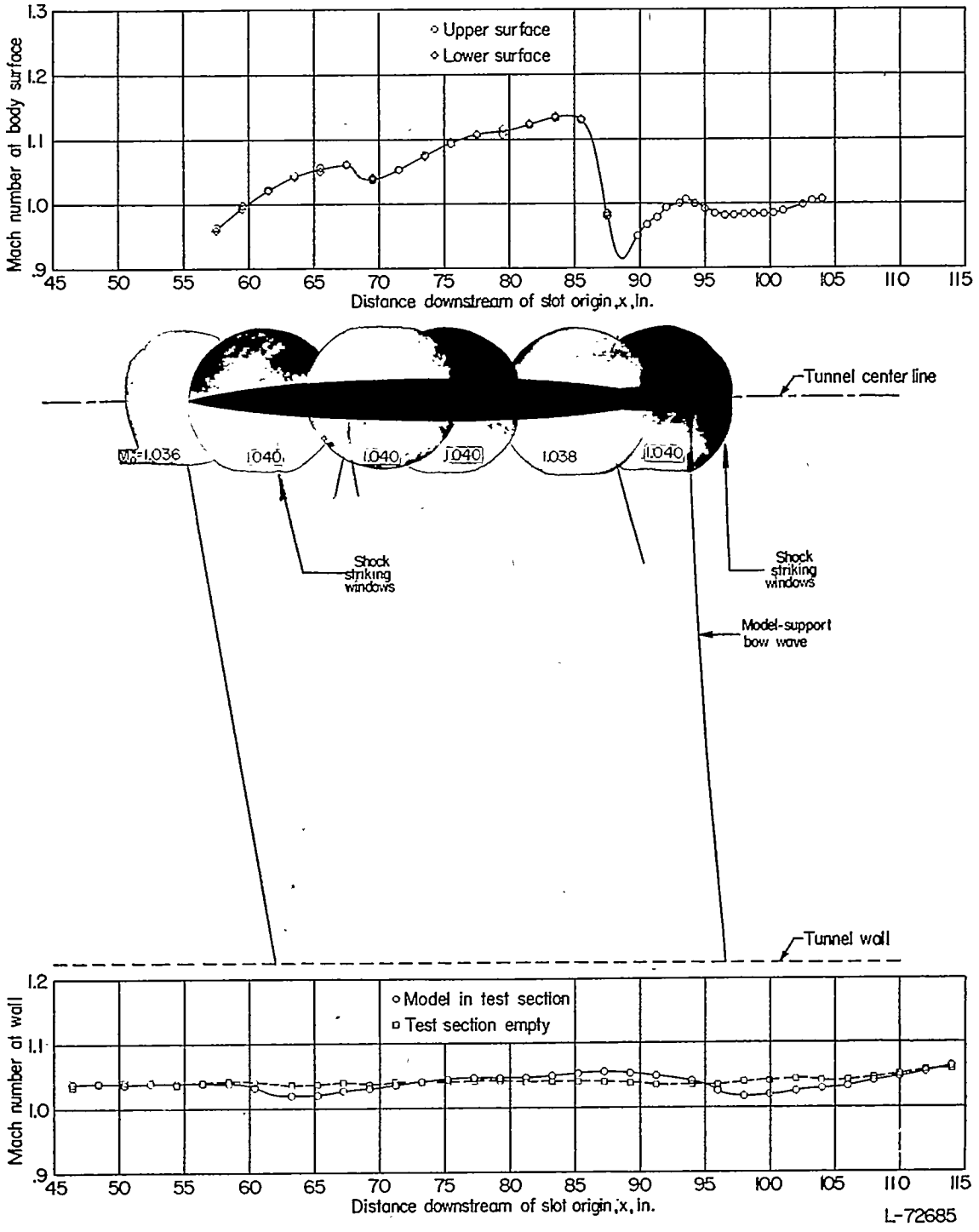

(g) M_o=1.042.

FIGURE 31.—Continued.

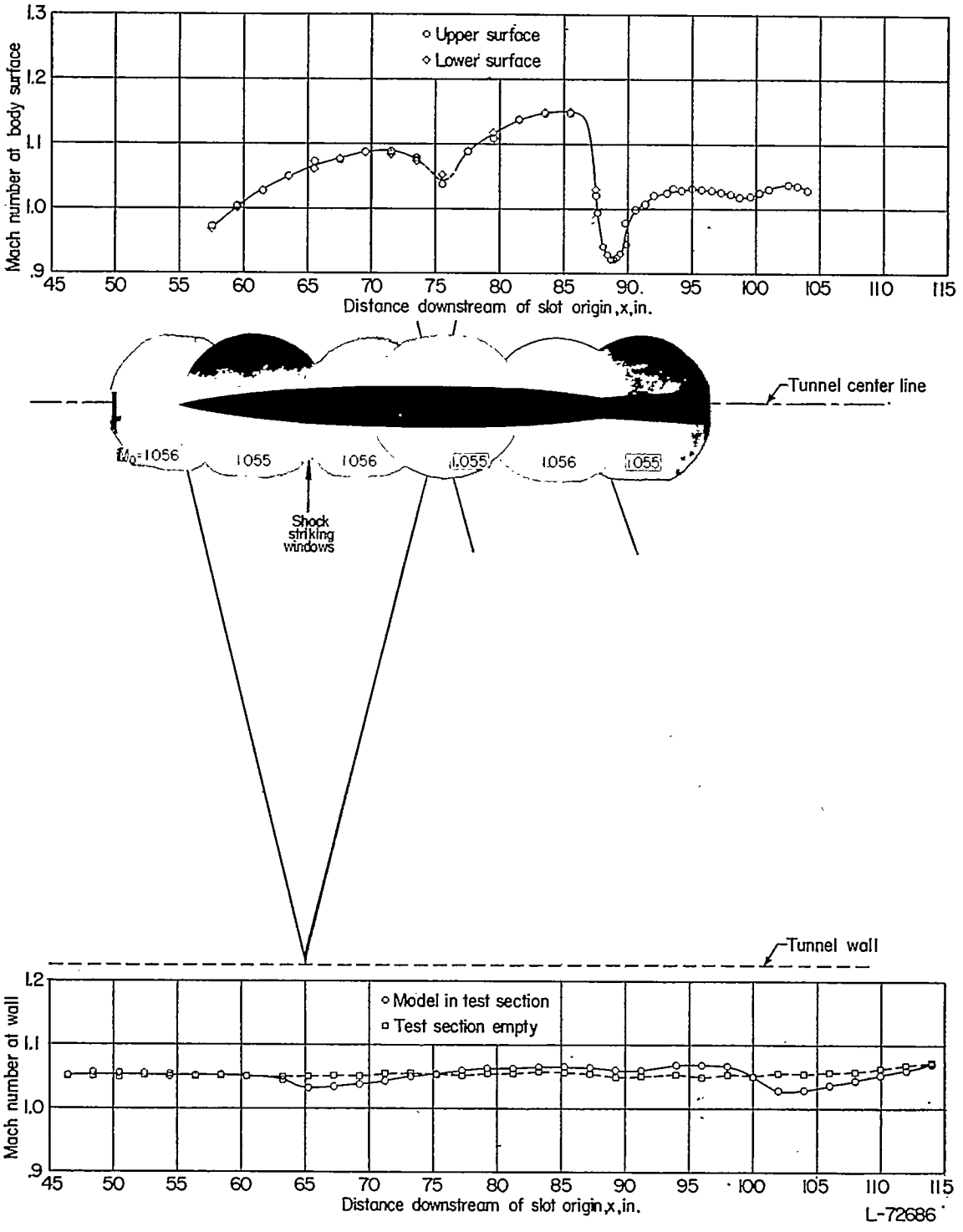

(h) $M_o = 1.056$.

FIGURE 31.—Continued.

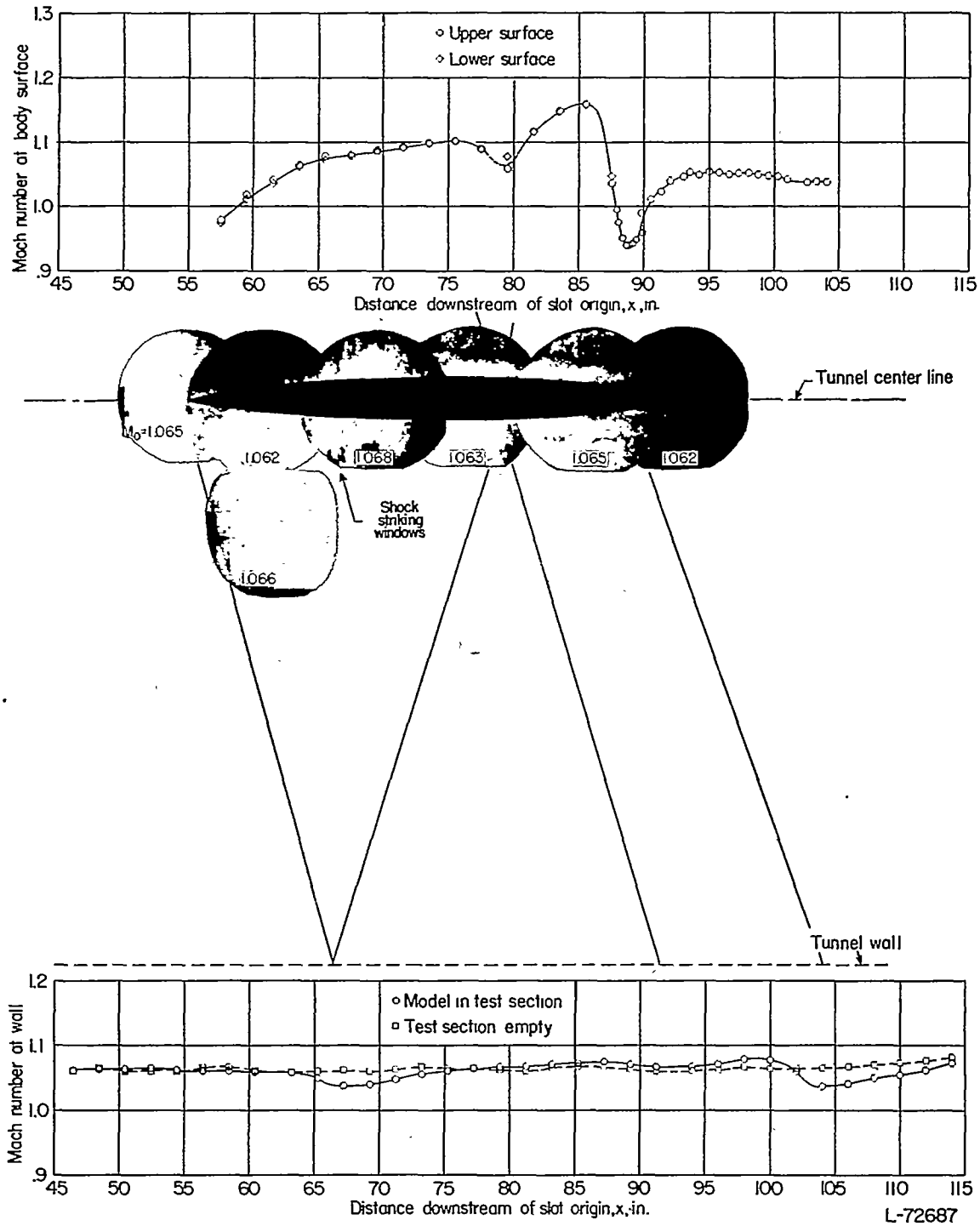

(i) M_o=1.065.

FIGURE 31.—Continued.

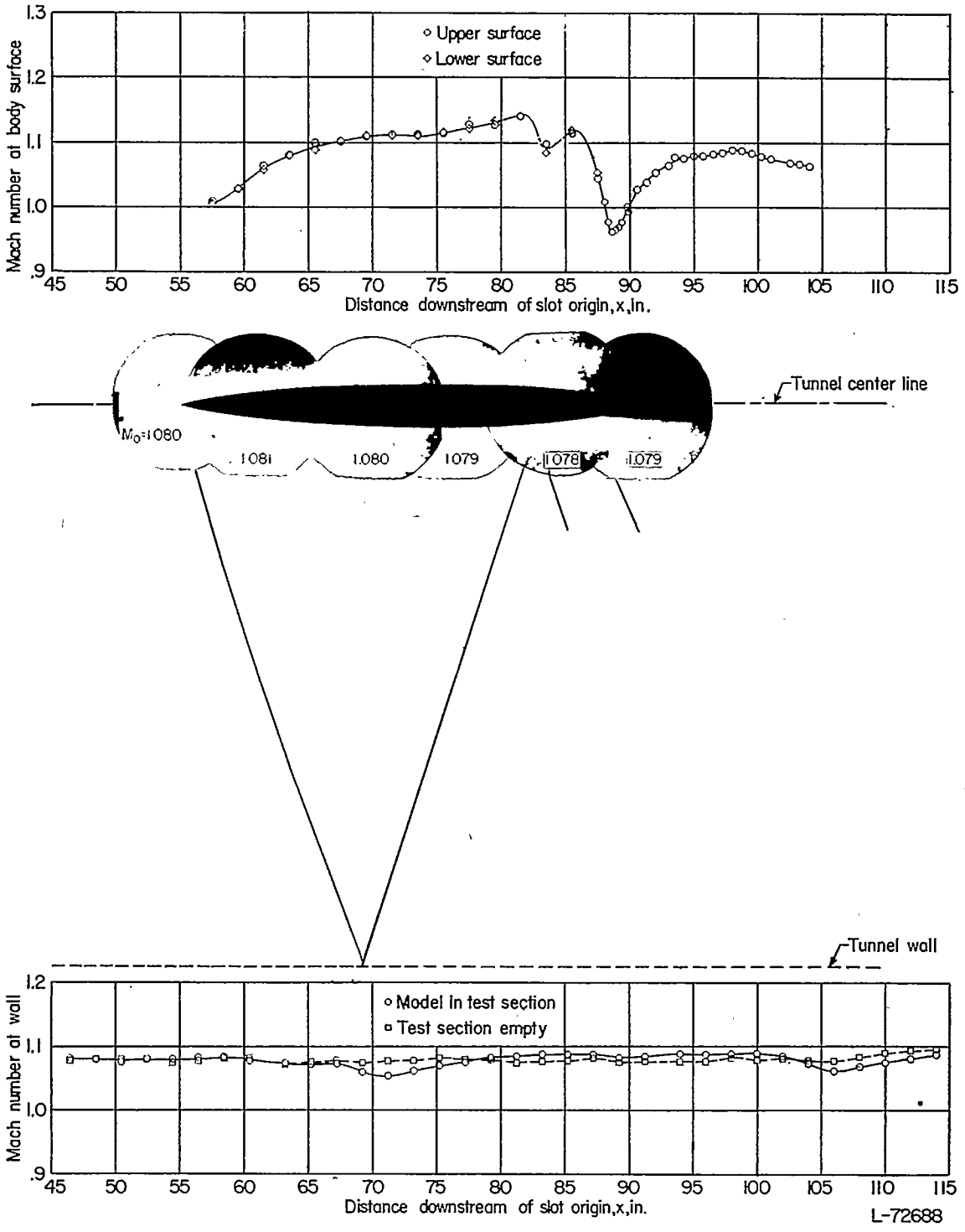

(j) M_o=1.080.

FIGURE 31.—Continued.

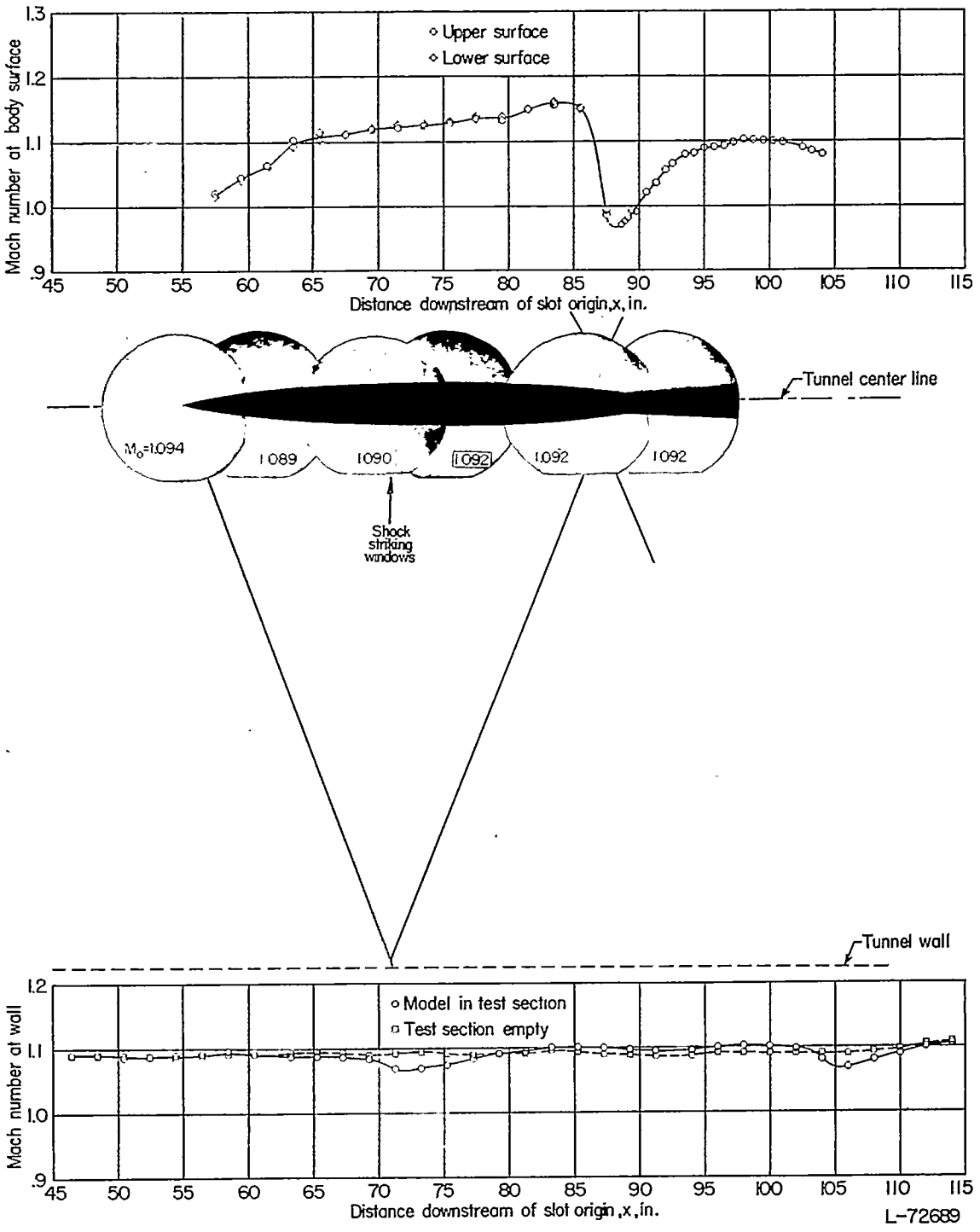

(k) M_o=1.092.

FIGURE 31.—Continued.

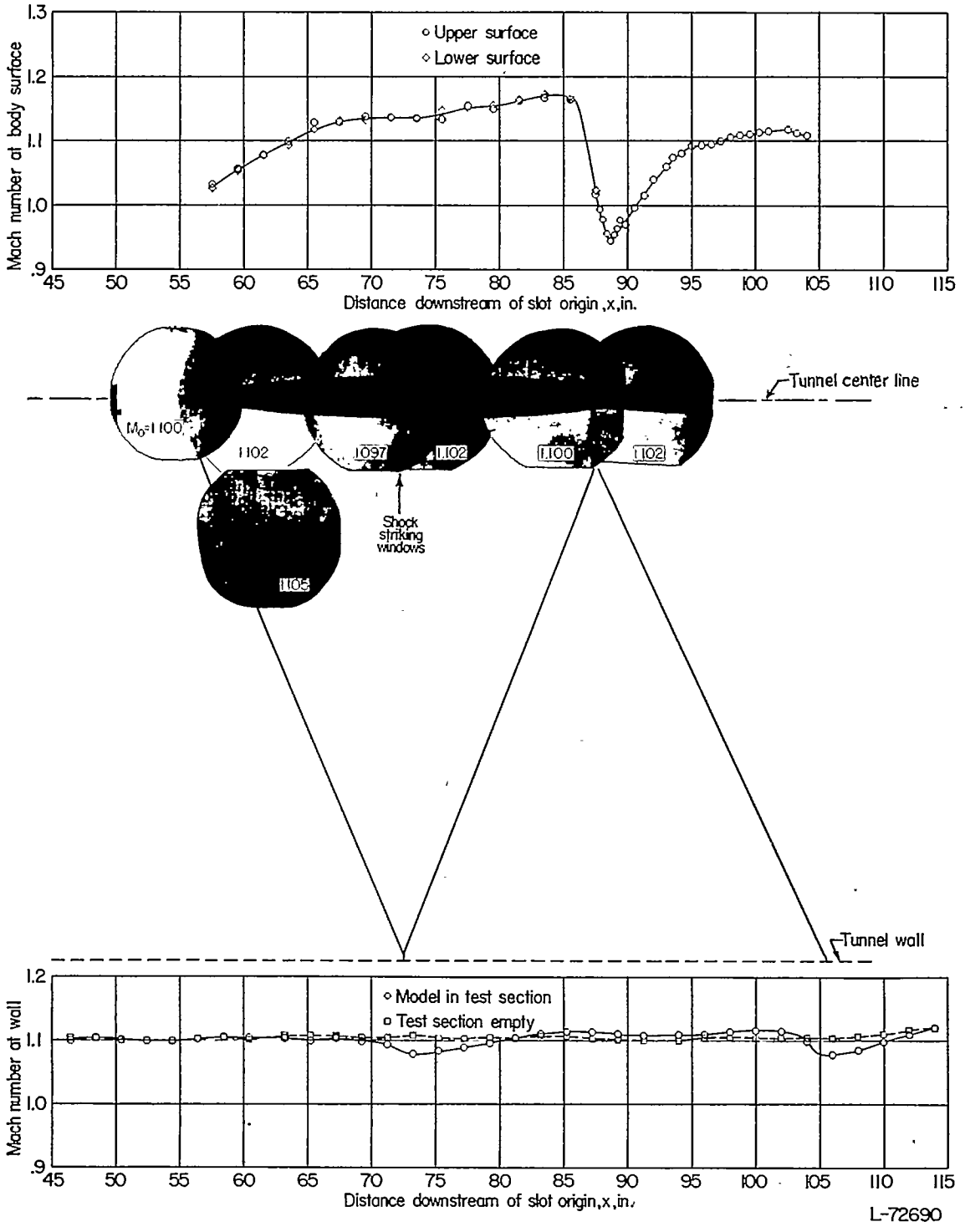

(*l*) M_o=1.105.

FIGURE 31.—Continued.

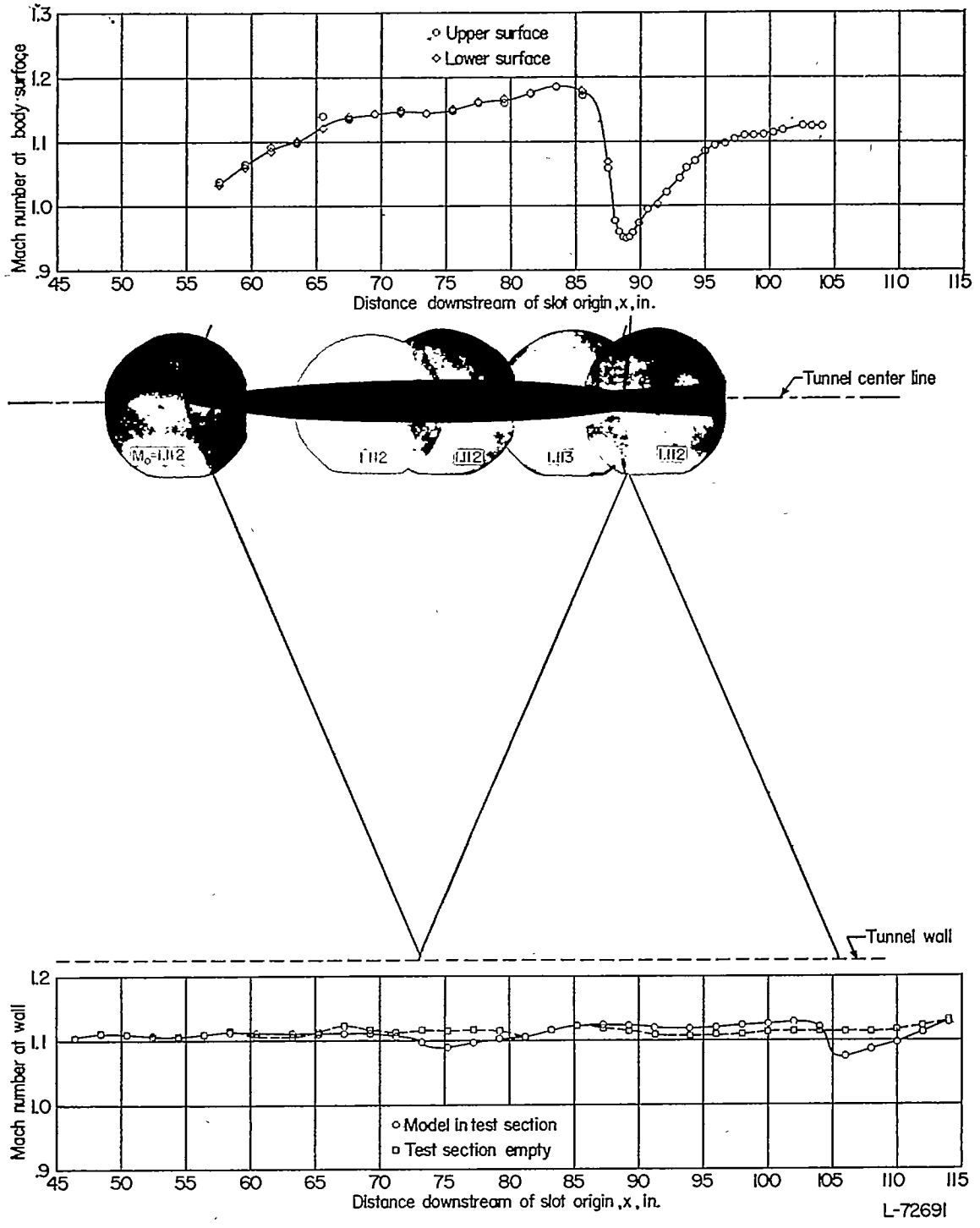

(m) $M_o = 1.113$.

FIGURE 31.—Continued.

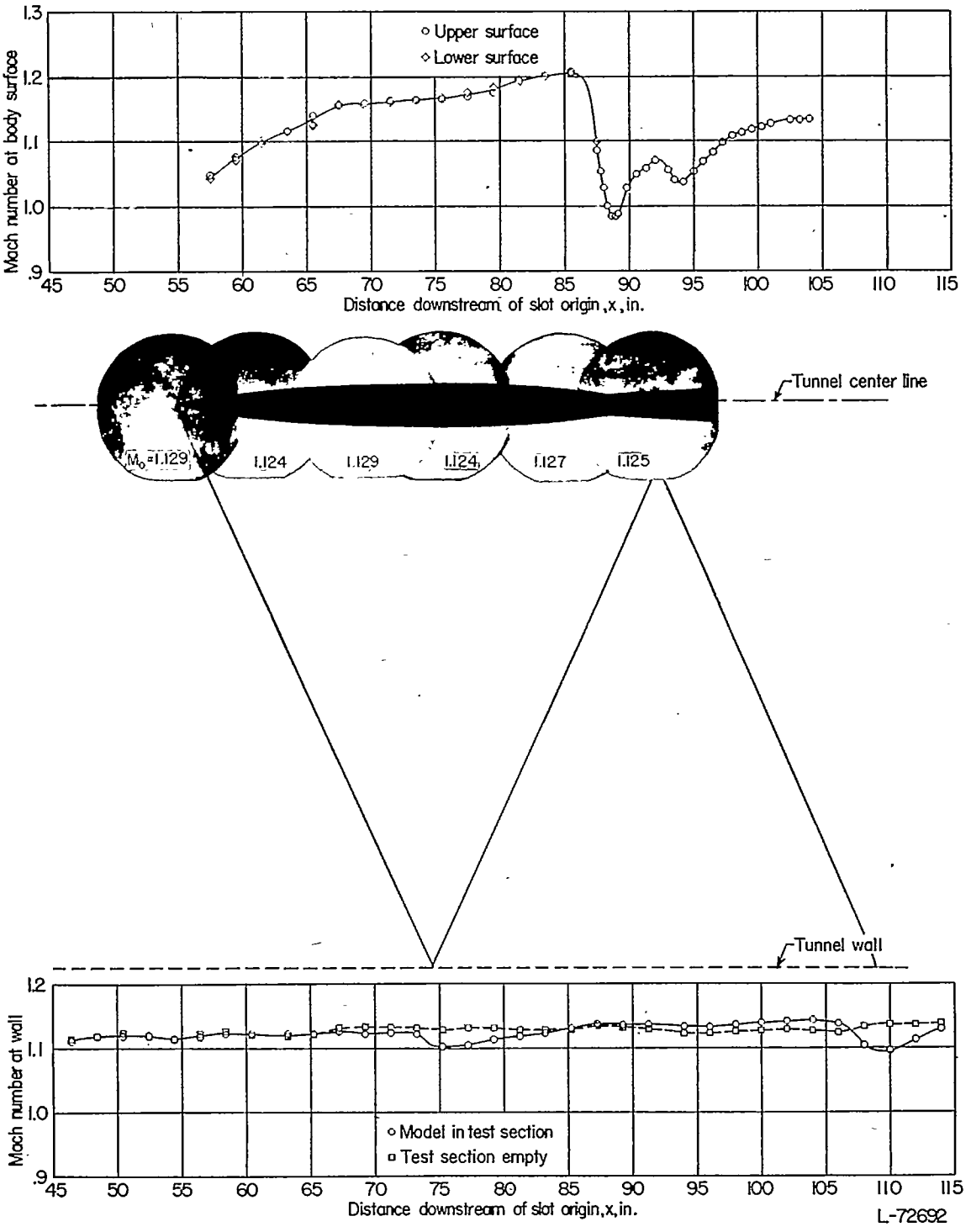

(n) M_o=1.129.

FIGURE 31.—Concluded.

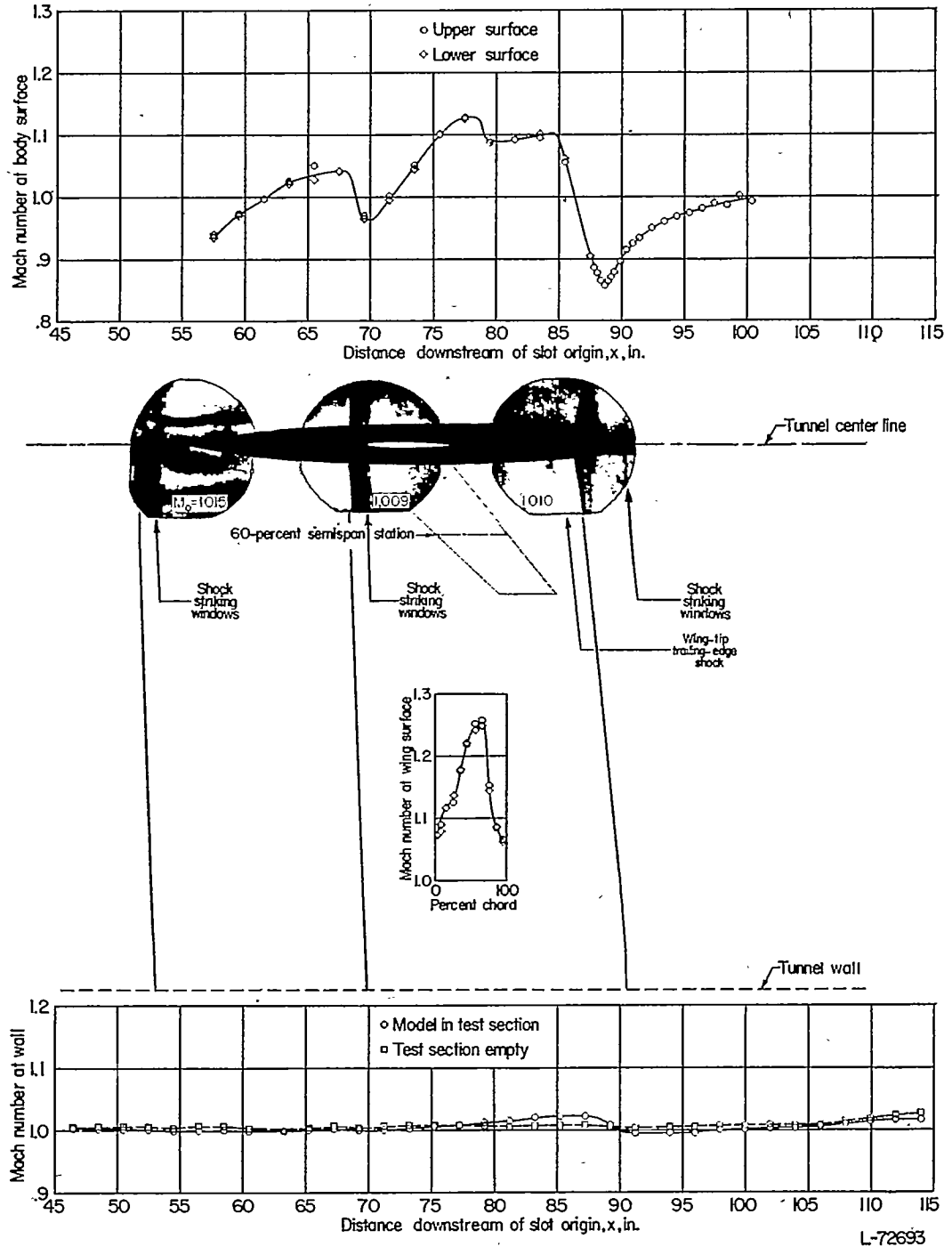

(a) M_o=1.009.

FIGURE 32.—Shock formations and reflections at low-supersonic speeds with wing-body model at center line of slotted test section. α=0°; diffuser-entrance nose A; slot shape 11.

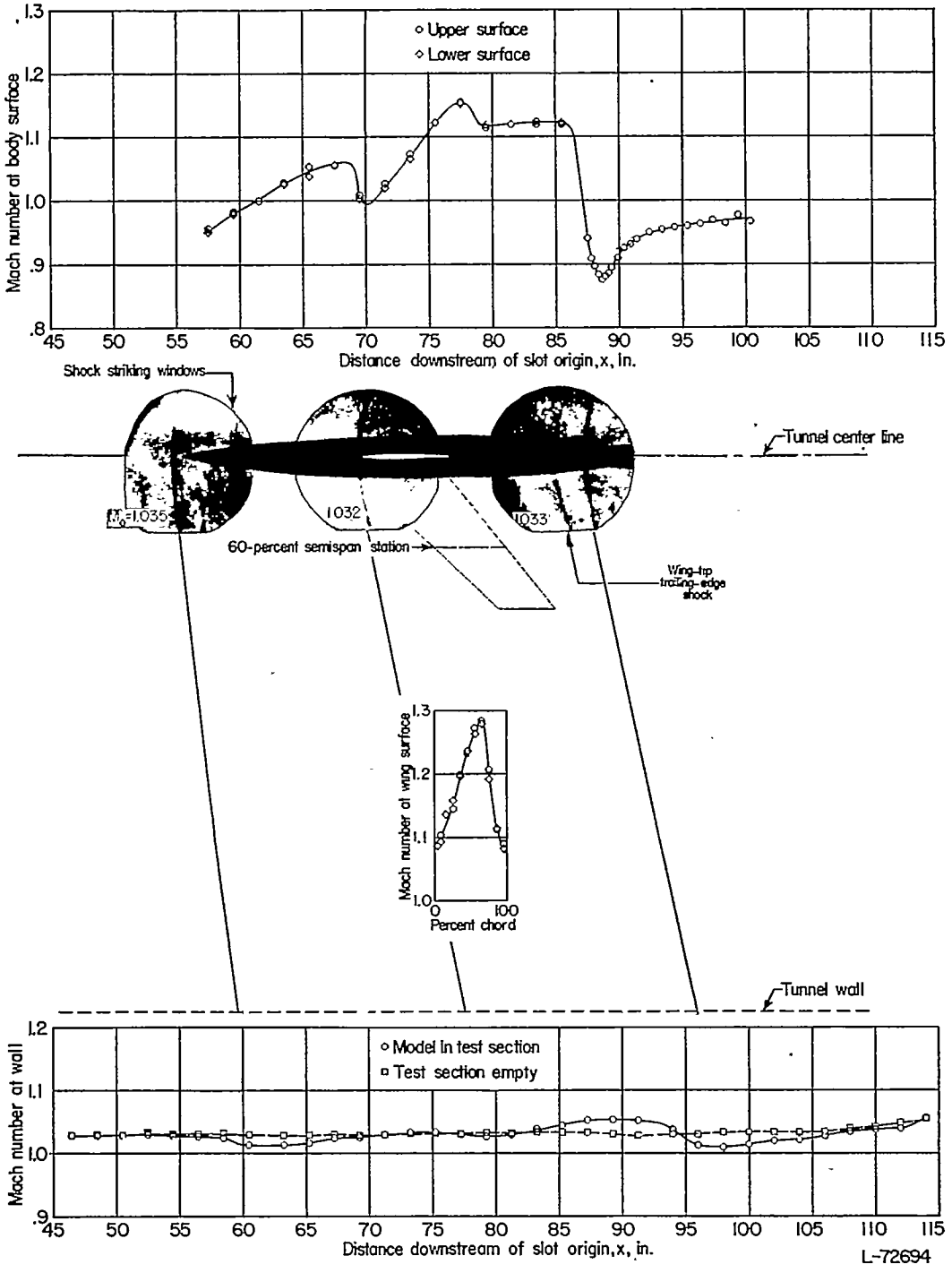

(b) $M_o = 1.034$.

FIGURE 32.—Continued.

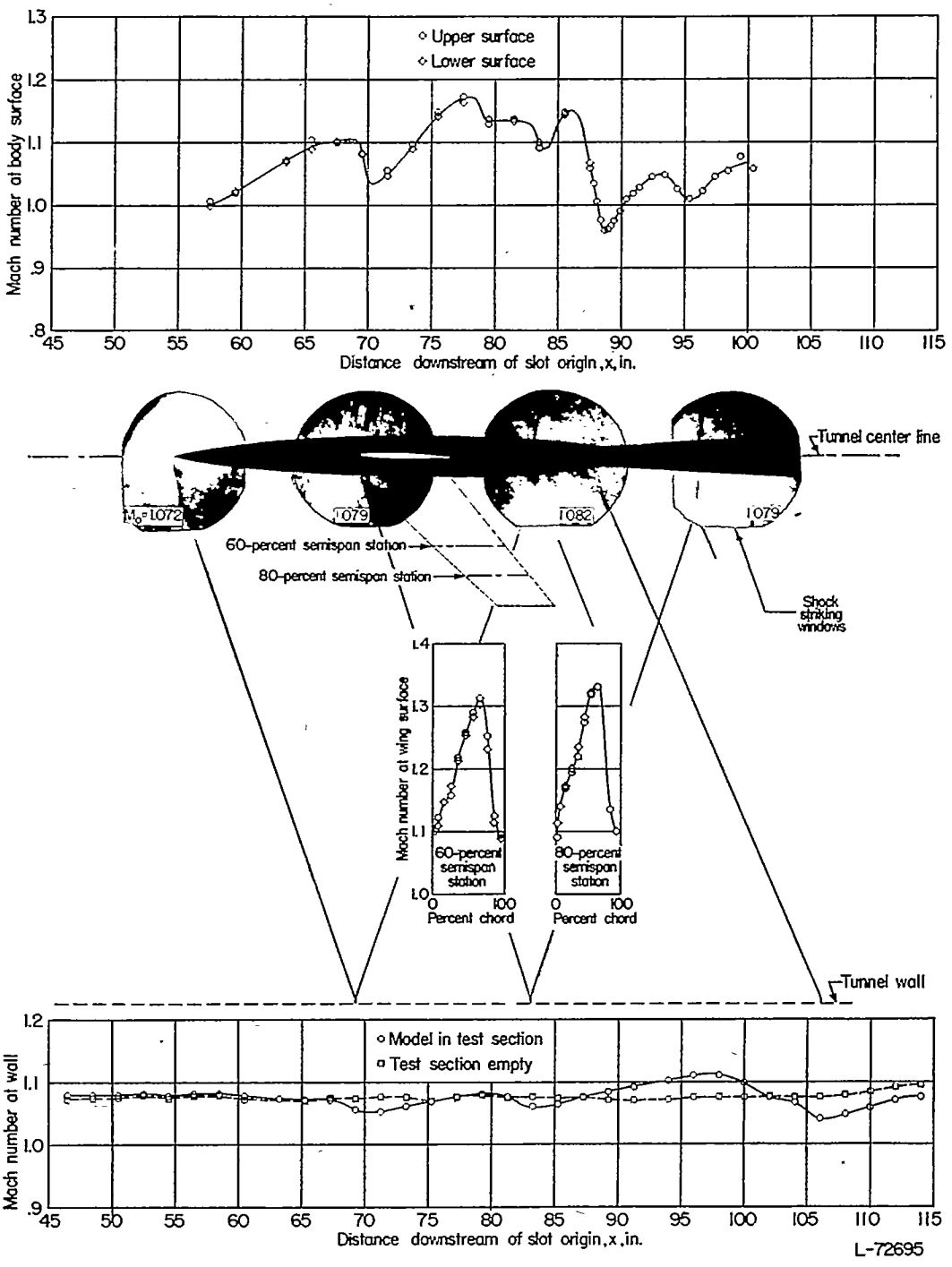

(c) M_o=1.079.

FIGURE 32.—Continued.

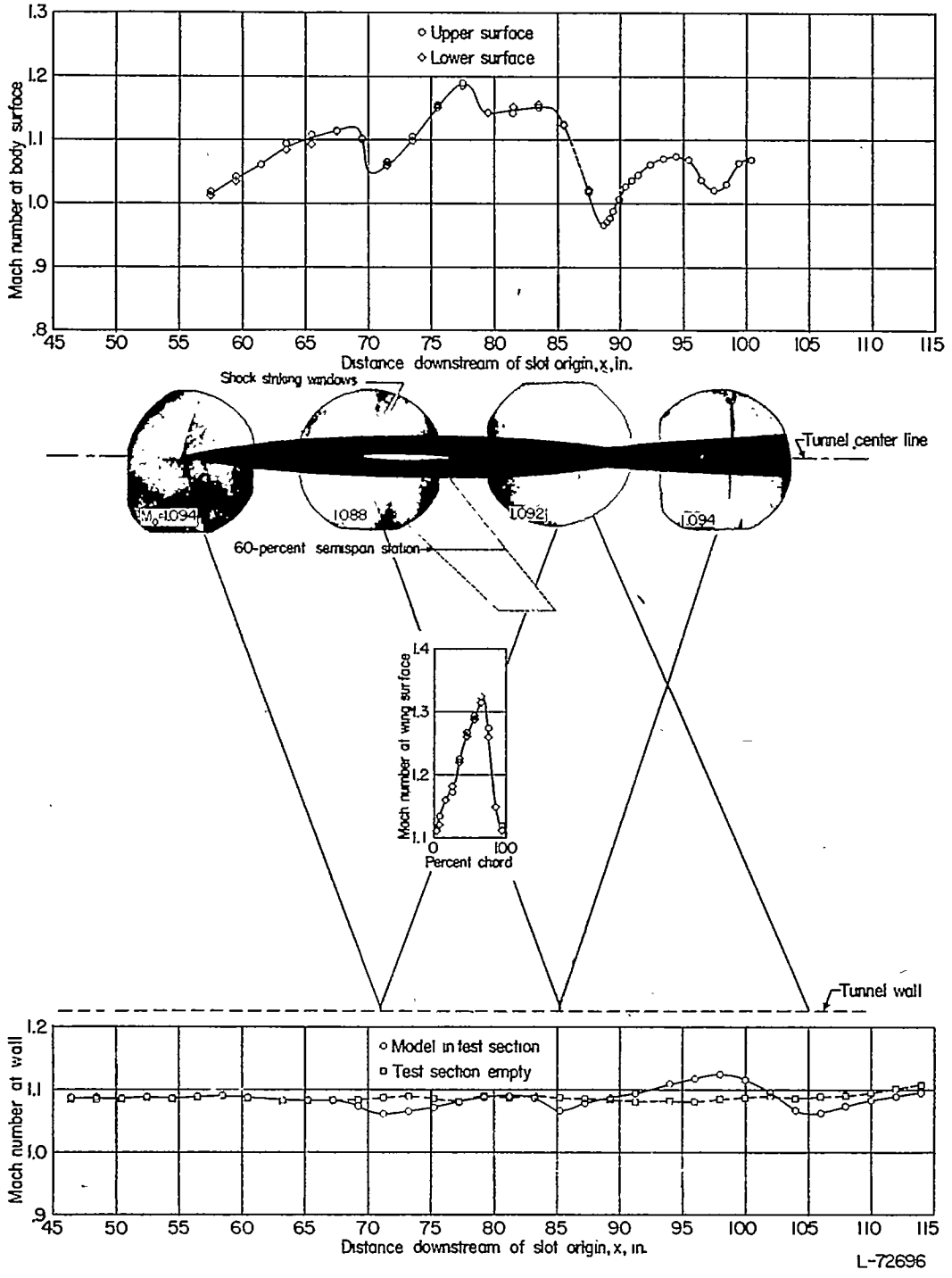

(d) M_o=1.088.

FIGURE 32.—Continued.

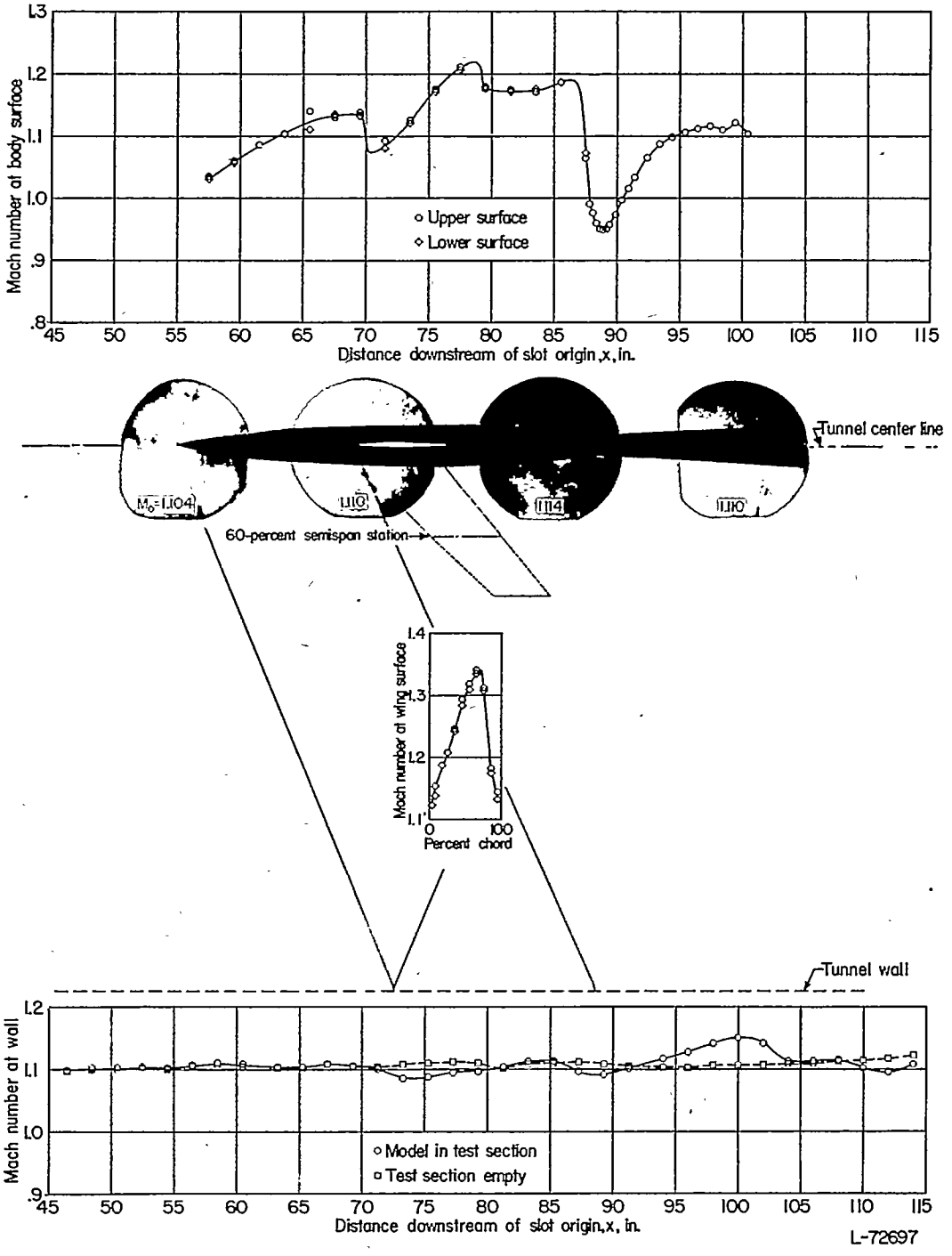

(e) M_o=1.110.

FIGURE 32.—Continued.

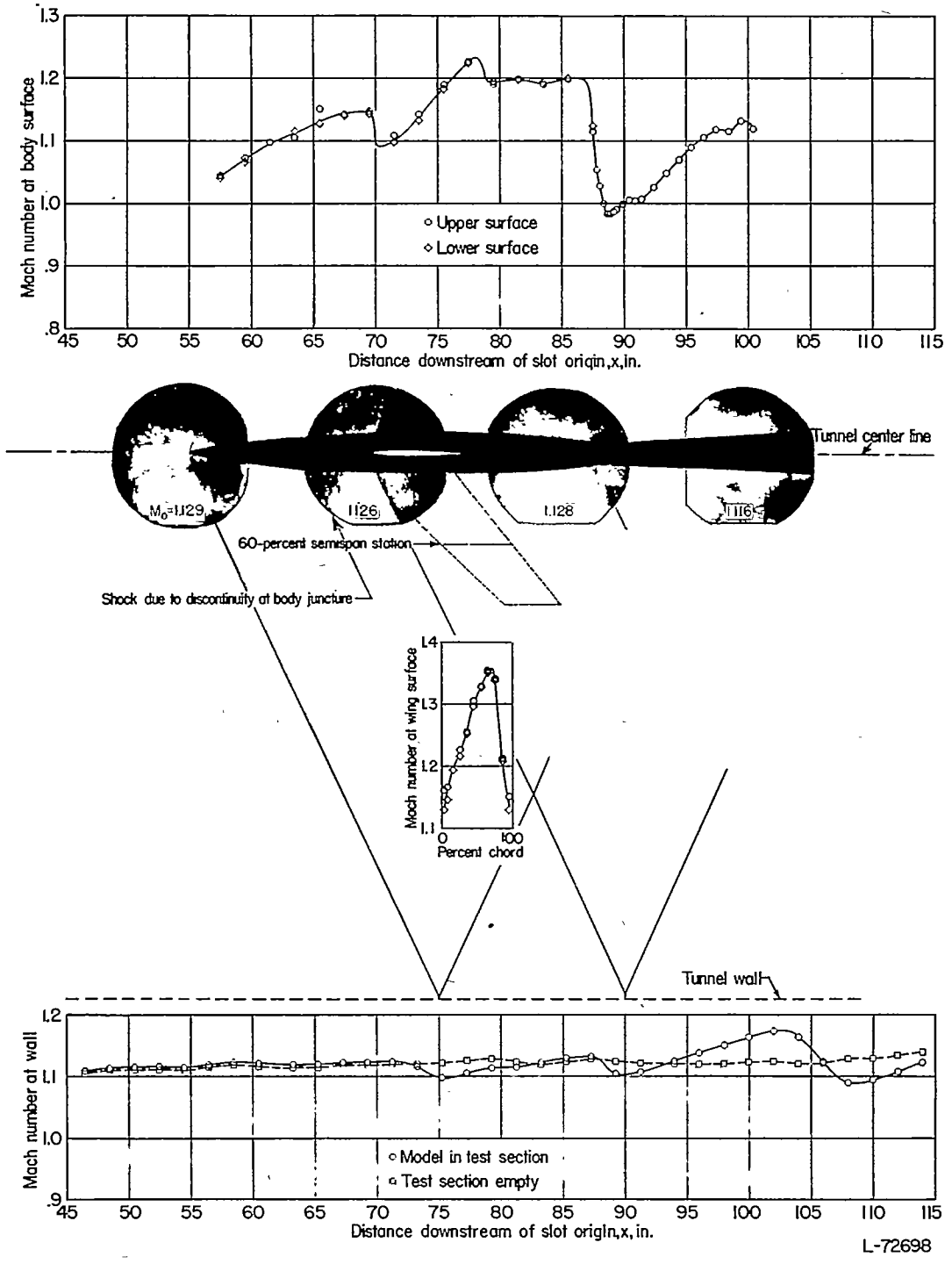

(f) M_o=1.126.

FIGURE 32.—Concluded.

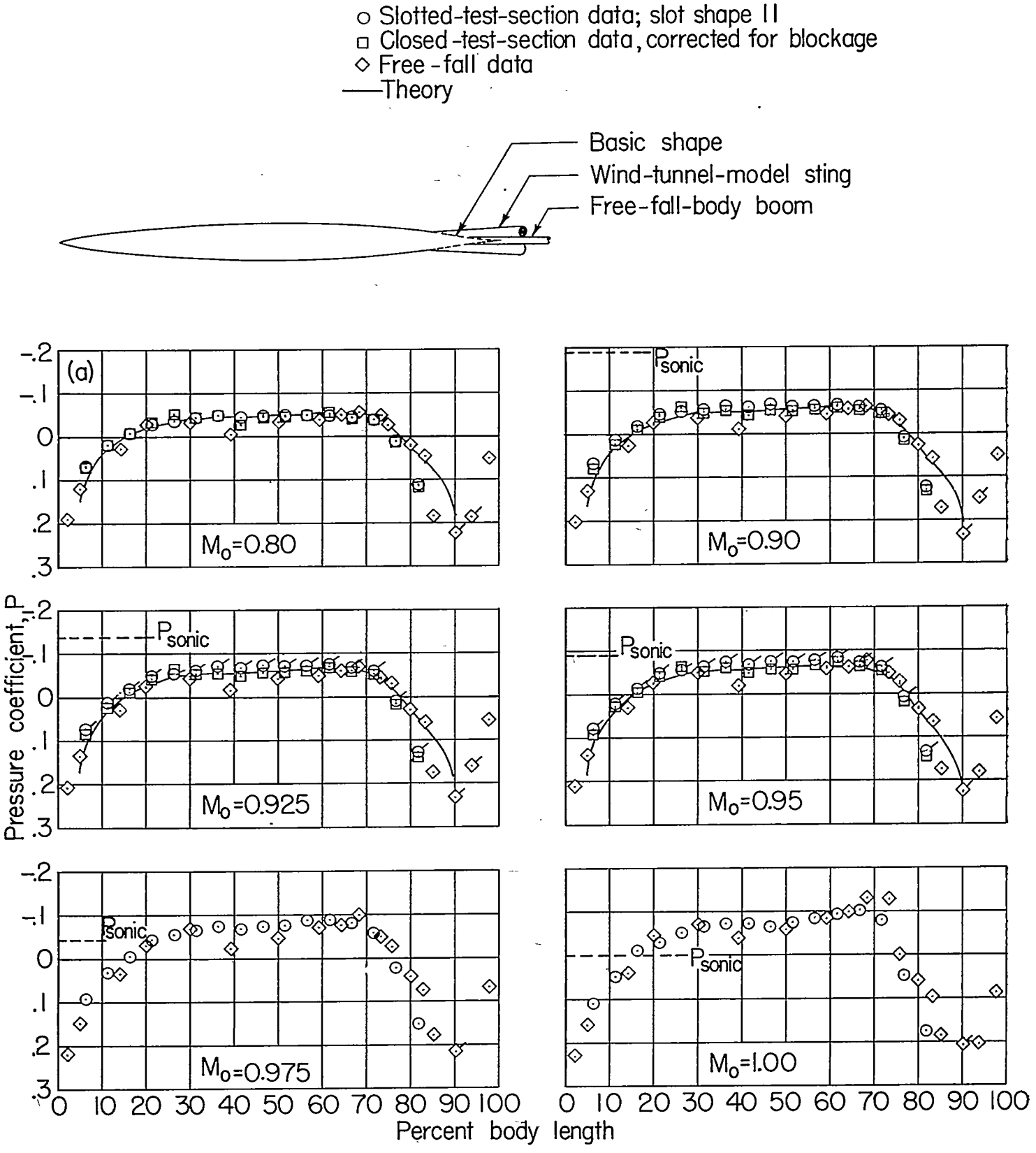

(a) Subsonic and sonic speeds.

FIGURE 33.—Comparison of body-surface pressure distributions obtained from tests of a body of revolution in the slotted test section with those from closed-test-section tests, free-fall tests, and theory. Flagged symbols indicate data obtained from faired curves.

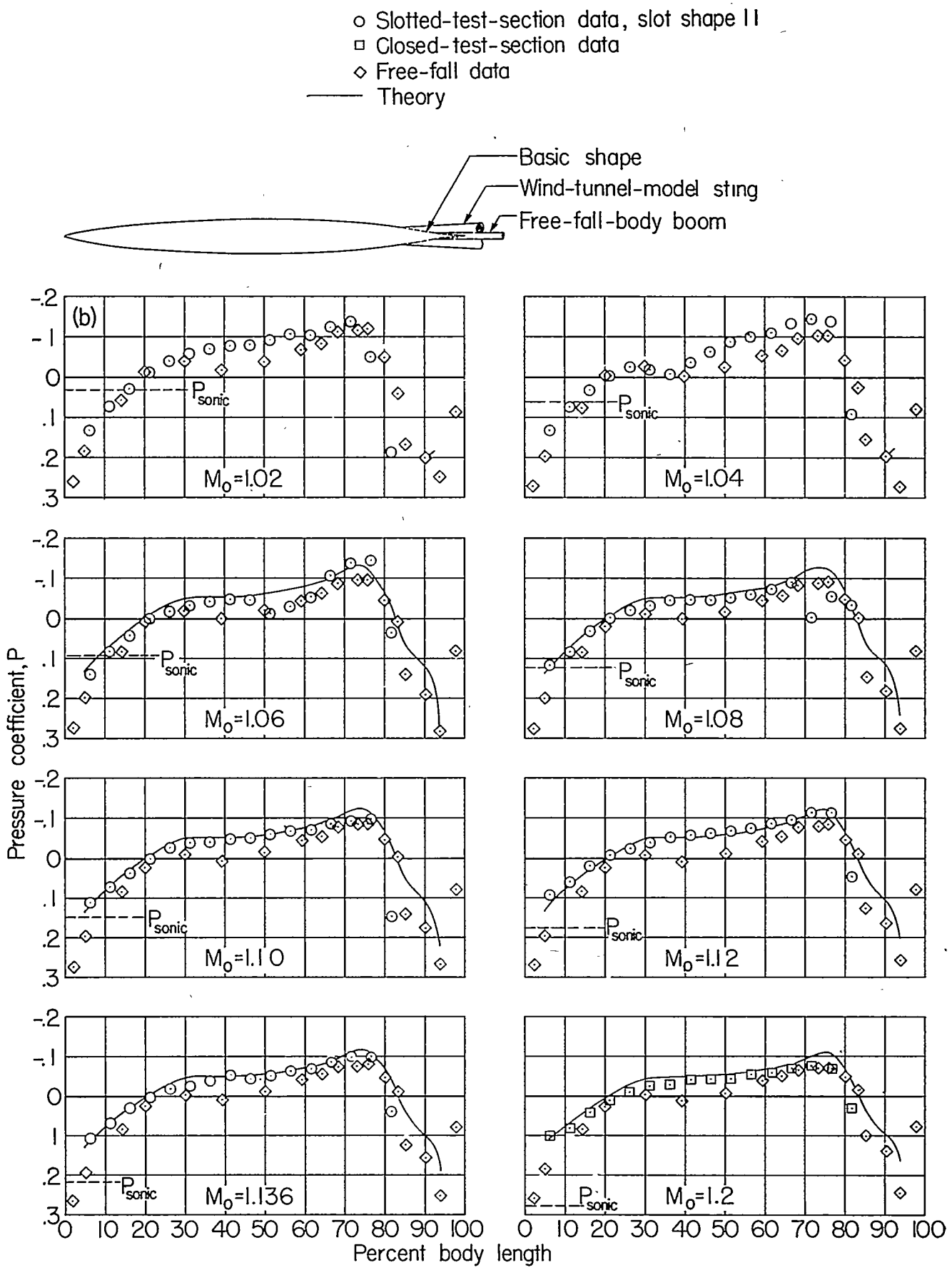

(b) Supersonic speeds.

FIGURE 33.—Concluded.

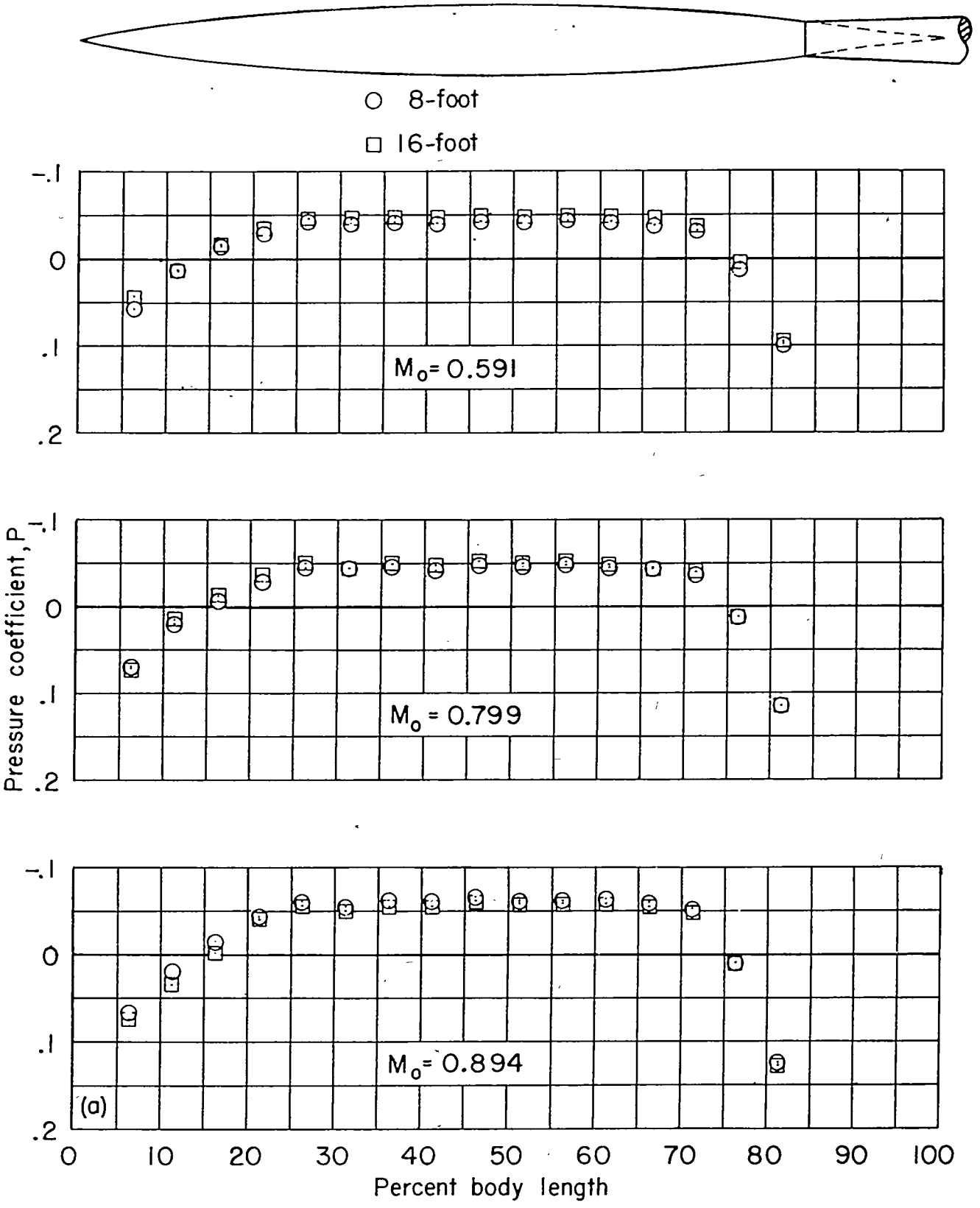

(a) Subsonic speeds (M_0 from 0.591 to 0.894).

FIGURE 34.—Comparison of body-surface pressure distributions obtained from tests of a body of revolution at zero angle of attack in the slotted test sections of the Langley 8-foot and 16-foot transonic tunnels.

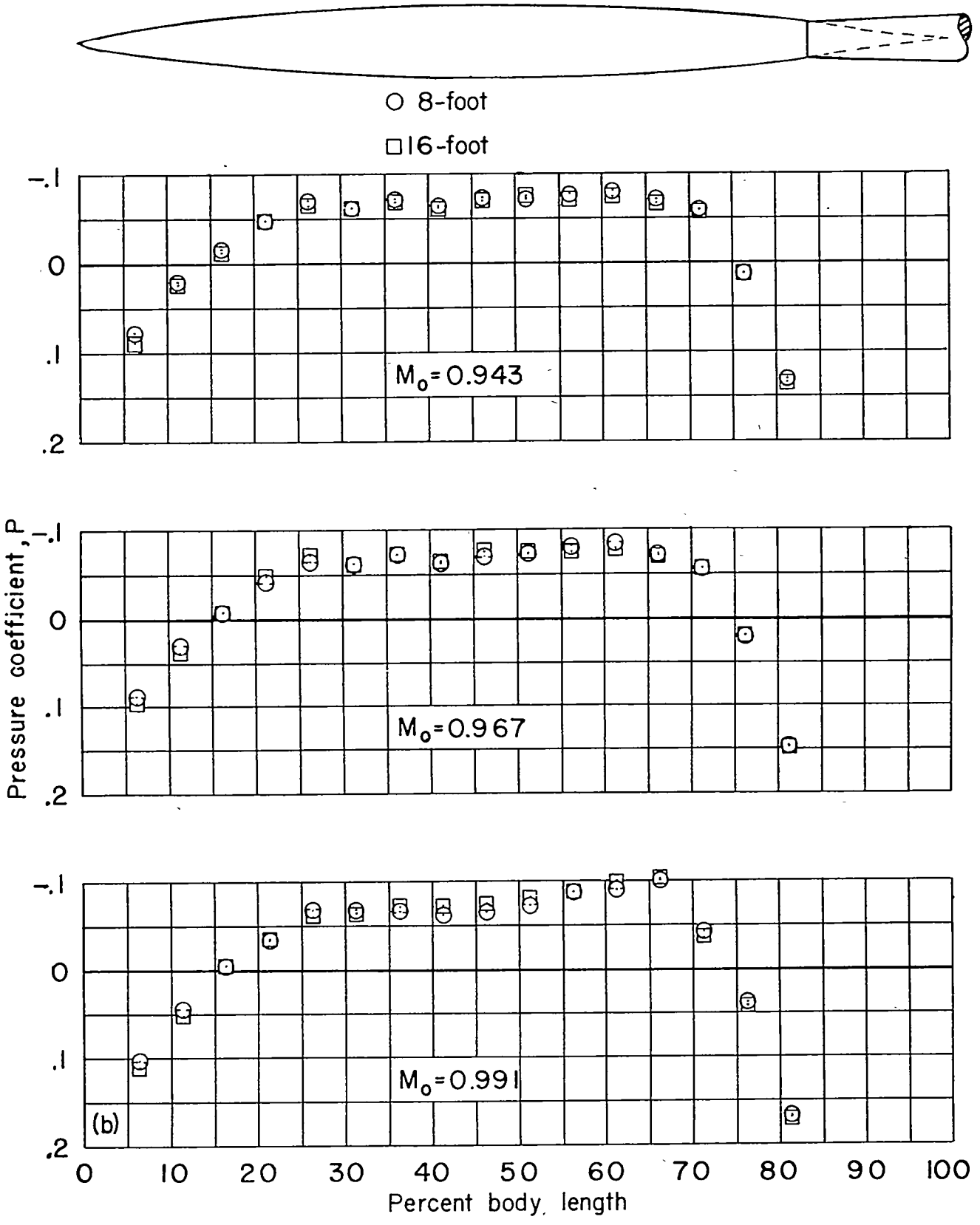

(b) Subsonic speeds (M_o from 0.943 to 0.991).

FIGURE 34.—Continued.

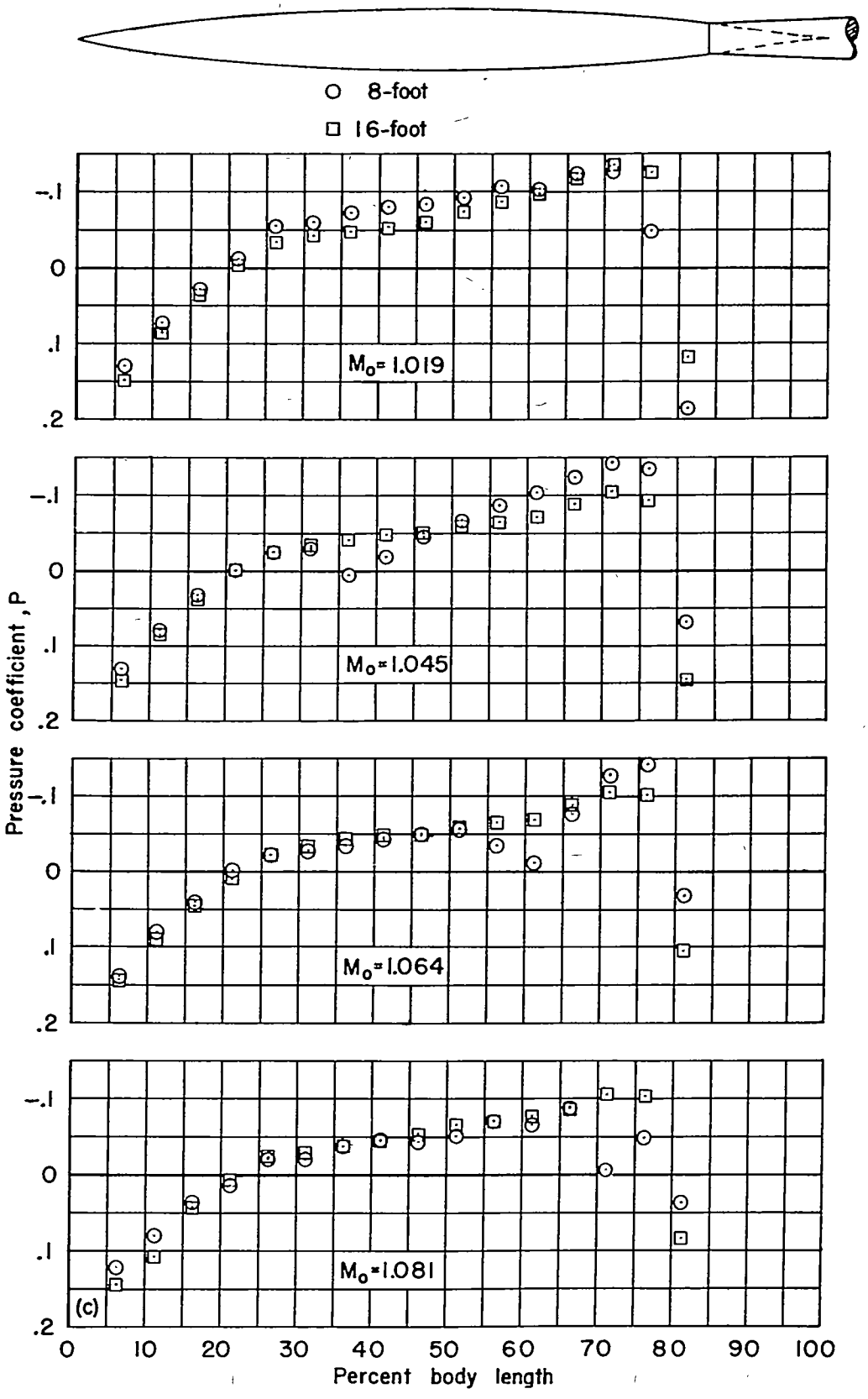

(c) Supersonic speeds (M_o from 1.019 to 1.081).

FIGURE 34.—Concluded.

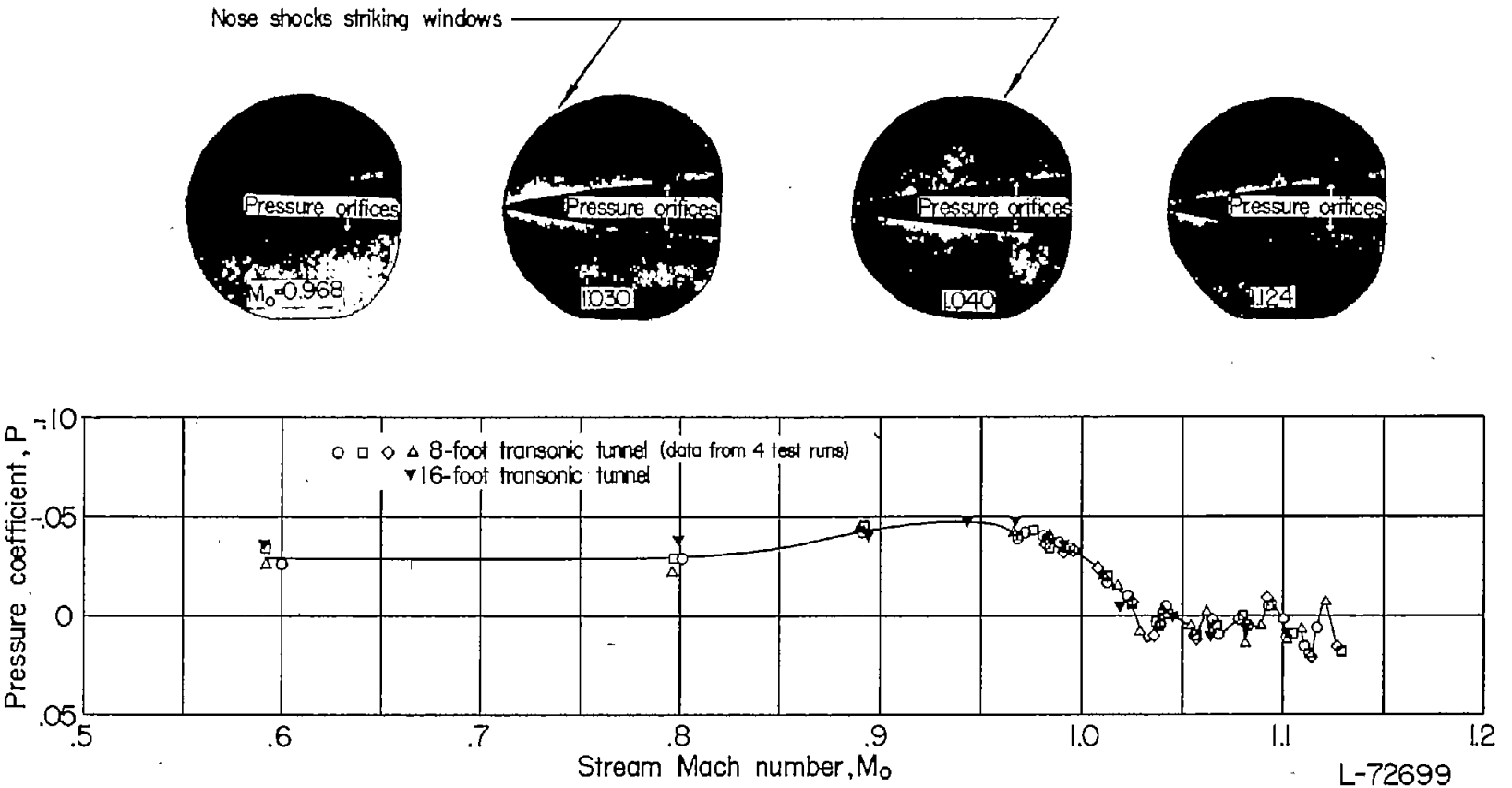

(a) $\frac{x}{l}$=0.2125.

FIGURE 35.—Variation with stream Mach number of the pressure coefficients at six axial stations on the body of revolution in the slotted test sections of the Langley 8-foot and 16-foot transonic tunnels.

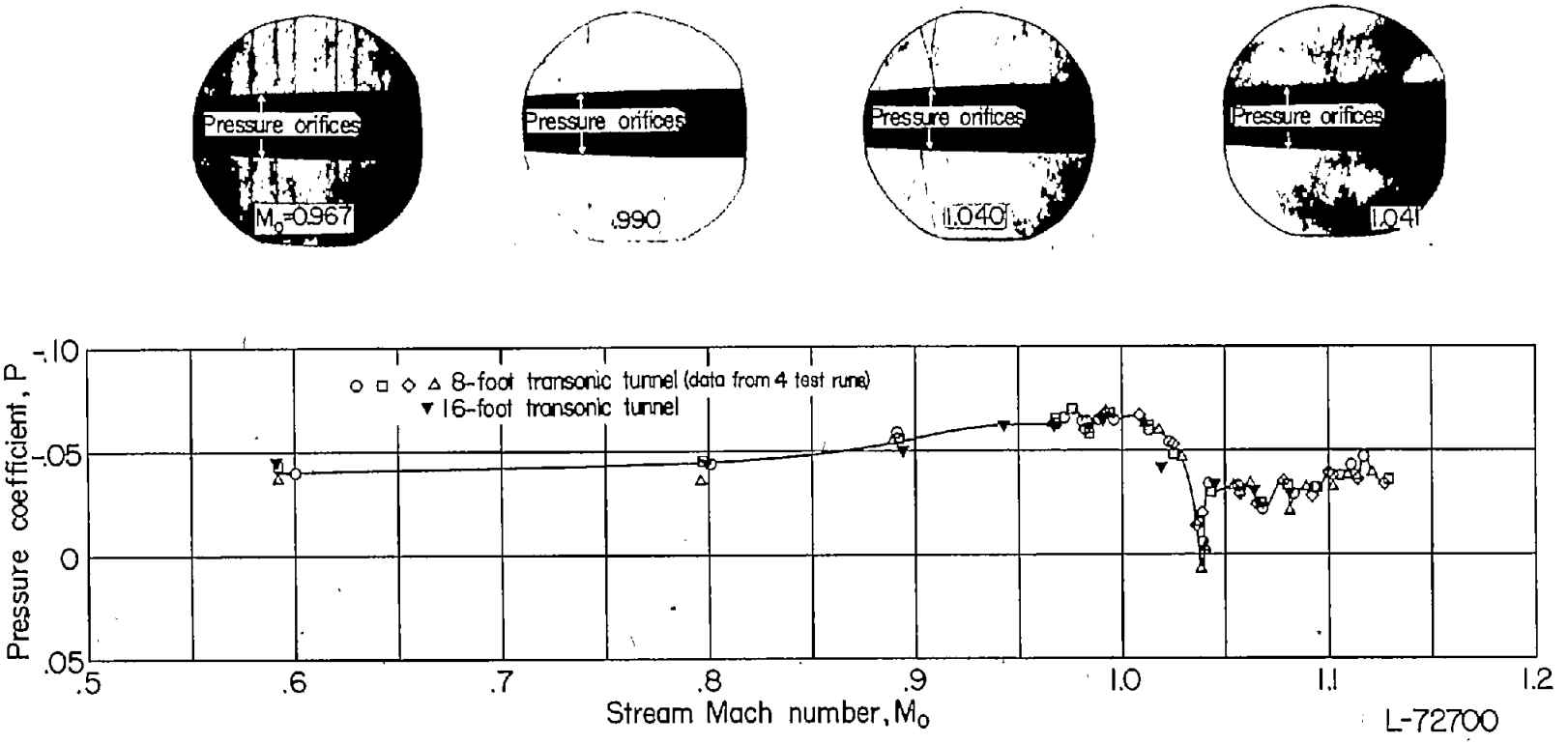

(b) $\frac{x}{l}$=0.3125.

FIGURE 35.—Continued.

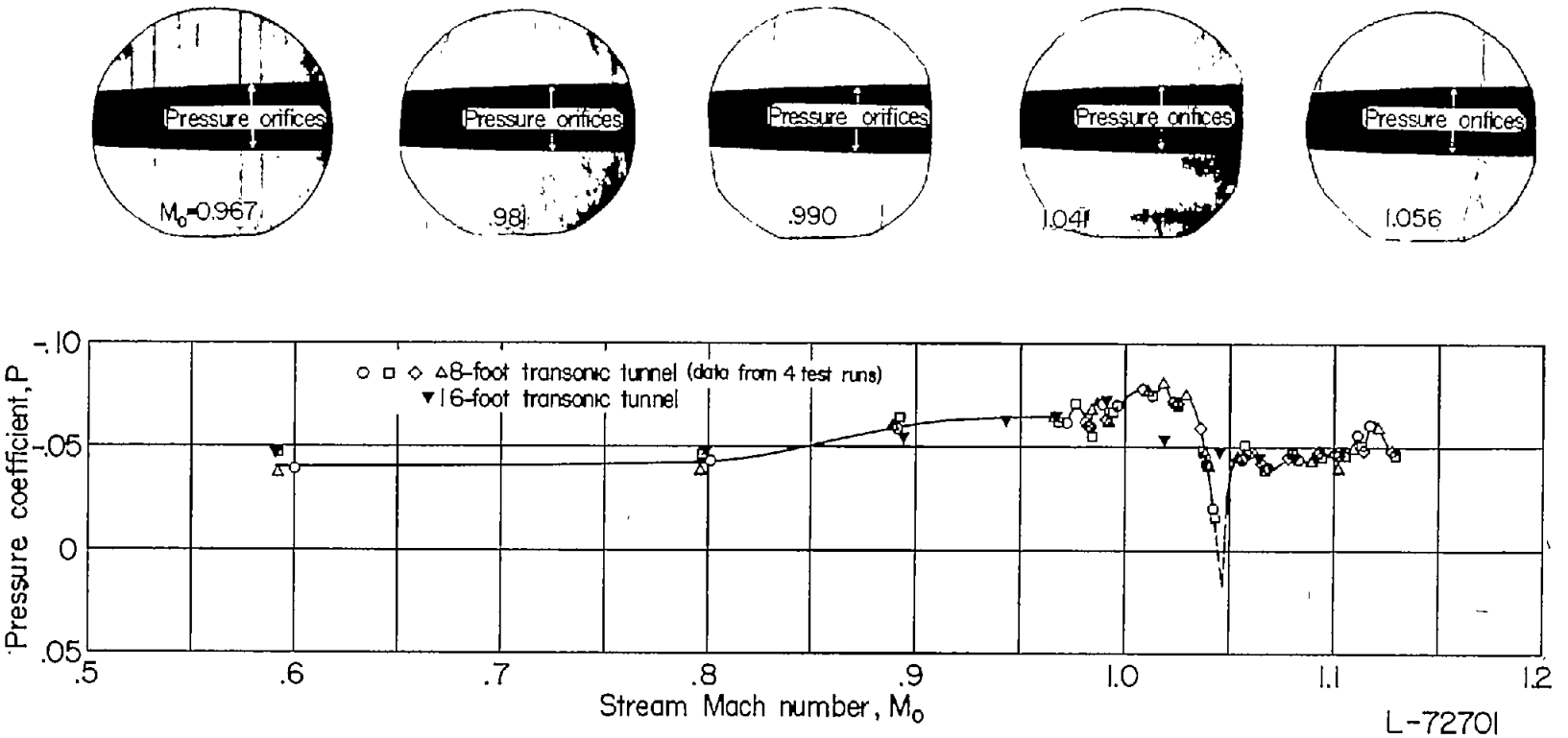

(o) $\frac{x}{l}$ = 0.4125.

FIGURE 35.—Continued.

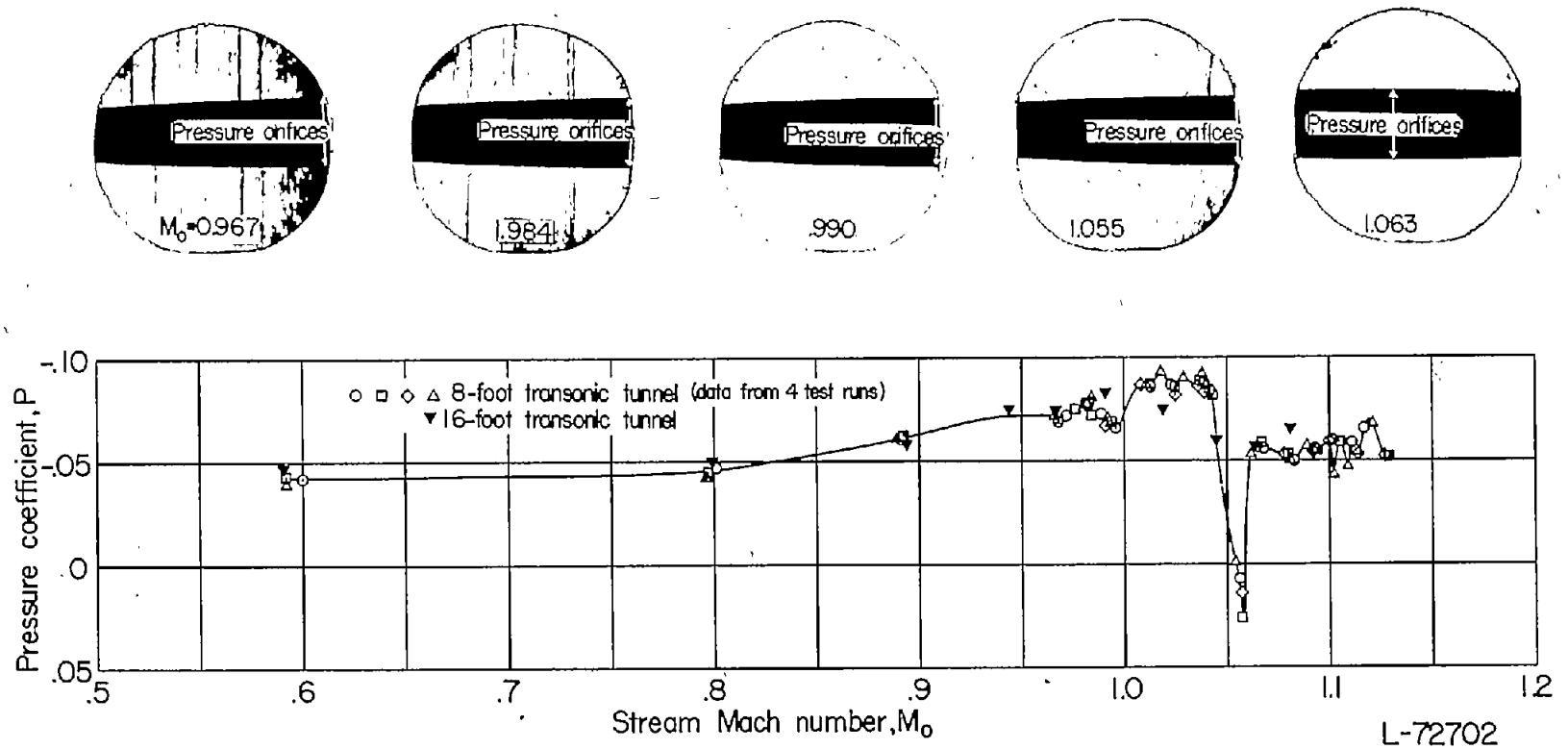

(d) $\frac{x}{l}=0.5125$.

FIGURE 35.—Continued.

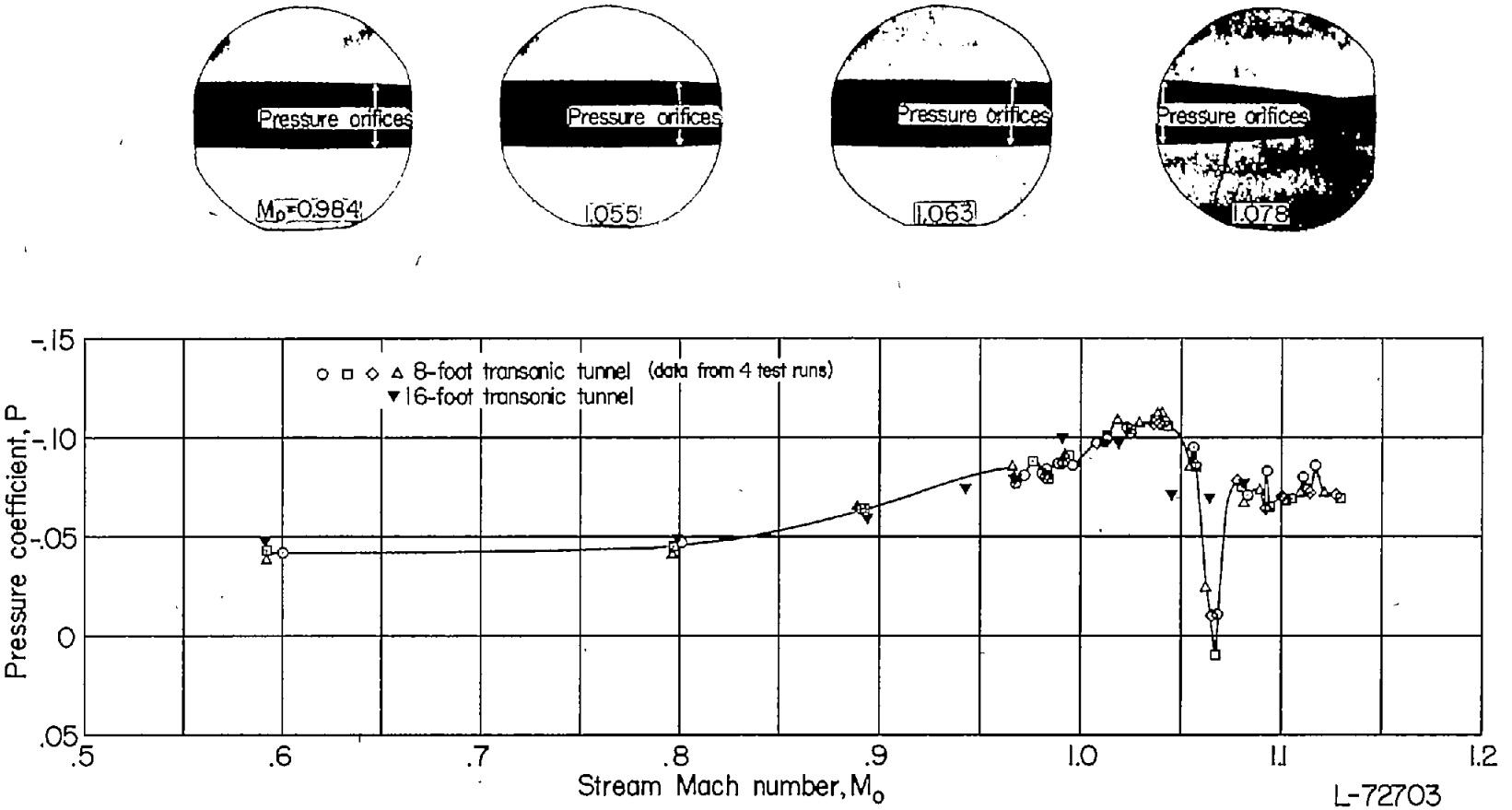

(e) $\frac{x}{l}$=0.6125.

FIGURE 35.—Continued.

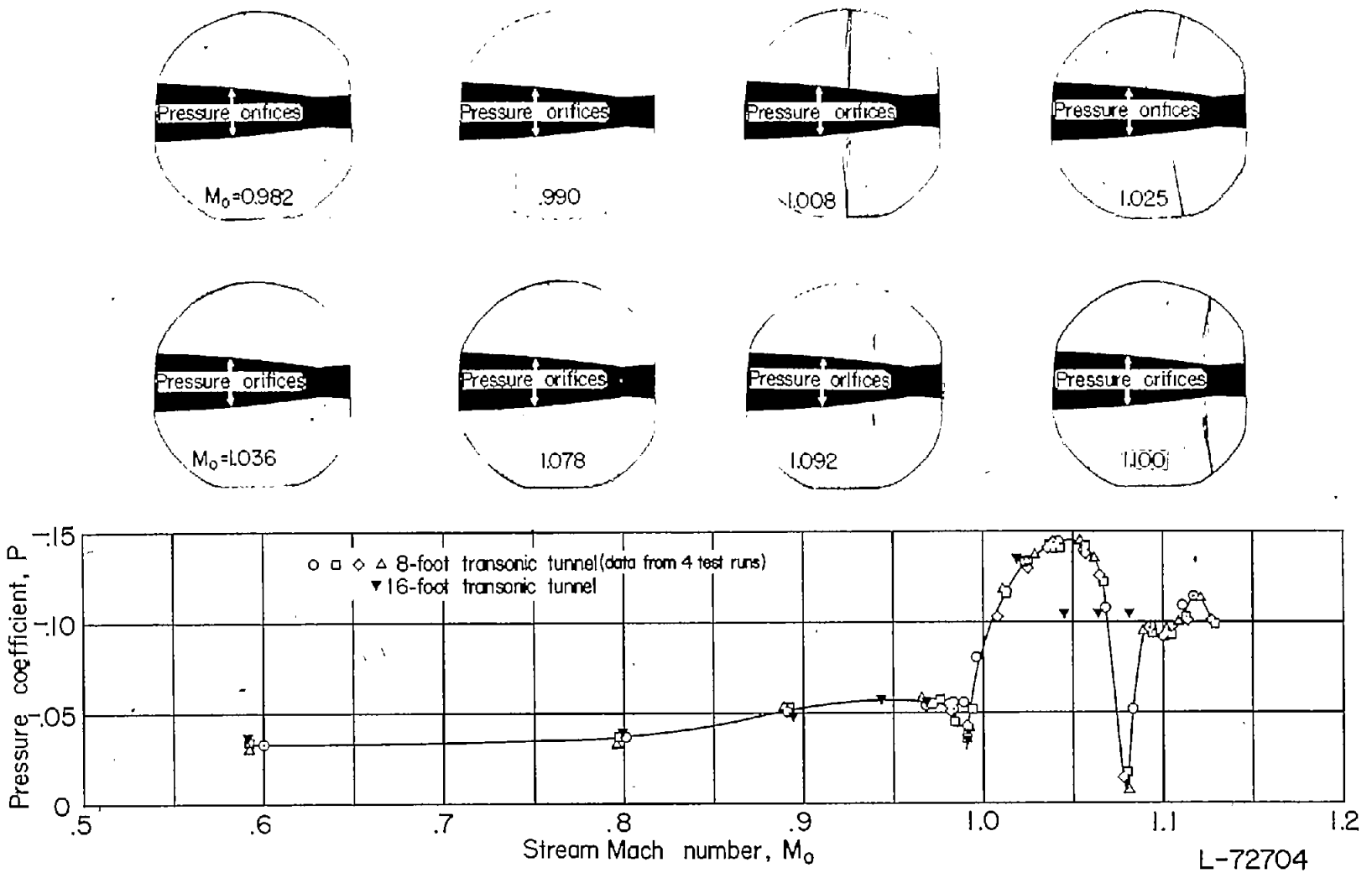

(f) $\frac{x}{l}$=0.7125.

FIGURE 35.—Concluded.

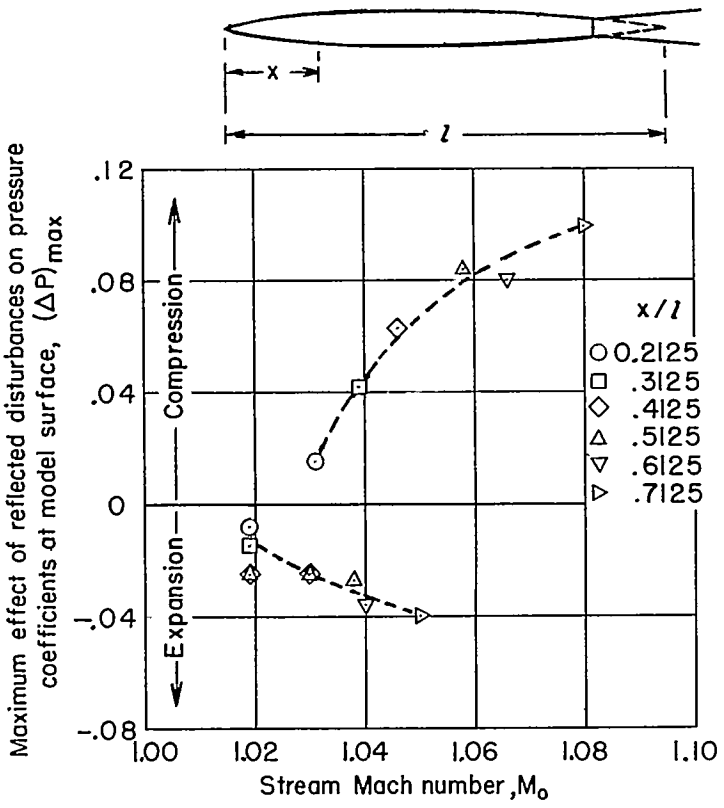

FIGURE 36.—Maximum effect of reflected compressions and expansions on pressure coefficients at model surface, as indicated by differences between measurements in the Langley 8-foot and 16-foot transonic tunnels.

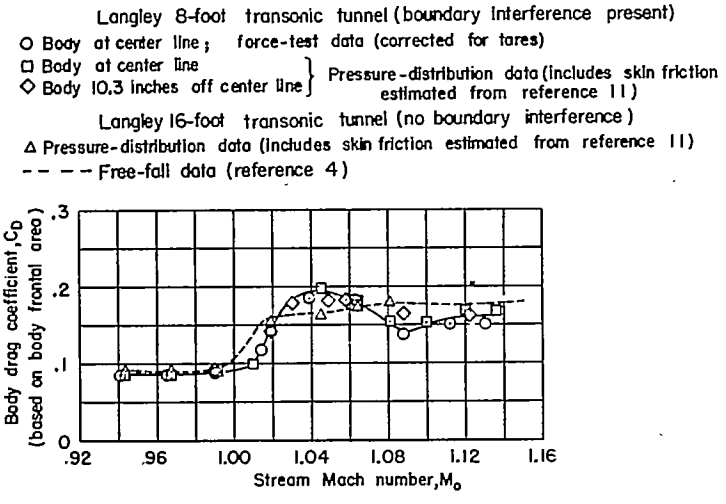

FIGURE 37.—Effect of boundary-reflected disturbances on body drag coefficients for a 33.5-inch-long nonlifting body of revolution in the slotted test section.

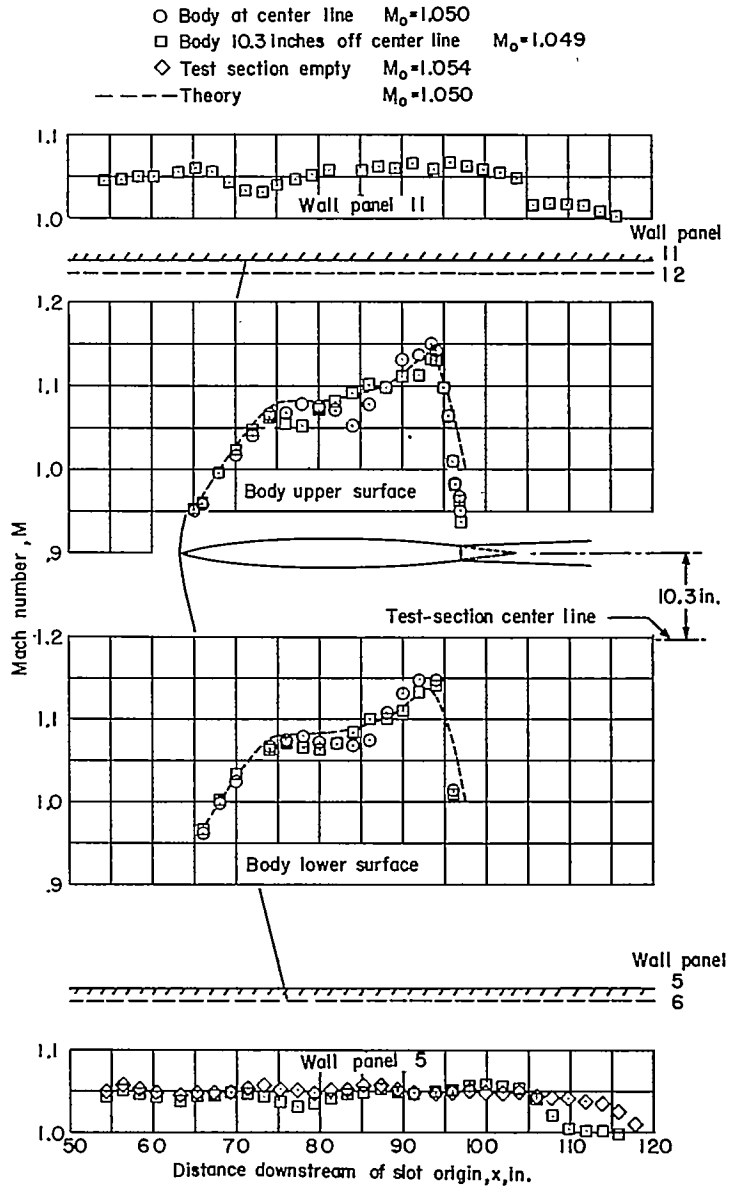

FIGURE 38.—Comparison of body-surface Mach number distributions obtained from tests of a body of revolution at the center line and approximately 10.3 inches off the center line of the slotted test section. $\alpha=0°$; $M_o=1.050$ (approximately).

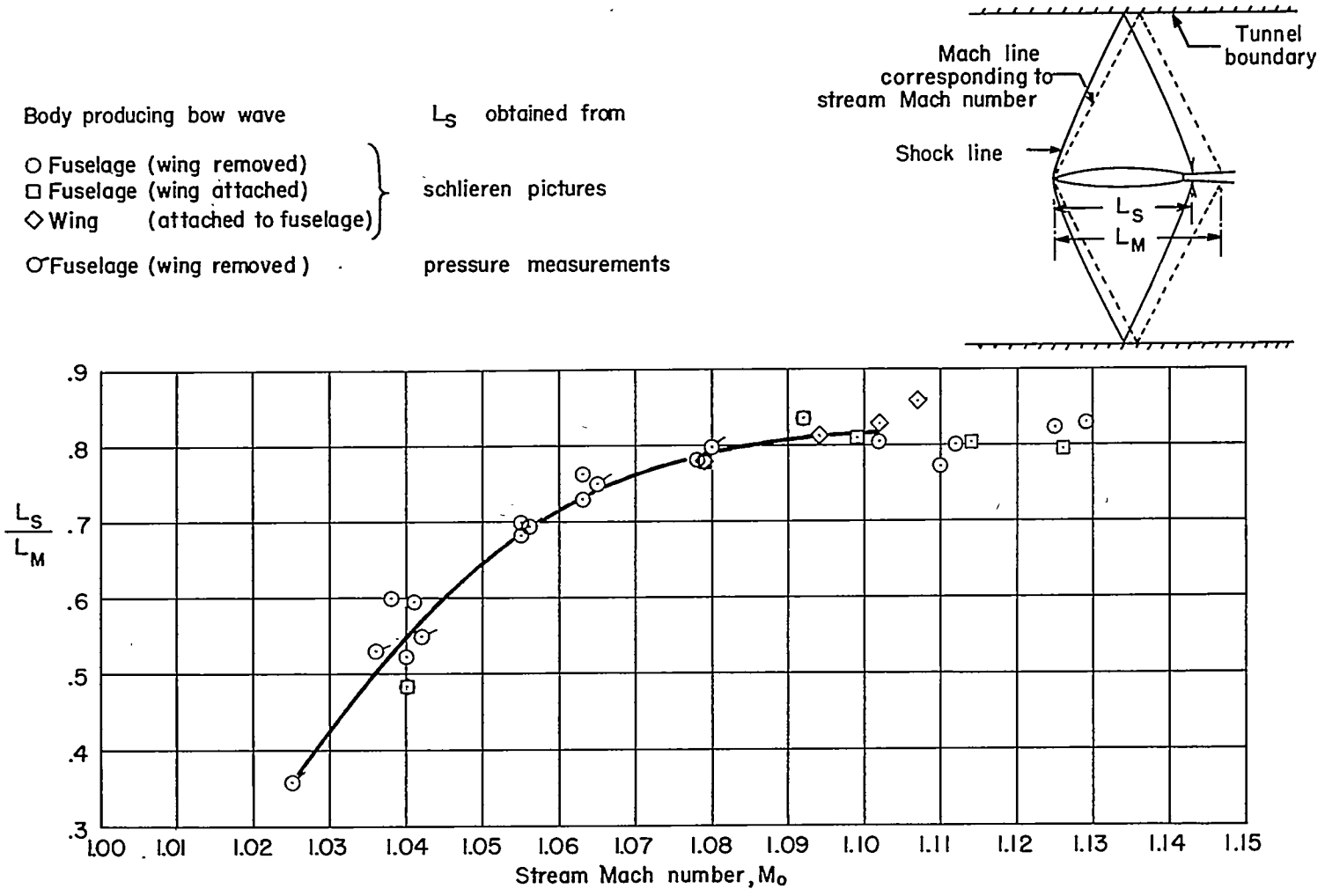

FIGURE 39.—Axial distance required for model bow wave to reflect from test-section wall and strike surface of model near center line. $\alpha=0°$

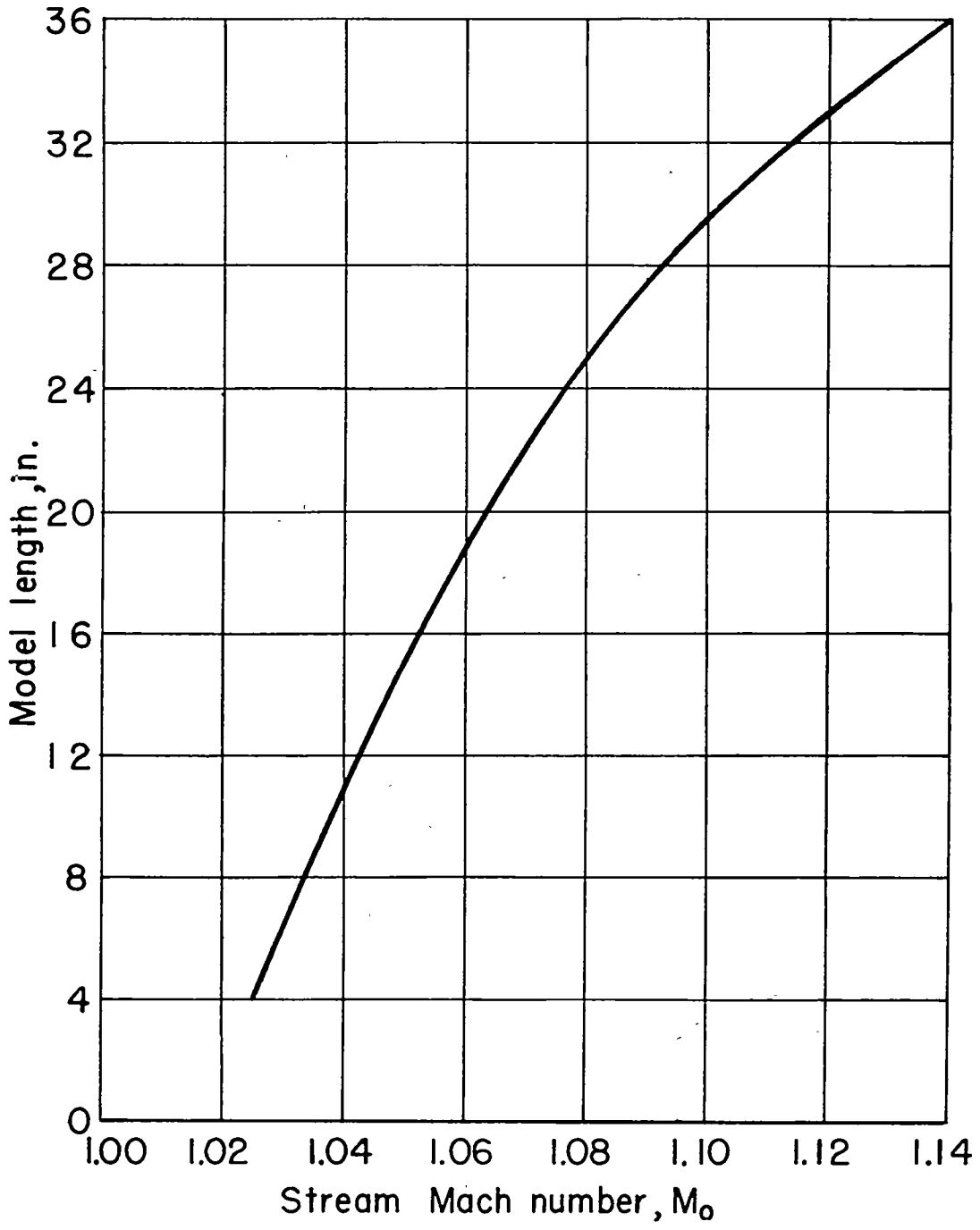

FIGURE 40.—Approximate model lengths for interference-free supersonic testing at center line of slotted test section measuring approximately 43.8 inches from center line to wall.

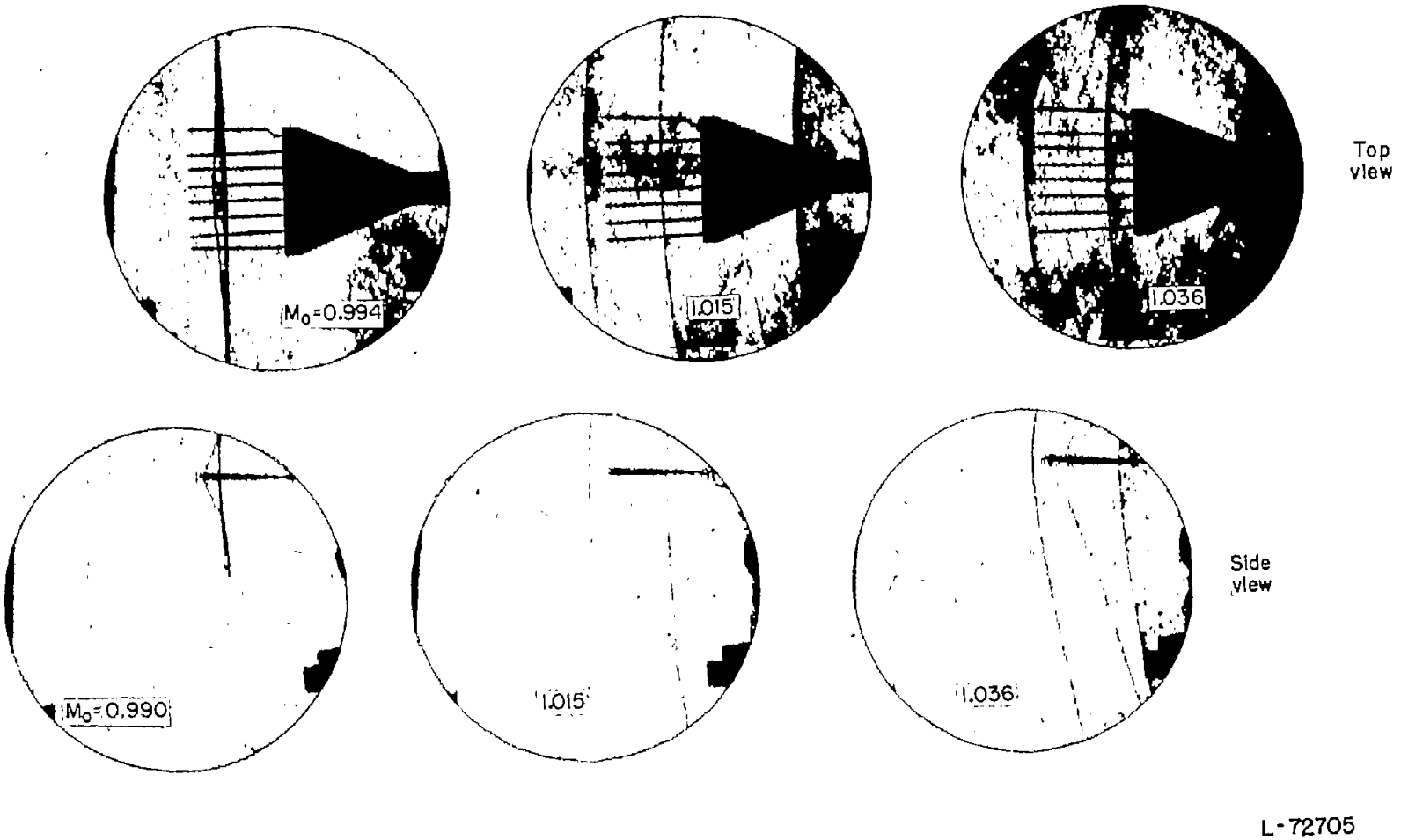

FIGURE 41.—Shock formations at transonic speeds with total-pressure rake (0.050-inch-diameter tubes projecting 3 inches ahead of 1° included-angle wedge) near center line of slotted test section.

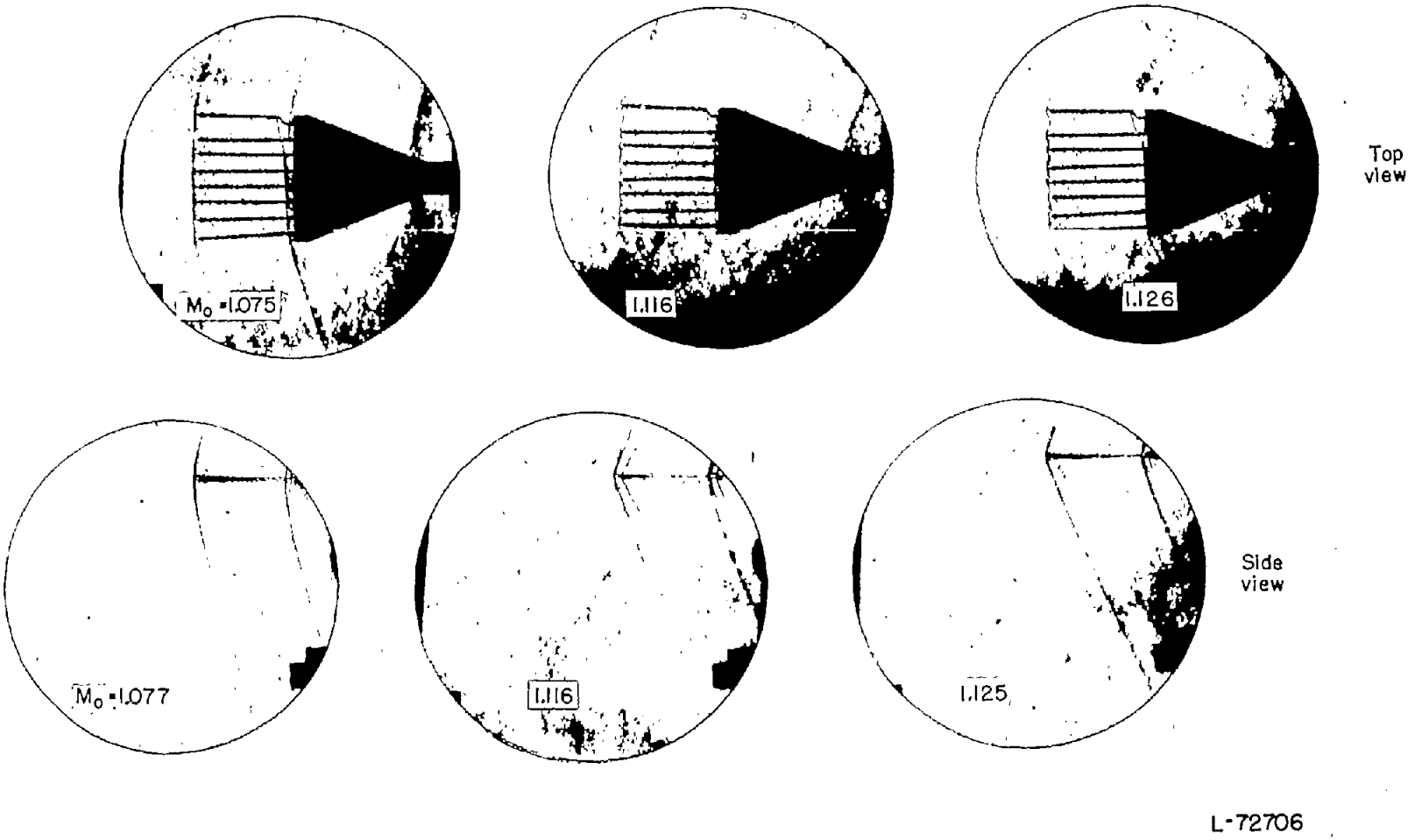

FIGURE 41.—Concluded.

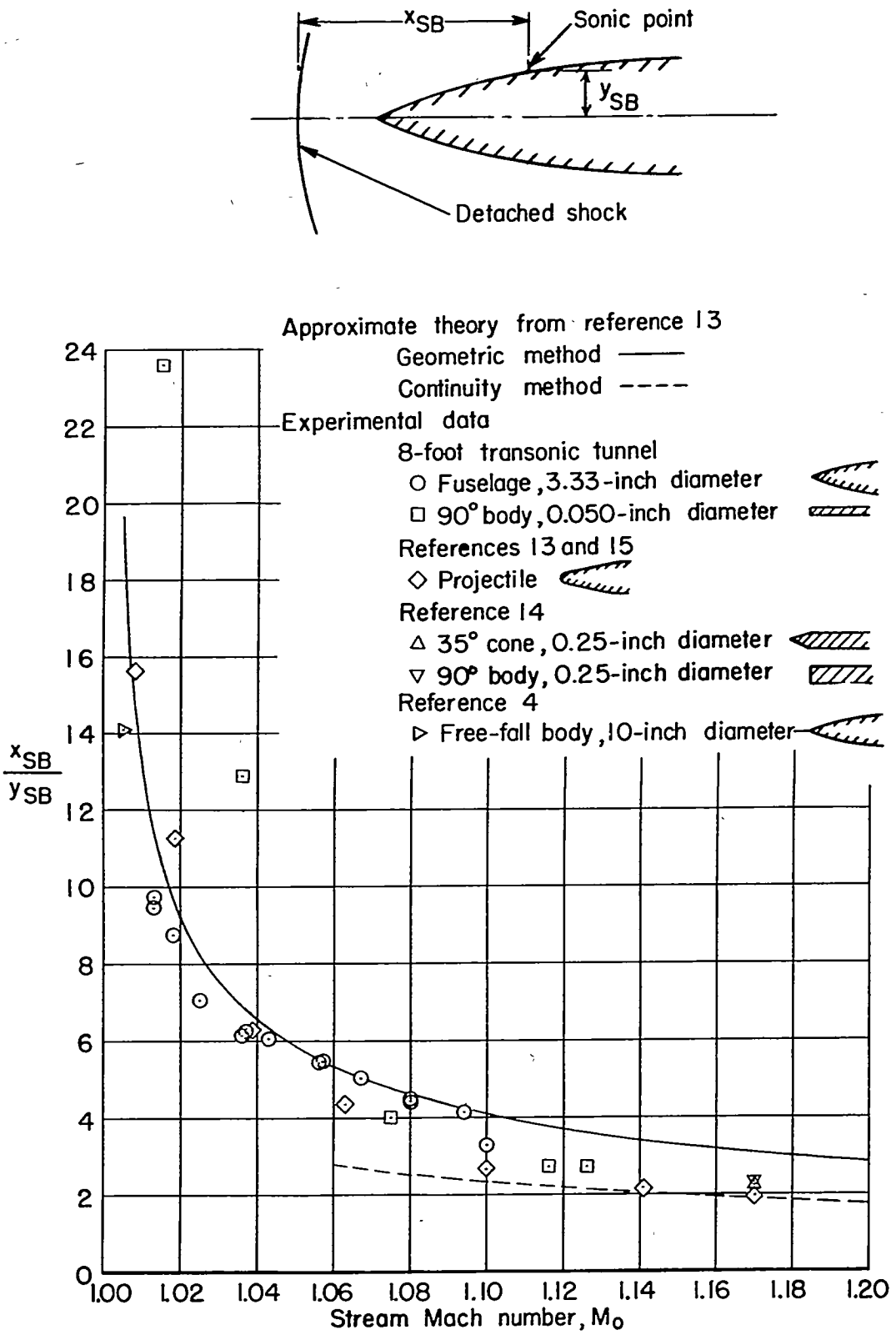

FIGURE 42.—Location of detached shock waves ahead of various axially symmetric bodies at low-supersonic speeds. $\alpha=0°$.

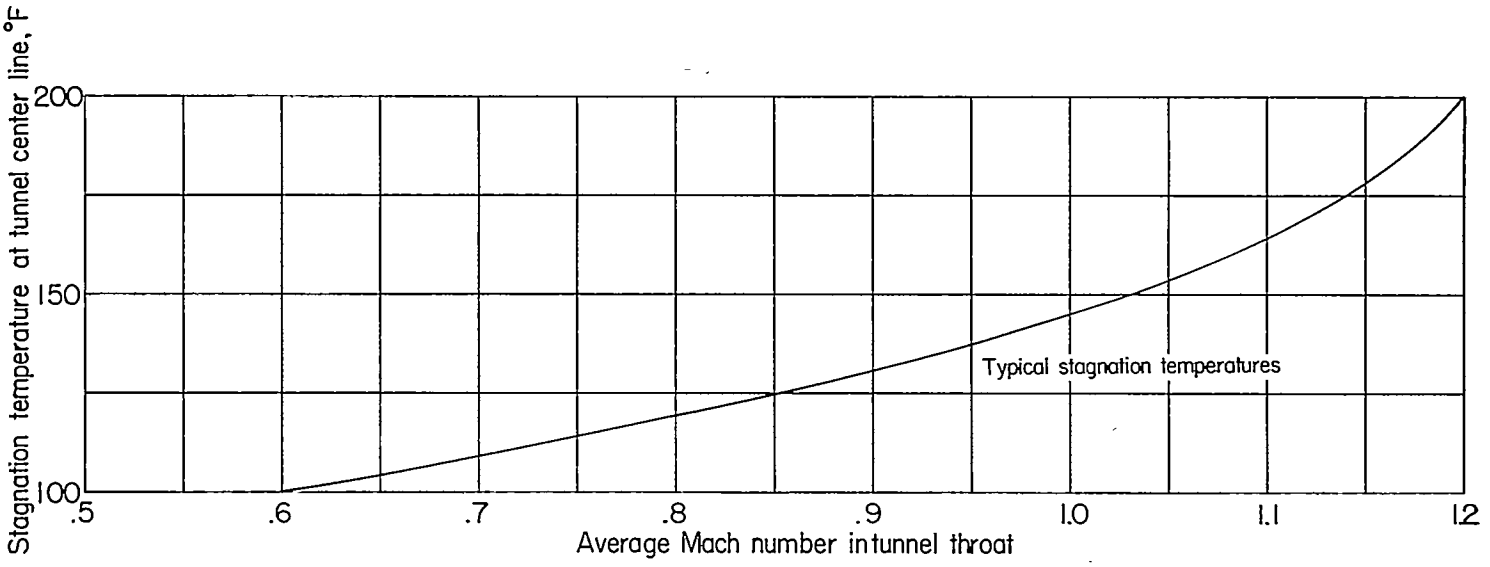

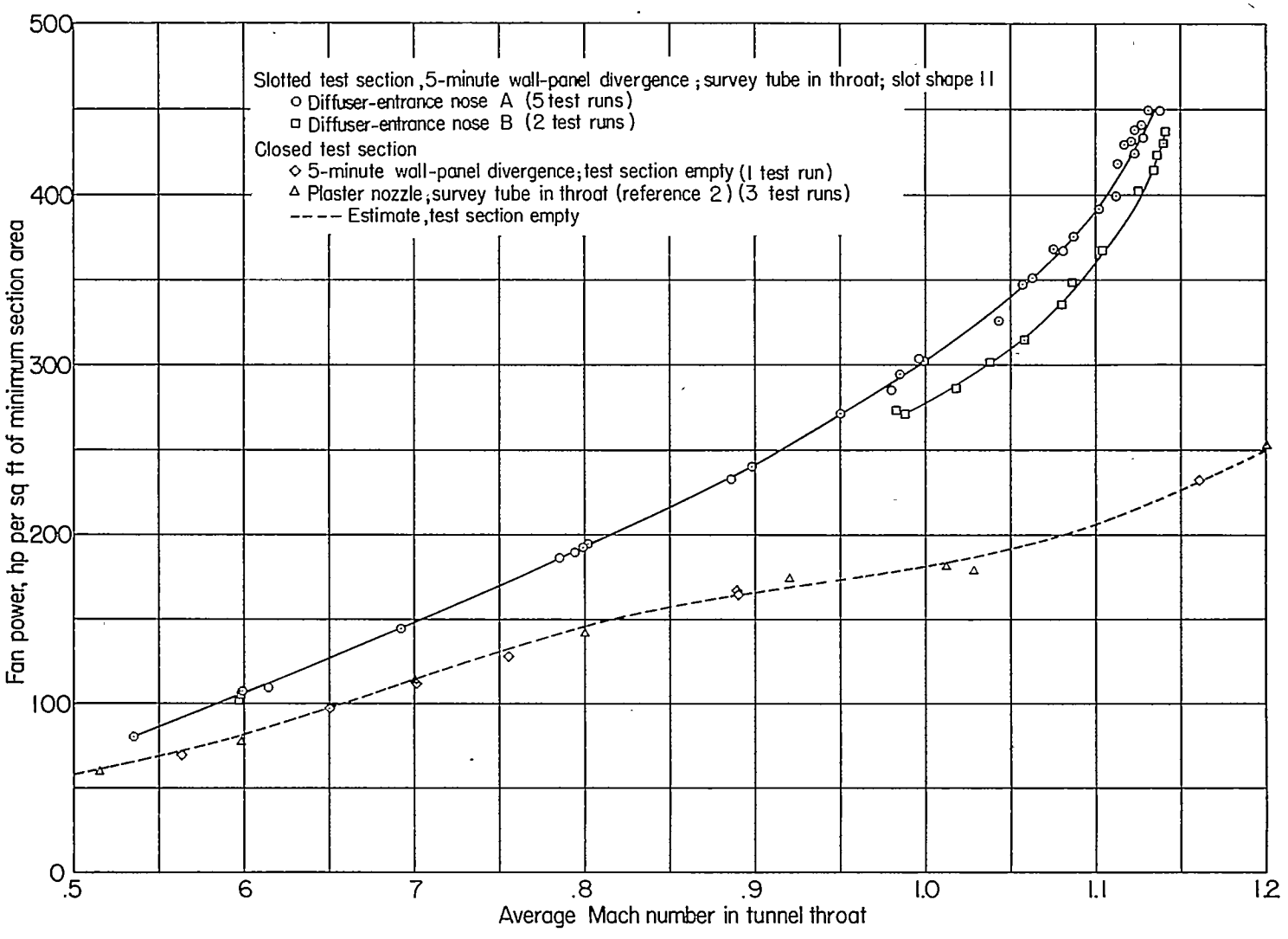

FIGURE 43.—Power requirements for transonic operation of 8-foot tunnel with closed and slotted test sections. All power data reduced to typical stagnation temperatures shown and to stagnation pressure of 2,120 pounds per square foot.

526597—60——89